

INFORMATION TO USERS

This manuscript has been reproduced from the microfilm master. UMI films the text directly from the original or copy submitted. Thus, some thesis and dissertation copies are in typewriter face, while others may be from any type of computer printer.

The quality of this reproduction is dependent upon the quality of the copy submitted. Broken or indistinct print, colored or poor quality illustrations and photographs, print bleedthrough, substandard margins, and improper alignment can adversely affect reproduction.

In the unlikely event that the author did not send UMI a complete manuscript and there are missing pages, these will be noted. Also, if unauthorized copyright material had to be removed, a note will indicate the deletion.

Oversize materials (e.g., maps, drawings, charts) are reproduced by sectioning the original, beginning at the upper left-hand corner and continuing from left to right in equal sections with small overlaps.

Photographs included in the original manuscript have been reproduced xerographically in this copy. Higher quality 6" x 9" black and white photographic prints are available for any photographs or illustrations appearing in this copy for an additional charge. Contact UMI directly to order.

**Bell & Howell Information and Learning
300 North Zeeb Road, Ann Arbor, MI 48106-1346 USA
800-521-0600**

UMI[®]



UNIVERSITY OF OKLAHOMA
GRADUATE COLLEGE

DISSECTING THE REACTION MECHANISM OF SHEEP LIVER
6-PHOSPHOGLUCONATE DEHYDROGENASE

A Dissertation

SUBMITTED TO THE GRADUATE FACULTY

in partial fulfillment of the requirements for the

degree of

Doctor of Philosophy

By

LEI ZHANG
Norman, Oklahoma
2000

UMI Number: 9985568

UMI[®]

UMI Microform 9985568

Copyright 2000 by Bell & Howell Information and Learning Company.

All rights reserved. This microform edition is protected against
unauthorized copying under Title 17, United States Code.

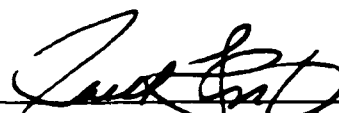
Bell & Howell Information and Learning Company
300 North Zeeb Road
P.O. Box 1346
Ann Arbor, MI 48106-1346

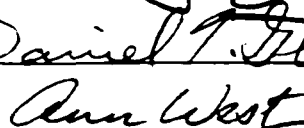
**© Copyright by LEI ZHANG 2000
All Rights Reserved.**


DISSECTING THE REACTION MECHANISM OF SHEEP LIVER
6-PHOSPHOGLUCONATE DEHYDROGENASE

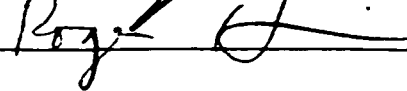
A Dissertation APPROVED FOR THE
DEPARTMENT OF CHEMISTRY AND BIOCHEMISTRY

BY



Daniel T. Blatzky


Ann West


Bruce O'Byrne


Roy J. ...

ACKNOWLEDGEMENTS

I would like to thank my research advisor, Professor Paul F. Cook, for his guidance, inspiration, and support during my graduate studies. Thanks for being my teacher and best friend for the past five years. I would also like to extend my appreciation to the other members of my graduate advisory committee, Dr. Bruce A. Roe, Dr. Ann H. West, Dr. Daniel T. Glatzhofer, and Dr. Roger G. Harrison, for their assistance. I also acknowledge the National Institutes of Health and the University of Oklahoma for financial support.

A special thanks goes to Drs. Bill Karsten and Lillian Chooback for their guidance on the project, for the weekends of BBQ, and a friendship that will last a lifetime. I would like to thank Jean Keil for her tremendous help during the process of completing my research studies. I also thank Qingping Xu for helping me prepare most of the color figures in this dissertation. I wish to thank everyone in the Cook and West Labs, Chia-Hui Tai, Chi-Ching Hwang, Corey Johnson, Weal Rabeh, Jason Sanders, Fabiola Janiak-Spens, Stace Porter, David Sparling, Daniel Copeland, Jennifer Gray, and Hui Tan, who have shared so many interesting events and conversations with me, and made the lab such a fun place to work.

Most importantly, I would like to express my sincere gratitude to my parents, Lianzhong Zhang and Shuqin Wang for their unwavering support and love. Mom and

Dad, thanks for your encouragement and advice, and for always being there for me. I also wish to thank my sister, Hui Zhang, for her encouragement.

Last but certainly not least, I would like to thank my husband, Dali Liu, who also works in the same lab with me, for his constant love and continuous support at both home and work. Thanks for helping me with the experiments, thanks for cooking for me when I am so tired after work, and thanks for making my last five years the best in my life.

TABLE OF CONTENTS

LIST OF TABLES	x
LIST OF FIGURES	xi
LIST OF ABBREVIATIONS	xiv
ABSTRACT	xvi
CHAPTER 1 INTRODUCTION	1
1.1 Pentose Phosphate Pathway	1
1.2 Pyridine-Nucleotide Linked Oxidative Decarboxylases	6
1.3 6-Phosphogluconate Dehydrogenase	11
1.3.1 Kinetic Mechanism	11
1.3.2 Chemical Mechanism	15
1.3.3 Structure of 6-Phosphogluconate Dehydrogenase	21
1.3.4 Important Catalytic and Substrate Binding Residues	21
1.3.5 Cloning and Sequencing of the Sheep Liver 6-Phosphogluconate Dehydrogenase cDNA	33
1.3.6 Altered Site II <i>in vitro</i> Mutagenesis System	34
1.3.7 QIAexpress Protein Expression and Purification System	36
1.4 Specific Goals of This Study	39
CHAPTER 2 EXPERIMENTAL METHODS	42
2.1 Materials	42

2.1.1	Chemical and Reagents	42
2.1.2	Bacterial Strains and Plasmids	43
2.2	Site-Directed Mutagenesis	43
2.2.1	Subcloning of 6PGDH into the pAlter-1 Vector	43
2.2.2	Preparation of Single-Stranded DNA	43
2.2.3	Site-Directed Mutagenesis	45
2.2.4	Subcloning of the Mutants into the pQE-30 Expression Vector	49
2.3	Expression and Purification of the Mutant Proteins	53
2.4	Characterization of the Mutant Proteins	54
2.4.1	Circular Dichroism Spectroscopy	54
2.4.2	Initial Velocity Studies	54
2.4.3	Product Inhibition Studies	55
2.4.4	pH Studies	55
2.4.5	Primary Deuterium Isotope Effects	56
2.4.6	Chemical Rescue	56
2.4.7	Data Processing	57
CHAPTER 3	RESULTS	59
3.1	Site-Directed Mutagenesis	59
3.2	Subcloning of the Mutants into the pQE-30 Expression Vector	59
3.3	Expression and Purification of the Mutant Proteins	61
3.4	Circular Dichroism Spectroscopy	64

3.5	Characterization of K183 Mutant Proteins	64
3.5.1	Kinetic Parameters	64
3.5.2	pH Dependence of Kinetic Parameters	67
3.5.3	Kinetic Deuterium Isotope Effect	71
3.5.4	Chemical Rescue	71
3.6	Characterization of the Substrate Binding Mutant Proteins	75
3.6.1	Kinetic Parameters	75
3.6.2	Product Inhibition by NADPH	78
3.6.3	Deuterium Isotope Effect	82
CHAPTER 4 DISCUSSION		85
4.1	Circular Dichroism Spectroscopy	85
4.2	K183 Mutant Proteins	85
4.2.1	Interpretation of Kinetic Data	86
4.2.2	Interpretation of the pH-Rate Profiles for the K183 Mutant Enzymes	90
4.3	Substrate Binding Mutants	91
4.3.1	Interpretation of Kinetic Data	98
4.3.2	Interpretation of Product Inhibition Data	103
4.3.3	Interpretation of Deuterium Isotope Effects	104
4.4	Mechanism	105
4.5	Summary	108
4.6	Future Studies	109

LITERATURE CITED	111
APPENDIX SEQUENCE ALIGNMENT OF 6-PHOSPHOGLUCONATE DEHYDROGENASES	122

LIST OF TABLES

1.	Sequence of Mutagenic Oligonucleotides	48
2.	Kinetic Parameters for K183 Mutant 6PGDHs	70
3.	pK Values for the Wild Type 6PGDH and K183R Mutant Protein	74
4.	Kinetic Parameters for Mutants of Binding Residues in 6PGDH Active Site	77
5.	K _s Values (μM) of the Product Inhibition (NADPH vs. NADP) Studies for Mutant 6-Phosphogluconate Dehydrogenases	81
6.	Primary Deuterium Kinetic Isotope Effects for Mutant 6-Phosphogluconate Dehydrogenases	84
7.	Interactions between Enzyme and Coenzymes	97
8.	Distances from Specific Enzyme Side Chains to Substrate and Coenzymes	99
9.	Interactions between Enzyme and 6PG	100

LIST OF FIGURES

1.	The Pentose Phosphate Pathway	2
2.	The General Reaction Catalyzed by Pyridine-Nucleotide Linked Oxidative Decarboxylases	8
3.	The Proposed General Acid-General Base Mechanism for Pyridine-Nucleotide Linked Oxidative Decarboxylases	9
4.	The Reaction Catalyzed by 6-Phosphogluconate Dehydrogenase	12
5.	The Rapid Equilibrium Random Kinetic Mechanism Proposed for Both the Sheep Liver and <i>C. utilis</i> 6PGDHs	14
6.	The Proposed General Acid-General Base Mechanism for 6-Phosphogluconate Dehydrogenase	16
7.	Structure of a Monomer of 6-Phosphogluconate Dehydrogenase from Sheep Liver	22
8.	Structure of the Dimer of 6-Phosphogluconate Dehydrogenase from Sheep Liver	24
9.	Stereopair of the 6PG Binding Site of Sheep Liver 6-Phosphogluconate Dehydrogenase	27
10.	Alignment of 6PGDH Sequences in the Active Site Region	30
11.	Binding Interaction between 6xHis Tag and Ni-NTA Resin	38
12.	Map of pPGDH.LC5	44

13.	Schematic Diagram of the Altered Sites II <i>in vitro</i> Mutagenesis Procedure from Promega	46
14.	Schematic Representation of Subcloning of Mutated 6PGDH cDNA into pQE-30 Expression Vector	51
15.	Map of Mutated 6PGDH Gene in pQE-30 Vector	52
16.	Agarose Gel Electrophoresis of K183A.pAlter Plasmids Digested with <i>EcoR</i> I and <i>Hind</i> III	60
17.	Agarose Gel Electrophoresis of K183A.pQE30 Plasmids Digested with <i>Hind</i> III	62
18.	Elution Profile of the K183E Mutant Protein	63
19.	SDS-PAGE of K183E Mutant Protein	65
20.	Far-UV CD Spectrum of K183E Mutant Protein Compared with the Wild Type Enzyme	66
21.	Lineweaver-Burk Plot for the K183C Mutant Protein	68
22.	Initial Velocity Pattern for K183R Mutant Protein	69
23.	pH Dependence of Kinetic Parameters for Wild Type 6-PGDH	72
24.	The pH Dependence of Kinetic Parameters for the K183R Mutant of 6-PGDH	73
25.	Initial Velocity Pattern for H186A Mutant Protein	76
26.	Inhibition Pattern for H186A Mutant Protein at Saturating 6PG Concentration	79
27.	Dixon Plot for N187A Mutant Protein at Saturating 6PG Concentration	80

28.	Primary Deuterium Isotope Effects for H186A mutant protein	83
29.	Stereopair of the Active Site Region of the 6PGDH:Nbr ⁸ ADP Binary Complex	93
30.	Stereopair of the Active Site Region of the 6PGDH:NADPH Binary Complex	95
31.	Active Site Regions of the Enzyme-Substrate and Enzyme-Coenzyme Binary Complexes	106

LIST OF ABBREVIATIONS

APADP, 3-acetylpyridine adenine dinucleotide 2'-phosphate

Bis-Tris, Bis(2-hydroxyethyl)imino-tris(hydroxymethyl)methane

bp, base pair

CD, circular dichroism

Ches, cyclohexylaminoethanesulfonic acid

3-*d*-6PG, 3-*deuterio*-6-phosphogluconate

E, enzyme

GST, glutathione S-transferase

Hepes, N-(2-hydroxyethyl)piperazine-N'-2-ethanesulfonic acid

ICDH, isocitrate dehydrogenase

IPTG, isopropylthio- β -galactoside

kb, kilobase

LB, Luria-Bertani

NADP, nicotinamide adenine dinucleotide 2'-phosphate (the plus sign is omitted for convenience)

NADPH, reduced nicotinamide adenine dinucleotide 2'-phosphate

Ni-NTA, Ni²⁺-nitrilo-tri-acetic acid

6PG, 6-phosphogluconate

6PGDH, 6-phosphogluconate dehydrogenase

3-h-6PG, 3-phosphogluconate

PCR, polymerase chain reaction

PEG, polyethylene glycol

RT-PCR, reverse transcription-polymerase chain reaction

Ru-5-P, ribulose-5-phosphate

ssDNA, single-stranded deoxyribonucleic acid

SDS-PAGE, sodium dodecyl sulfate-polyacrylamide gel electrophoresis

WT, wild type

ABSTRACT

6-Phosphogluconate dehydrogenase (6PGDH) catalyzes the reversible oxidative decarboxylation of 6-phosphogluconate to ribulose-5-phosphate and CO₂ with the concomitant reduction of NADP to NADPH. Site-directed mutagenesis was used to change K183 of sheep liver 6-phosphogluconate dehydrogenase to A, E, H, C, Q, R, and M to probe its possible role as a general base catalyst. Each of the mutant proteins was characterized with respect to its kinetic parameters at pH 7, and the pH dependence of kinetic parameters for the K183R mutant enzyme. The only mutant enzyme that gives a significant amount of catalysis is the K183R mutant. Its activity is decreased by about 3 orders of magnitude, and the general base pK is perturbed to a value greater than pH 9. All other mutant enzymes have rates that are decreased by about 4 orders of magnitude compared to the wild type enzyme. Data are consistent with the general base function of K183.

In the second part of the research, three additional mutants, S128A, H186A and N187A were characterized in the same manner as the K183 mutant enzymes. The decrease in the activity compared to the wild type enzyme is about 200-fold for the H186A and N187A mutant enzymes, but only 12-fold for the S128A mutant enzyme. Dissociation constant for 6PG from the E:NADP:6PG complex (K_{6PG}) is increased by around 6-fold for both S128A and H186A and 16-fold for N187A. Product inhibition studies by NADPH give a dissociation constant for the E:NADPH complex (K_{is}) that

is increased by 5- to 6-fold for the S128A and H186A mutant enzymes at nonsaturating 6PG. No significant change is found in K_m value for the N187A mutant enzyme. The primary deuterium isotope effects decrease for S128A and H186A, and increase in the case of N187A compared to those of the wild type enzyme. The kinetic data suggest that all of the three enzyme side chains are responsible for binding the substrates, and that both S128 and H186 play an important role in the decarboxylation process, while N187 facilitates the hydride transfer step.

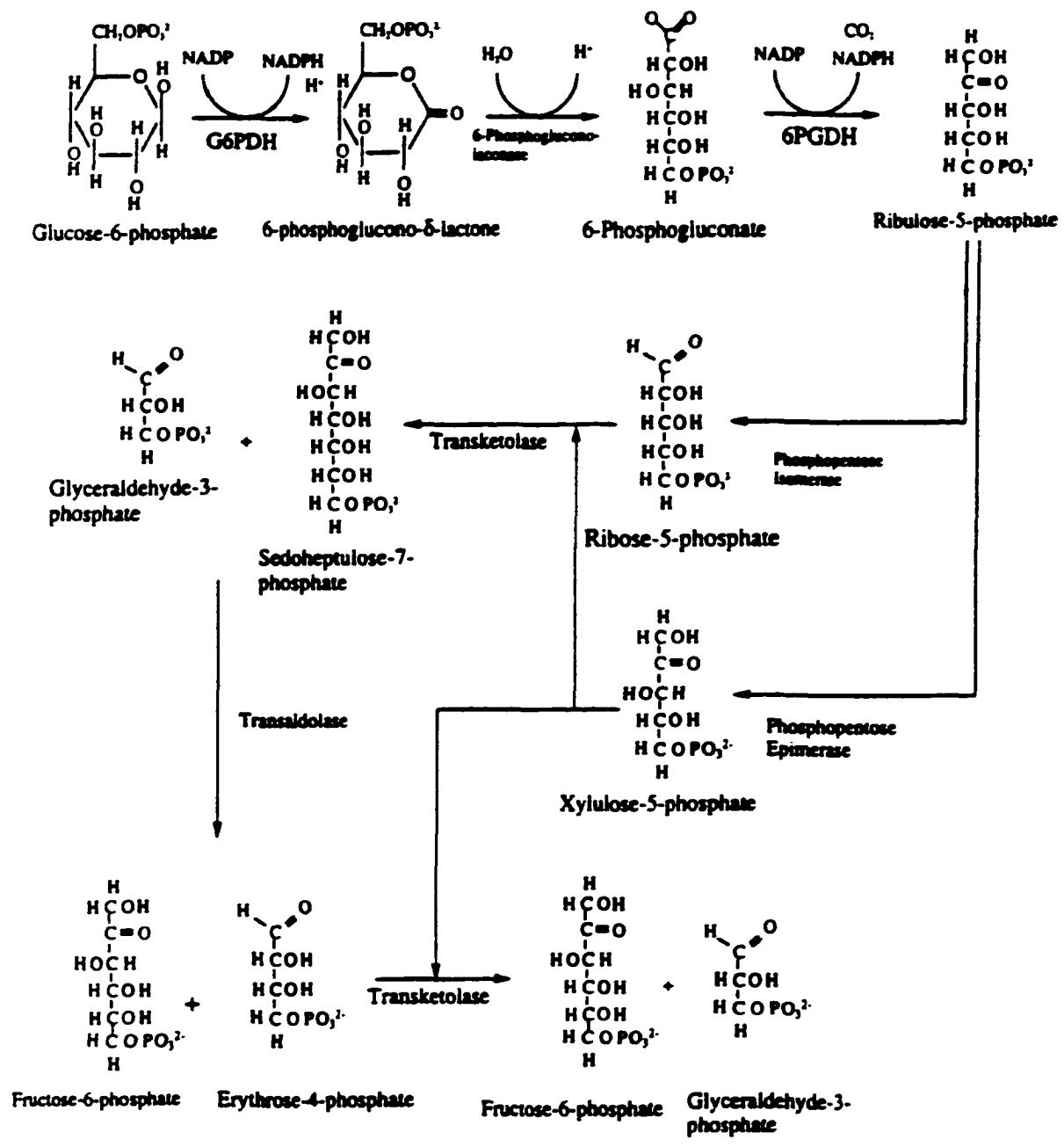
CHAPTER 1

INTRODUCTION

1.1 Pentose Phosphate Pathway.

6-Phosphogluconate dehydrogenase (EC 1.1.1.44) is the third enzyme in the pentose phosphate pathway [also called the hexose monophosphate (HMP) shunt or the phosphogluconate pathway; Figure 1]. The pentose phosphate pathway is an alternate mode of glucose oxidation and is important for the synthesis of NADPH, the reducing power for reductive biosynthesis. Many endergonic reactions, such as the biosynthesis of fatty acids and cholesterol, as well as photosynthesis, require NADPH to utilize the free energy of metabolite oxidation. Thus, the pentose phosphate pathway is most active in tissues involved in fatty acid and cholesterol biosynthesis, and the $[NADP]/[NADPH]$ ratio is maintained near 0.01, which favors metabolite reduction. Although NADPH and NADH differ only by a phosphate group at the 2'-OH group of the adenosine moiety, they are not metabolically interchangeable, because of the high degree of specificity towards the coenzymes shown by the dehydrogenase involved. On the other hand, NADPH is also required for maintaining the erythrocyte membrane integrity by regenerating reduced glutathione (GSH), catalyzed by glutathione reductase. In addition to NADPH, another product of the pentose phosphate pathway is ribose-5-phosphate (R5P) which is a precursor in the

Figure 1. The Pentose Phosphate Pathway. The pathway consists of an oxidative branch and a non-oxidative branch. 6-Phosphogluconate dehydrogenase is the third enzyme in the oxidative branch.



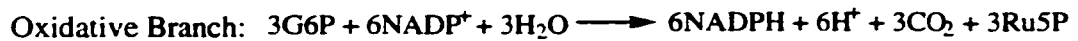
biosynthesis of nucleic acids as well as a component of nucleotide cofactors (Voet and Voet, 1995).

The overall reaction of the pentose phosphate pathway is:



The pathway consists of an oxidative branch and a non-oxidative one. In the oxidative branch, glucose-6-phosphate is oxidized to 6-phosphoglucono- δ -lactone by glucose-6-phosphate dehydrogenase (G6PDH) with the concomitant production of NADPH. Next, 6-phosphogluconolactonase hydrolyses 6-phosphoglucono- δ -lactone to 6-phosphogluconate. Finally, 6-phosphogluconate dehydrogenase (6PGDH) catalyzes the oxidative decarboxylation of 6-phosphogluconate to ribulose-5-phosphate and CO_2 with the concomitant production of a second NADPH. The NADPH produced is used for reductive biosynthesis, while the other product, ribulose-5-phosphate enters the non-oxidative branch of the pathway. In this part of the pathway, ribulose-5-phosphate can be converted either to ribose-5-phosphate by ribulose-5-phosphate isomerase or to xylulose-5-phosphate (Xu5P) by ribulose-5-phosphate epimerase. The next step involves a series of carbon-carbon bond cleavage and formation reactions catalyzed by two enzymes, transaldolase and transketolase. Transketolase transfers a C_2 unit from xylulose-5-phosphate to ribose-5-phosphate, producing glyceraldehyde-3-phosphate (GAP) and sedoheptulose-7-phosphate (S7P). The reaction is followed by the transfer of a C_3 unit from sedoheptulose-7-phosphate to glyceraldehyde-3-phosphate catalyzed by transaldolase, yielding erythrose-4-

phosphate (E4P) and fructose-6-phosphate (F6P). A second transketolase is needed to transfer another C₂ unit from xylulose-5-phosphate to erythrose-4-phosphate, giving the final product glyceraldehyde-3-phosphate and the second molecule of fructose-6-phosphate. The overall reactions for oxidative and non-oxidative branches are summarized as follows:



The balance between the oxidative and non-oxidative branches depends largely on the metabolic need for NADPH and ribose-5-phosphate. When the cell needs more NADPH than ribose-5-phosphate, the excess ribose-5-phosphate can enter the non-oxidative branch to be converted to glyceraldehyde-3-phosphate and fructose-6-phosphate, which can be reconverted to G6P for additional rounds of the pentose phosphate pathway. On the other hand, if more ribose-5-phosphate is required than NADPH, glucose-6-phosphate can be isomerized to fructose-6-phosphate. The latter enters the non-oxidative branch for ribose-5-phosphate synthesis through the reverse reactions of the pathway. The regulation of the flux through the pentose phosphate pathway is achieved by controlling the rate of the glucose-6-phosphate dehydrogenase reaction, which is the first step of the pathway. One of the substrates of the reaction, NADP, acts as an activator of the enzyme (Voet and Voet, 1995).

Genetic deficiency involving the pentose phosphate pathway enzymes may cause severe diseases such as hemolytic anemia. One of the pentose phosphate products, NADPH, is required to maintain the integrity of the cell membrane, especially in erythrocytes due to their lack of mitochondria and constant exposure to an oxidizing environment. Hemolytic anemia is traced to gene mutations of glucose-6-phosphate dehydrogenase, the first enzyme in the pathway. Defective enzyme is produced from the altered gene and does not have sufficient activity to maintain normal levels of NADPH in red blood cells. No hemolytic syndrome has ever been related to 6-phosphogluconate dehydrogenase deficiency (Luzzato and Mehta, 1989). Since the pentose phosphate pathway provides ribose phosphate for nucleic acids biosynthesis, it has been suggested to play an important role in the tumor proliferation process (Boros et al., 1997). Cancer researchers are focusing on glucose-6-phosphate dehydrogenase and transketolase, and the latter two have become targets for new anticancer drug designs. As to 6PGDH, it has been reported that carbamylation of 6-phosphogluconate dehydrogenase may cause cataract formation in populations with high levels of blood urea (Ganea and Harding, 1996). 6PGDH from *Trypanosoma brucei* is also considered a key enzyme involved in parasitic infections (Hanau et al., 1996).

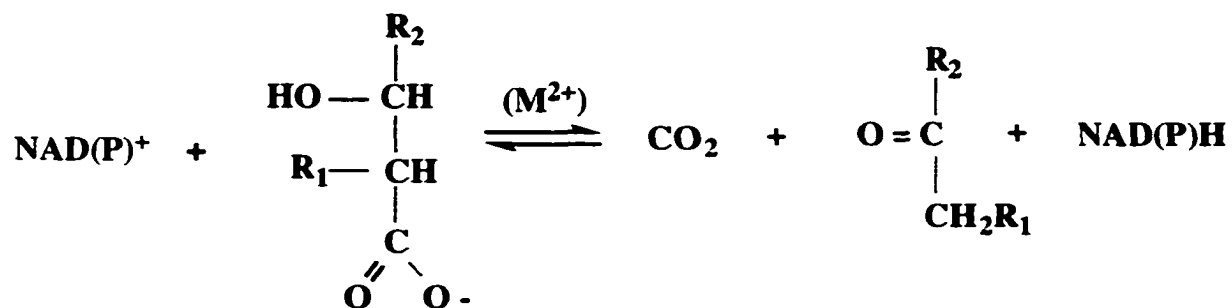
1.2 Pyridine-Nucleotide Linked Oxidative Decarboxylases.

Pyridine-nucleotide linked oxidative decarboxylases are an enzyme class which uses a pyridine nucleotide (NAD or NADP) as a cofactor. In general, this class of

enzyme catalyzes the oxidative decarboxylation of a β -hydroxyacid to a ketone product and CO_2 with the concomitant reduction of NAD(P) to NAD(P)H. The general reaction is shown in Figure 2.

Among the enzymes in this class, previous studies have primarily focused on isocitrate dehydrogenase (ICDH), malic enzyme and 6-phosphogluconate dehydrogenase (6PGDH). These dehydrogenases can be divided into two groups: metal ion dependent and metal ion independent enzymes. The first two enzymes, malic enzyme and isocitrate dehydrogenase require a divalent metal ion for catalytic activity (malic enzyme, Hsu and Lardy, 1967; ICDH, Villafranca and Colman, 1974), while 6-phosphogluconate dehydrogenase is metal ion independent (Pontremoli et al., 1961). This difference may be due to the lack of an electron withdrawing functional group on the carbon α to the leaving group in isocitrate and malate, which are the substrates for ICDH and malic enzyme, respectively. Different enzymes require different divalent metal ions, and the metal ion has been proposed to act as a Lewis acid to facilitate the decarboxylation of the keto intermediate (Grissom and Cleland, 1988). While most 6PGDHs from different sources show no dependence on a divalent metal ion, some can be inhibited by divalent metal ions (Niehuas et al., 1996), and there are examples of 6PGDHs that can be activated by divalent metal ions such as Co^{2+} and Mn^{2+} (Tsai and Chen, 1998).

A general acid-general base mechanism has been proposed for this class of enzyme (Fig. 3). In the proposed mechanism, a general base accepts a proton to facilitate the hydride transfer and further catalyzes the decarboxylation to form an

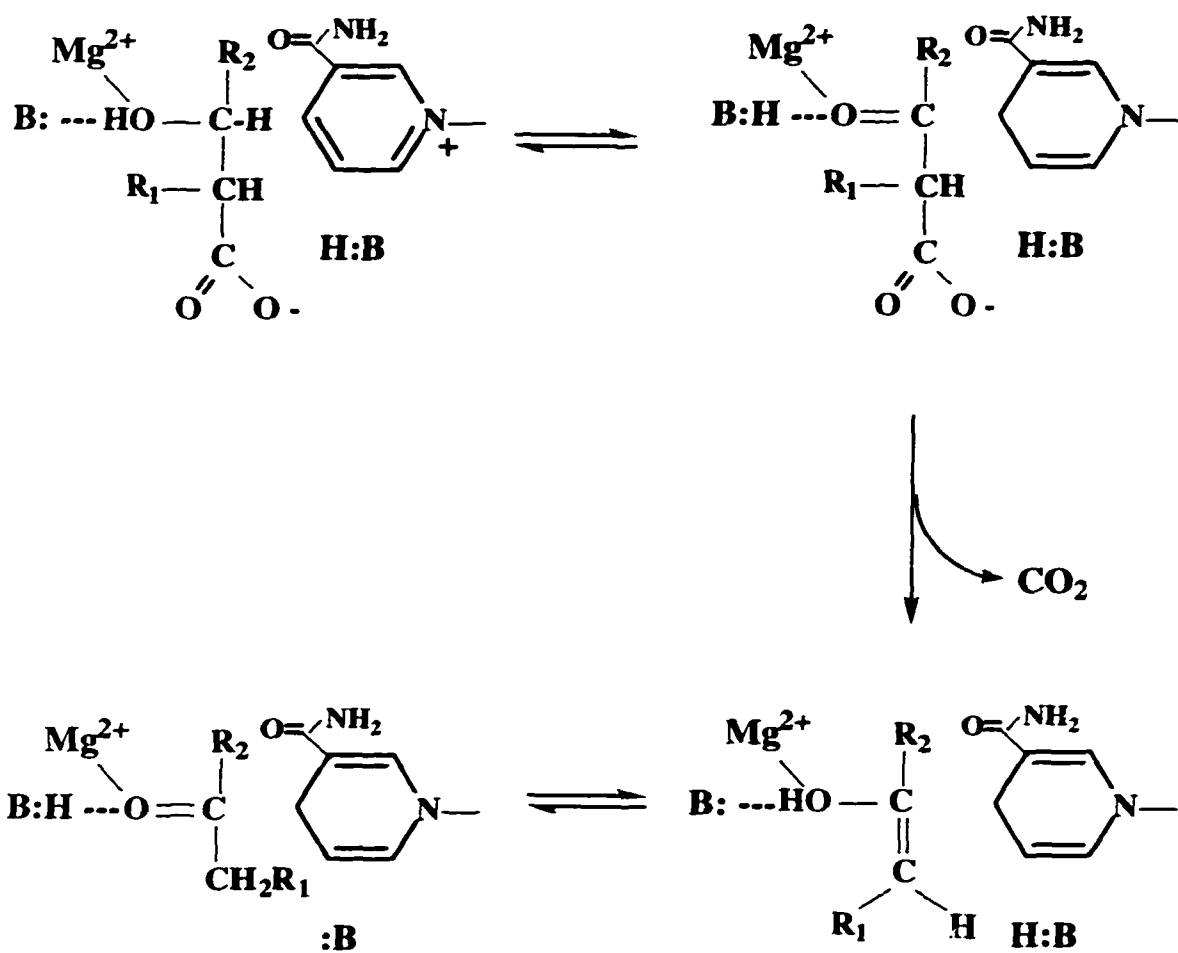


R₁ = H, OH, CH₂CO₂⁻, CH(CH₃)₂

R₂ = CO₂⁻, CH(OH)CH(OH)CH₂OPO₃⁼

Figure 2. The General Reaction Catalyzed by Pyridine-Nucleotide Linked Oxidative Decarboxylases. This class of enzyme catalyzes the oxidative decarboxylation of β-hydroxyacids to their ketone product and CO₂ with the concomitant reduction of NAD(P) to NAD(P)H.

Figure 3. The Proposed General Acid-General Base Mechanism for Pyridine-Nucleotide Linked Oxidative Decarboxylases. The mechanism includes three steps: oxidation, decarboxylation, and tautomerization. A metal ion is required for the activity of this class of enzyme with the exception of 6PGDH.



$R_1 = \text{H, OH, CH}_2\text{CO}_2^-, \text{CH}(\text{CH}_3)_2$

$R_2 = \text{CO}_2^-, \text{CH}(\text{OH})\text{CH}(\text{OH})\text{CH}_2\text{OPO}_3^-$

enol or enediol intermediate, while a general acid is needed to catalyze the tautomerization of the enol or enediol to the final ketone product (malic enzyme, Kiick et al., 1986; Hermes et al., 1982; ICDH, Cook and Cleland, 1981; Grissom and Cleland, 1988; 6PGDH, Berdis and Cook, 1993b; Price and Cook, 1996).

1.3 6-Phosphogluconate Dehydrogenase.

6-Phosphogluconate dehydrogenase is the third enzyme in the pentose phosphate pathway. It catalyzes the reversible oxidative decarboxylation of 6-phosphogluconate to ribulose-5-phosphate and CO₂ with the concomitant reduction of NADP to NADPH. There is no divalent metal ion requirement for the reaction (Siebert et al., 1957; Pontremoli et al., 1961). The reaction catalyzed by 6PGDH is shown in Figure 4.

1.3.1 Kinetic Mechanism.

Kinetic studies have been carried out for 6-phosphogluconate dehydrogenase from several sources, including *Candida utilis*, sheep liver, *Trypanosoma brucei*, human erythrocyte, *Haemophilus influenzae*, *Cryptococcus neoformans*, *Lactococcus lactis*, and *Schizosaccharomyces pombe* (Berdis and Cook, 1993a; Price and Cook, 1996; Hanau et al., 1996; Dallochio et al., 1985; Yoon et al., 1989; Niehaus et al., 1996; Tetaud et al., 1999; Tsai and Chen, 1998). Among them, the *Candida* enzyme and the sheep liver enzyme have been characterized most extensively for their kinetic mechanism, using initial velocity and isotope effect studies.

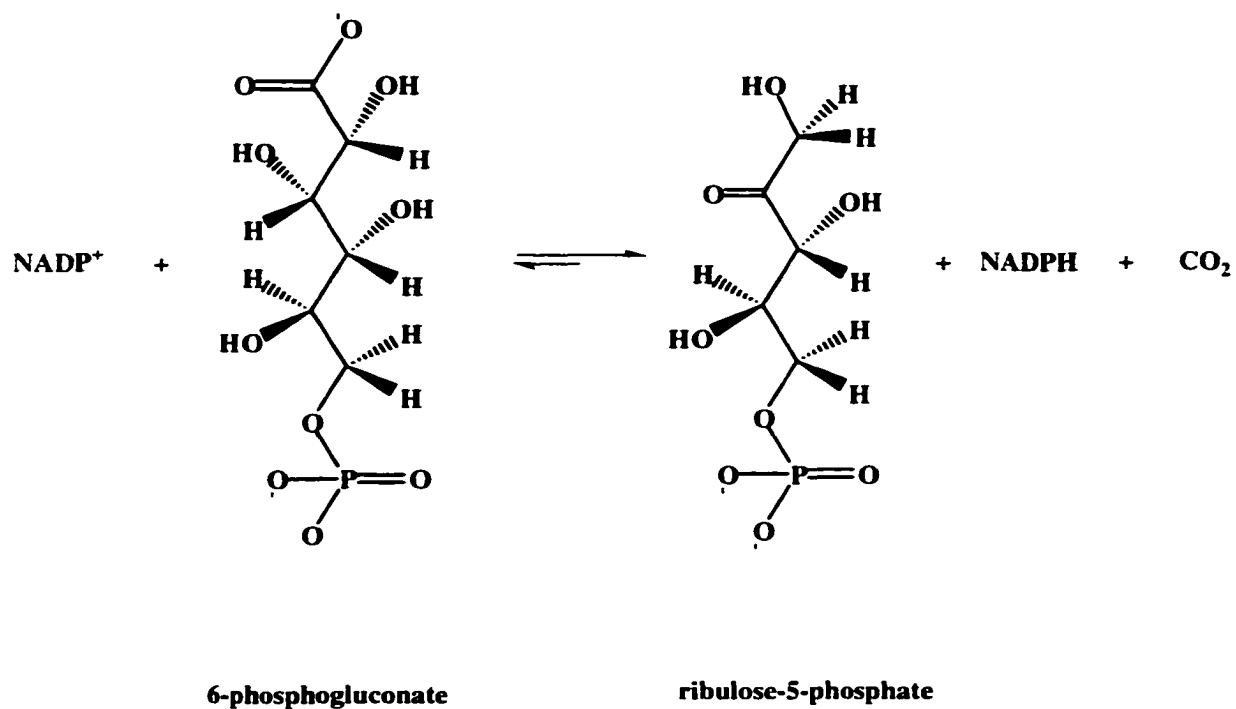


Figure 4. The Reaction Catalyzed by 6-Phosphogluconate Dehydrogenase. The enzyme catalyzes the reversible oxidative decarboxylation of 6-phosphogluconate to ribulose-5-phosphate and CO_2 with the concomitant reduction of NADP to NADPH .

A complete initial velocity study including product and dead-end inhibition has been carried out for 6PGDH from *Candida utilis* (Berdis and Cook, 1993a). The results suggest a rapid equilibrium random kinetic mechanism with dead-end E:NADP:(ribulose-5-phosphate) and E:NADPH:(6-phosphogluconate) complexes (Figure 5). Equal deuterium isotope effects on V , V/K_{NADP} , and V/K_{6PG} have been obtained, indicating that the chemical portion of the reaction limits the overall rate (Cook and Cleland, 1981; Rendina et al., 1984). These results are consistent with the rapid equilibrium mechanism. The mechanism of 6PGDH is different from that of the malic enzyme and isocitrate dehydrogenase, since the latter two have a steady-state random mechanism in which catalysis is not the only slow step.

The steady-state kinetic studies for 6PGDH from sheep liver were carried out initially by Dalziel and co-workers (Topham et al., 1986). Data suggest an asymmetric sequential mechanism in which the substrates bind randomly and product release is ordered. A complete kinetic characterization of sheep liver 6PGDH including product and dead-end inhibition patterns as well as primary deuterium isotope effects has been performed more recently by Price and Cook (1996). The results of the latter authors are consistent with a rapid equilibrium random kinetic mechanism, as proposed for the *Candida* enzyme (Figure 5). The primary deuterium isotope effects suggest that hydride transfer is at least partially rate limiting in the overall reaction. The V/E_t value of sheep liver 6PGDH is 2.0 s^{-1} , while the K_m values for 6PG and NADP are $19 \mu\text{M}$ and $5 \mu\text{M}$, respectively.

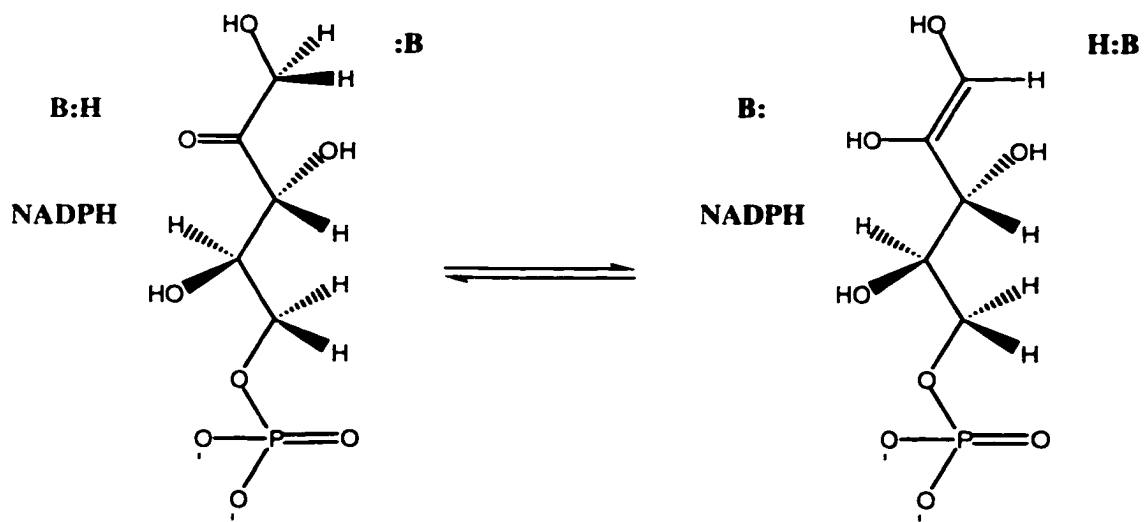
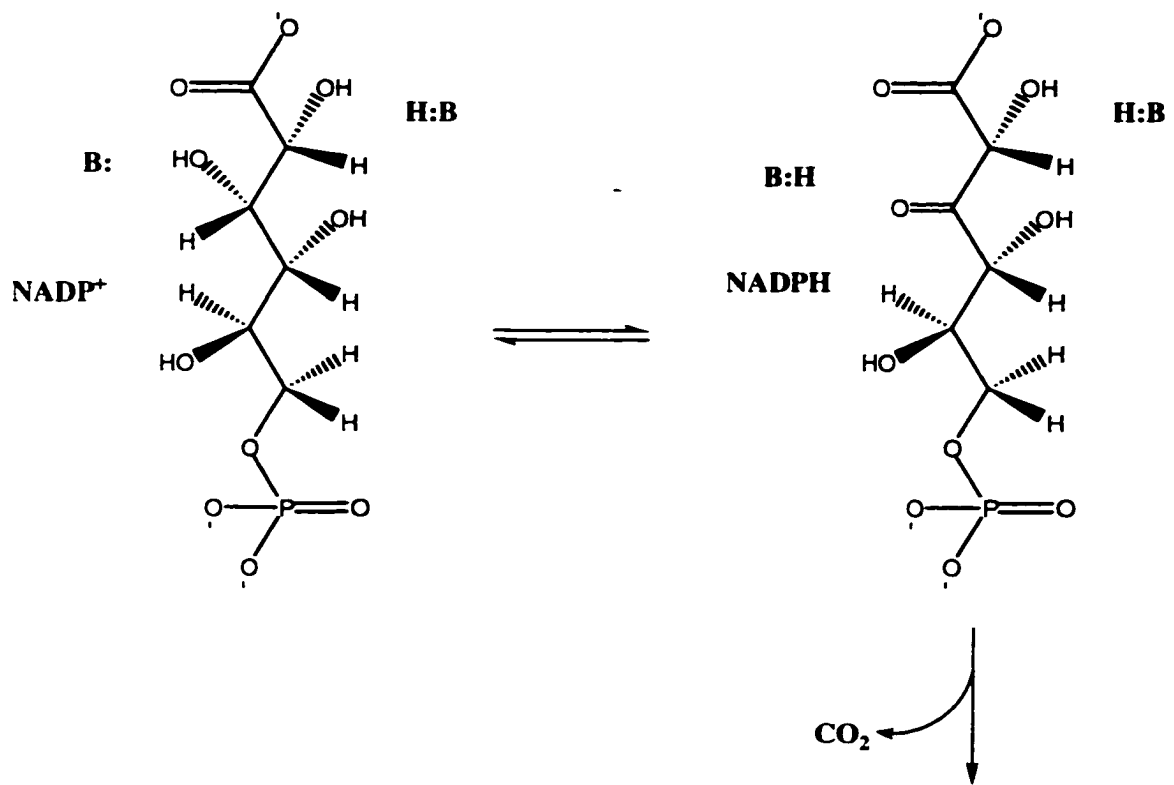
1.3.2 Chemical Mechanism.

The oxidative decarboxylation reaction catalyzed by 6-phosphogluconate dehydrogenase is very similar to the metal ion dependent reactions catalyzed by malic enzyme and isocitrate dehydrogenase, with the exception that 6PGDH does not require a divalent metal ion. Therefore, there is an interest in a study of the chemical mechanism of 6PGDH, particularly in comparison to that of one of the metal ion dependent enzyme.

The hypothesis of a Schiff-base intermediate involved in this reaction was tested by Topham and Dalziel (1986). [2-¹⁸O] Ribulose-5-phosphate was prepared as a substrate for the reductive carboxylation reaction, while H₂¹⁸O was used for the oxidative decarboxylation reaction. If a Schiff-base mechanism is involved in the decarboxylation step, solvent exchange will occur with the C-2 oxygen of the 3-keto intermediate during formation of the enamine. A complete retention of the heavy atom has been observed for the reductive carboxylation, and the product of the oxidative decarboxylation remained unlabeled. These results exclude the possibility of a Schiff-base mechanism. Another reasonable mechanism for 6PGDH consists of the enzyme-mediated protonation of the carbonyl group of the 3-keto intermediate.

pH studies of both the *Candida utilis* and sheep liver 6PGDHs have been carried out (Berdis and Cook, 1993b; Price and Cook, 1996), with a general acid-general base mechanism proposed (Figure 6). In this mechanism, an active site general base is required to accept the proton from the 3-hydroxyl group of 6PG as the

Figure 6. The Proposed General Acid-General Base Mechanism for 6-Phosphogluconate Dehydrogenase. In this mechanism, an active site general base is required to accept the proton from the 3-hydroxyl group of 6PG as the hydride transfers from C-3 of 6PG to NADP. The resulting 3-keto-6-phosphogluconate intermediate is decarboxylated to give the enediol of ribulose-5-phosphate, with the same enzyme residue restoring the proton to the C-3 carbonyl group of the keto intermediate. Finally, a general acid is needed to assist the tautomerization of the enediol intermediate to form the final ketone product.



hydride transfers from C-3 of 6PG to NADP. The resulting 3-keto-6-phosphogluconate intermediate is decarboxylated to give the enediol of ribulose-5-phosphate, with the same enzyme residue restoring the proton to the C-3 carbonyl group of the keto intermediate. Finally, a general acid is needed to assist the tautomerization of the enediol intermediate to form the final ketone product. Reverse protonation states between the general acid and the general base are proposed for the sheep liver 6PGDH (Price and Cook, 1996). The pattern of the pH dependence of kinetic parameters suggests that the general acid and general base must be in opposite protonation states for optimum catalysis, and the catalytic residues are also involved in substrate binding. Thus, the general base must be unprotonated for catalysis, while the general acid must be protonated. Since the pK of the general base is observed on the basic side of the pH profile, and the pK of general acid on the acid side, only a small proportion of enzyme is in the correct protonation state for catalysis.

Unlike malic enzyme and isocitrate dehydrogenase, 6PGDH does not require any divalent metal ion for its activity. A possible reason is that the α - and γ -hydroxyl groups of 6PG are electron-withdrawing and thus facilitate decarboxylation of the β -keto intermediate. 2-Deoxy-6-phosphogluconate has been used as the alternative substrate for sheep liver 6PGDH (Rippa et al., 1973). The 2-deoxy-3-keto intermediate is released from the enzyme due to the slow decarboxylation, and the decarboxylation can only occur in the presence of the reduced coenzyme. The results are consistent with the proposed electron-withdrawing function of the α -hydroxyl group of 6PG, and further support a stepwise mechanism with hydride transfer

preceding decarboxylation. However, 6PGDH from human erythrocytes and *Trypanosoma brucei* catalyze the oxidative decarboxylation of 2-deoxy-6-phosphogluconate without releasing the 2-deoxy-3-keto intermediate (Rippa et al., 1998), and the decarboxylation occurs in the absence of either NADPH or 6PG. According to Rippa, this difference is due to the higher affinity for 2-deoxy-6PG by the erythrocyte enzyme and the *T. brucei* enzymes. As a result, the electron-withdrawing ability of the α -hydroxyl group may not be the only thing to account for the metal ion independence of 6PGDH. Another possibility is the presence of a positively charged enzyme side chain that could perform the same function as the divalent ions, i.e. polarizing the 3-keto of the intermediate.

Multiple primary deuterium/primary ^{13}C isotope effect studies have been carried out for the *Candida* and sheep liver enzymes with both NADP and APADP as the dinucleotide substrates (Hwang et al., 1998). A decrease in $^{13}(\text{V}/\text{K}_{6\text{PG}})_\text{D}$ compared to $^{13}(\text{V}/\text{K}_{6\text{PG}})_\text{H}$ has been observed in all cases, indicating that the hydride transfer step becomes more rate-limiting due to the deuteration at C-3, and the ^{13}C -sensitive step becomes partially masked. The results of multiple isotope effects are consistent with a stepwise mechanism (Figure 6; Hermes et al., 1982; Weiss et al., 1991; Karsten and Cook, 1994; Rendina et al., 1984). The most likely sequence of steps for the oxidative decarboxylation of a β -hydroxy acid is oxidation to generate a β -keto acid, followed by decarboxylation. The ^{13}C -isotope effect on $\text{V}/\text{K}_{6\text{PG}}$ decreases as conditions change along the series NADP/6PG, NADP/6PG-3d, APADP/6PG, and APADP/6PG-3d. Thus, the hydride transfer step has become slower when APADP is

used as the dinucleotide substrate in place of NADP, and it becomes completely rate determining with APADP/6PG-3d. Based on the observed isotope effect data, intrinsic isotope effects have been estimated. Intrinsic isotope effects such as Dk and ^{13}k refer to the isotope effects on the microscopic rate constants in enzyme-catalyzed reactions. The intrinsic effects cannot be measured directly by experiment but must be calculated from observed isotope effects, *e.g.*, DV , $^D(V/K)$ and $^{13}(V/K)$, subtracting out the contribution of other slow steps. Intrinsic isotope effects provide information on transition state structure. However, the transition state structure for hydride transfer remains unknown due to the lack of the ability to distinguish between an early or late transition state. As to the decarboxylation step, it is likely that C₁-C₂ bond cleavage has a late transition state. The primary deuterium isotope effect on V/K_{6PG} is constant at pH values below the pK and decreases as the pH increases, suggesting that the pH sensitive step(s) is(are) not the same as the isotope sensitive step(s).

Furthermore, multiple solvent deuterium/substrate deuterium and multiple solvent deuterium/ ^{13}C isotope effects have been measured (Hwang and Cook, 1998). Data suggest proton transfer and hydride transfer occur in the same step. A significant medium effect has also been observed, suggesting a possible conformational change preceding all the chemical steps. Medium effects reflect the part of the solvent isotope effect that is not caused by isotope exchange between solute and solvent (Quinn and Sutton, 1991).

1.3.3 Structure of 6-Phosphogluconate Dehydrogenase.

The three-dimensional structures of 6-phosphogluconate dehydrogenase from sheep liver, *Trypanosoma brucei* and *Lactococcus lactis* have been solved by X-ray crystallography (Adams et al., 1994; Phillips et al., 1998; Tetaud et al., 1999). All 6PGDHs known from various sources are dimeric with the exception of the tetrameric enzyme from *Schizosaccharomyces pombe* (Tsai and Chen, 1998).

Sheep liver 6PGDH is a homodimer with a subunit molecular mass of 52,000. The crystal structures of the apo-enzyme as well as both enzyme-substrate binary complexes have been obtained by Adams and coworkers (1994). Figure 7 shows the structure of a monomer of the apo-enzyme. From the structure, each monomer consists of three domains. The first domain is a dinucleotide binding domain (amino acids 1-176). This amino terminal domain has a typical $\beta\alpha\beta$ fold which is often found in dinucleotide binding proteins. The $\beta\alpha\beta$ fold is followed by a short helix and another $\beta\alpha\beta$ unit anti-parallel to the first one. The second domain is a large helical domain (amino acids 177-434). The third domain is a carboxyl terminal tail (amino acids 435-482). The dimer has molecular two-fold symmetry, and the carboxyl terminal tail of each subunit burrows through the helical domain of the other subunit (Figure 8). Both the coenzyme domain and the helical domain of one subunit and the carboxyl terminal tail of the other subunit form the 6PG binding site.

1.3.4 Important Catalytic and Substrate Binding Residues.

Figure 7. Structure of a Monomer of 6-Phosphogluconate Dehydrogenase from Sheep Liver. Each monomer consists of three domains: a dinucleotide binding domain, a large helical domain, and a carboxyl terminal tail. The active site resides at the bottom of the cleft formed by the first two domains.

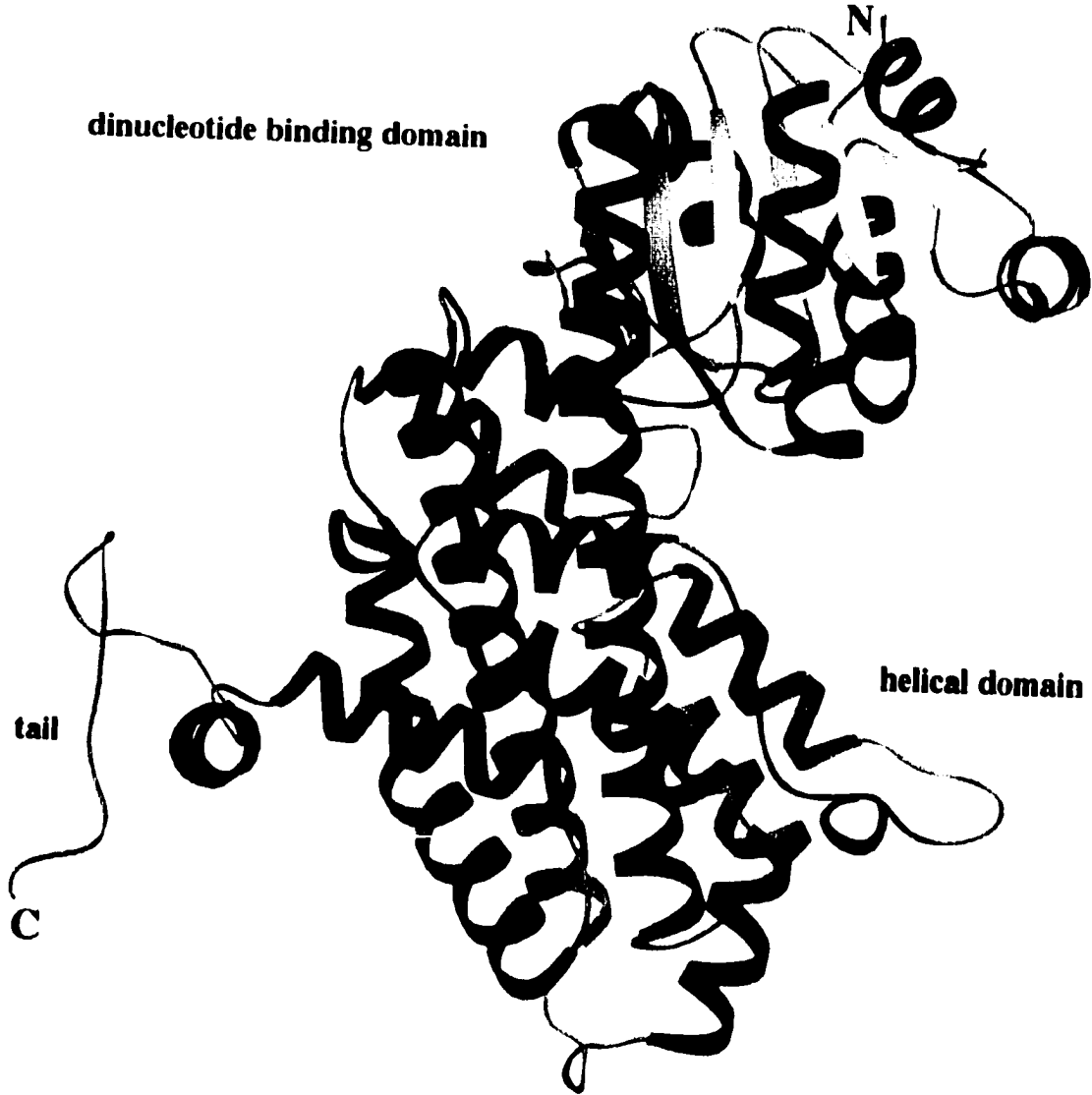
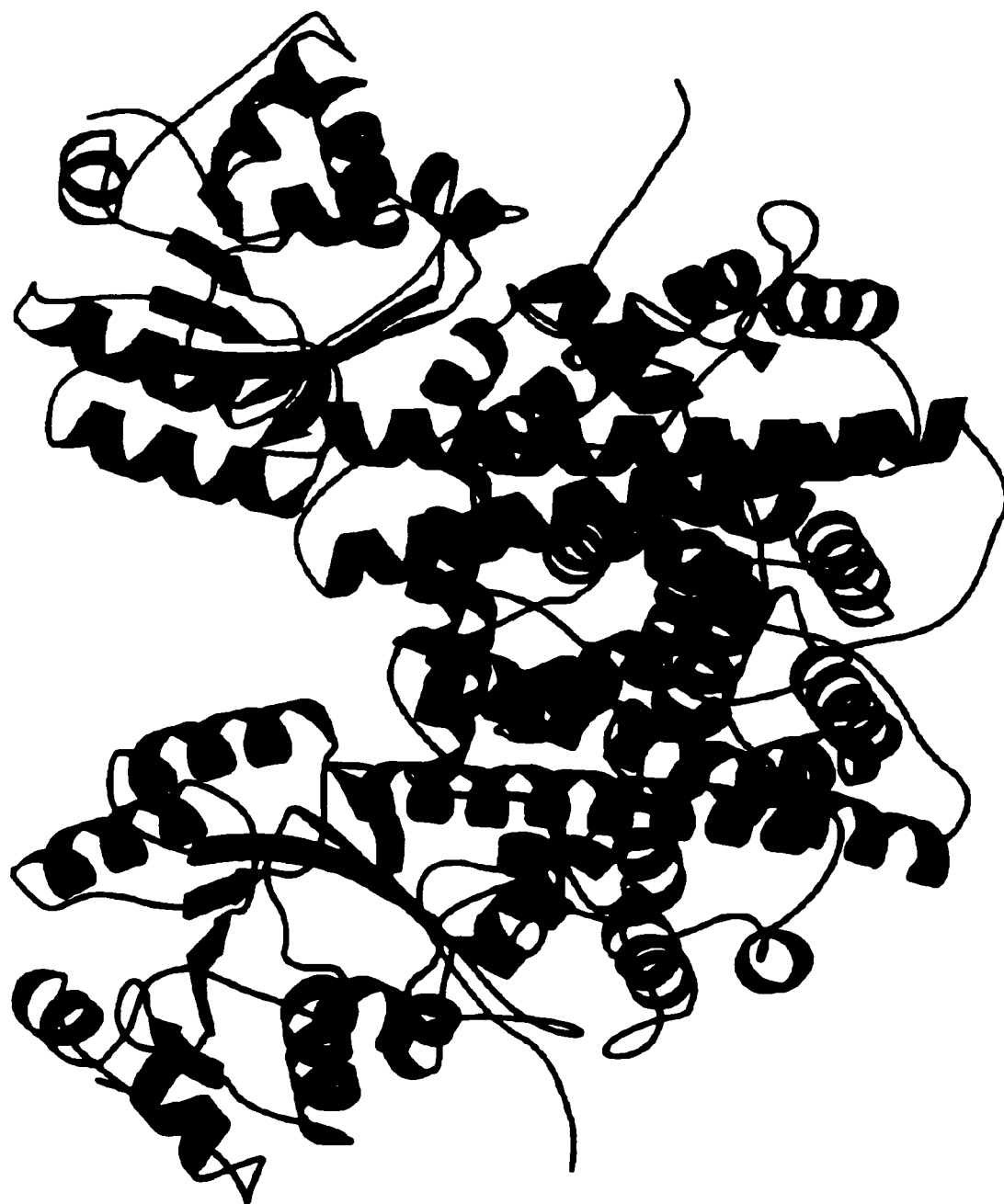
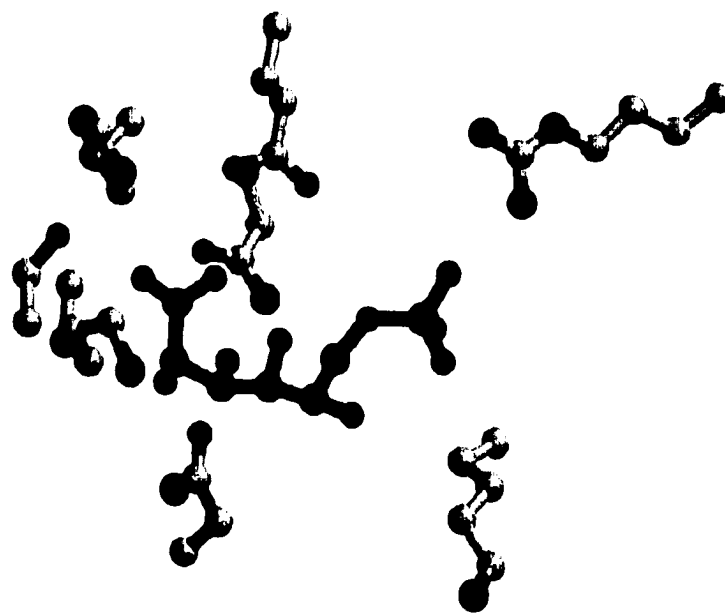
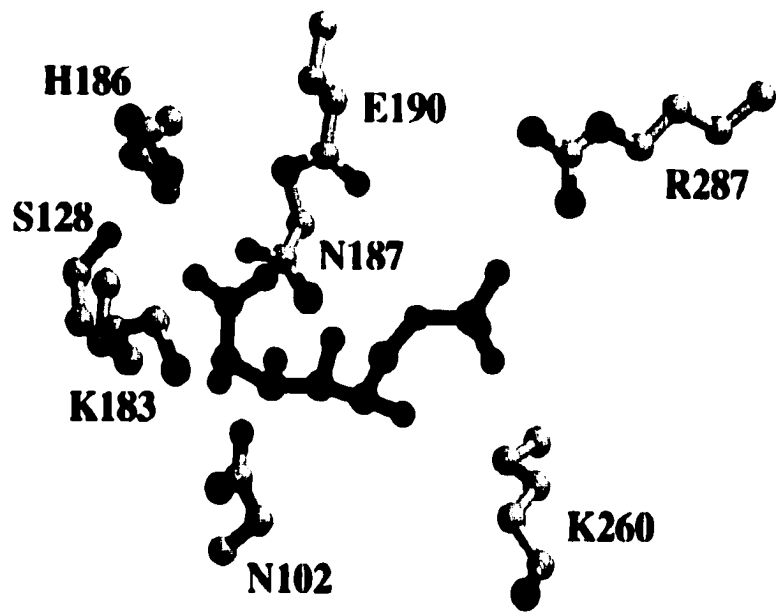


Figure 8. Structure of the Dimer of 6-Phosphogluconate Dehydrogenase from Sheep Liver. One subunit is in green, and the other subunit is in red. The tail domain of each subunit penetrates into the helical domain of the other subunit, and participates in the active site.



A general acid-general base mechanism has been proposed for sheep liver 6PGDH based on pH studies (Price and Cook, 1996). From the crystal structure of the E:6PG binary complex (Figure 9), two amino acid residues, Lys 183 and Asn 187, are within hydrogen-binding distance of the 3-hydroxyl group of 6PG. Since Asn 187 is not ionizable, it can only act to hydrogen bond the 3-hydroxyl group of 6PG, acting as a binding group. The N ϵ of Lys 183, on the other hand, is properly positioned to accept a proton from the 3-hydroxyl group of 6PG. As a result, Lys 183 appears to be the best candidate for the general base. From the pH profiles, the pK for the general base is around 8. Although this value is rather low for a lysine residue, it is possible if the lysine is placed in a positively charged or hydrophobic environment. As for the general acid involved in the last tautomerization step, the residue should be positioned near C-1 of the enediol intermediate. A water molecule hydrogen-bonded to Gly 130 has been suggested to participate in proton donation to C-1 of the enediol, which makes it a potential general acid candidate (Adams et al., 1994). However, Glu 190 turns out to be the most likely candidate for the proton donation. In the structure shown in Figure 9, Glu 190 is found hydrogen-bonded to the carboxyl group of 6PG and thus appears to be involved in substrate binding. The hydrogen bond must be eliminated after oxidation to facilitate the decarboxylation process. Although no direct evidence of a conformational change exists since no ternary complex structure is available, differences are observed in the structures of the E:NADP and E:NADPH complexes. A comparison reveals the reduced coenzyme as more extended than the oxidized form, likely due to the charge difference at the

Figure 9. Stereopair of the 6PG Binding Site of Sheep Liver 6-Phosphogluconate Dehydrogenase. 6-Phosphogluconate is shown with its carboxylate to the left and its 6-phosphate to the right. The atoms are labeled as, N, blue, O, red, and P, magenta. The carbon backbones of enzyme side chains are labeled in yellow, and the carbon backbone of 6PG is in green.



nicotinamide ring upon the reduction of NADP to NADPH. As a result, rearrangement of the nucleotide binding site may cause a conformational change in the substrate binding, which then positions C-2 of the keto intermediate closer to Glu 190. An additional contribution to this rearrangement may be provided by the change in the hybridization state of the C-3 group of 6PG upon oxidation. Again, based on the pH profile, the pK for Glu 190 has to be around 7 if it is the general acid. A hydrophobic environment should also help increasing the pK for the carboxyl group of Glu 190. In addition, sequence alignment of 6PGDH from different sources shows that both Lys 183 and Glu 190 are absolutely conserved among all the known sequences (Figure 10). This result further supports the hypothesis that these two residues are the general base and general acid, respectively. Site-directed mutagenesis of Glu 190 has been carried out recently, with data consistent with its catalytic role as the general acid (Karsten et al., 1998).

Besides Lys 183 and Glu 190, several other residues also contribute to binding 6PG, and may contribute to catalysis. The 6-phosphate group of 6PG makes hydrogen bonds to Tyr 191 and Arg 287 from the first subunit and to Arg 446 from the tail of the second subunit. Arg 447 of 6PGDH from *Lactococcus lactis* (same as Arg 446 for sheep liver enzyme) has been mutated to other amino acid residues (Tetaud et al., 1999). The loss of enzyme activity for all the mutants suggests that this residue plays a critical role in activity, presumably by anchoring the substrate. Other side chains are also important for 6PG binding. The carboxyl oxygens of 6PG

Figure 10. Alignment of 6PGDH Sequences in the Active Site Region. **S128, K183, H186, E190 and N187** are totally conserved and labeled in bold.

	120	180	190
Bakers yeast	ILFVGS	SG...HYV KM VHNGI	EYGDMLQICE
<i>Candida albicans</i>	ILFVGS	SG...HYV KM VHNGI	EYGDMLQICE
Fission yeast	ILFVGS	SG...HYV KM VHNGI	EYGDMLQICE
<i>Drosophila melanogaster</i>	LLFVGS	SG...HFV KM VHNGI	EYGDMLQICE
<i>Drosophila simulans</i>	LLYVGS	SG...HFV KM VHNGI	EYGDMLQICE
<i>Ceratitidis capitata</i>	ILYVGS	SG...HFV KM VHNGI	EYGDMLQICE
Human	ILFVGS	SG...HFV KM VHNGI	EYGDMLQICE
Sheep	ILFVGS	SG...HFV KM VHNGI	EYGDMLQICE
<i>Actinobacillus</i>	IRFIGT	GVSG...HFV KM VHNGI	EYGDMLQICE
<i>Haemophilus influenzae</i>	IRFIGS	GVSG...HFV KM VHNGI	EYGDMLQICE
<i>Treponema pallidum</i>	IHFIGT	GVSG...HYV KM IHNGI	EYGDMLQIAE
<i>Shigella boydii</i>	FNFIGT	GVSG...HYV KM VHNGI	EYGDMLQIAE
<i>Shigella dysenteriae</i>	FNFIGT	GVSG...HYV KM VHNGI	EYGDMLQIAE
<i>Shigella flexneri</i>	FNFIGT	GVSG...HYV KM VHNGI	EYGDMLQIAE
<i>Shigella sonnei</i>	FNFIGT	GVSG...HYV KM VHNGI	EYGDMLQIAE
<i>Salmonella typhimurium</i>	FNFIGT	GVSG...HYV KM VHNGI	EYGDMLQIAE
<i>Citrobacter diversus</i>	FNFIGT	GVSG...HYV KM VHNGI	EYGDMLQIAE
<i>Citrobacter freundii</i>	FNFIGT	GVSG...HYV KM VHNGI	EYGDMLQIAE
<i>Escherichia vulneris</i>	FNFIGT	GVSG...HYV KM VHNGI	EYGDMLQIAE
<i>Escherichia coli</i>	FNFIGT	GVSG...HYV KM VHNGI	EYGDMLQIAE
<i>Klebsiella pneumoniae</i>	FNFIGT	GVSG...HYV KM VHNGI	EYGDMLQIAE
<i>Klebsiella planticola</i>	FNFIGT	GVSG...HYV KM VHNGI	EYGDMLQIAE
<i>Klebsiella terrigena</i>	FNFIGT	GVSG...HYV KM VHNGI	EYGDMLQIAE
<i>Citrobacter amalonaticus</i>	FNFIGT	GVSG...HYV KM VHNGI	EYGDMLQIAE
<i>Bacillus subtilis</i>	IHFIGT	GVSG...HYV KM VHNGI	EYGDMLQISE
<i>Synechococcus</i> sp	LGFMGM	GVSG...HYV KM VHNGI	EYGDMLQIAE
<i>Synechocystis</i> sp	LGFVGM	GVSG...HYV KM VHNGI	EYGDMLQIAE
<i>Bacillus licheniformis</i>	IGYLGIGI	SG...HFV KM VHNGI	EYADMQLIAE
<i>Trypanosoma brucei</i>	LRFLGMGI	SG...SCV KM YHNSG	EYAILQIWGE
Primary consensus	FNFIGT	GVSG...HYV KM VHNGI	EYGDMLQIAE

form hydrogen bonds to Ser 128 and Glu 190, and the 3-OH forms hydrogen bonds to Lys 183 and Asn 187.

Sheep liver 6PGDH shows a high specificity towards the coenzyme required for the catalysis. NAD has been found to be a poor dinucleotide substrate for this enzyme. Studies with other alternative dinucleotide substrates suggest that the 2'-phosphate plays a very important role in dinucleotide binding (Berdis and Cook, 1993c). Selectivity towards NADP over NAD is provided by the tight binding between the 2'-phosphate and three active site residues: Asn 32, Arg 33 and Thr 34. Among them, Arg 33 is suggested to be important in providing one face of the adenine binding pocket and neutralizing the charge of the 2'-phosphate. Consistent with this theory, Arg 34 of the *L. lactis* enzyme (same as Arg 33 for the sheep liver enzyme) was mutated to tyrosine, and the affinity for NADP decreases nearly three orders of magnitude (Tetaud et al., 1999). As to the nicotinamide binding site, the difference between the conformations of the oxidized and reduced coenzyme binary complexes is quite obvious. In the reduced coenzyme binary complex, the amide of the nicotinamide ring is hydrogen-bonded to Ser 128, His 186, and Asn 187. All three of these residues are absolutely conserved among all known sequences (Figure 10). As indicated above, Ser 128 is also hydrogen-bonded to the carboxyl group of 6PG and Asn 187 interacts with the 3-hydroxyl group. Therefore, binding of reduced coenzyme may in a way facilitate the decarboxylation process. Consistent with the above postulate, it has been reported that decarboxylation of 3-keto-2-deoxy-6PG is

enhanced upon binding of the reduced (but not oxidized) coenzyme (Hanau et al., 1992).

1.3.5 Cloning and Sequencing of the Sheep Liver 6-Phosphogluconate Dehydrogenase cDNA.

Previously, several attempts were made to isolate a cDNA clone of the sheep liver 6PGDH. As a result of a failure to isolate cDNA clones, the cDNA sequence was obtained through PCR amplification to generate a family of overlapping cDNA clones encoding a mature protein of 482 amino acids (Somers et al., 1992).

In the later work of Chooback and coworkers (1998), a cDNA of the sheep liver enzyme was obtained by RT-PCR, and then cloned into a pBluescript phagemid. The cDNA was then subcloned into the expression vector pKK223-3. When the recombinant protein was expressed in *E. coli*, the host 6PGDH was also expressed, and the two 6PGDHs could not be separated from one another during purification. The amount of contamination was insignificant when the wild type enzyme was expressed. However, for many of the mutant enzymes, since enzyme activity decreases dramatically, the contaminating *E. coli* 6PGDH exhibited higher activity than the mutant enzymes. Therefore, another expression system was needed for site-directed mutagenesis studies.

Attempts were made to purify the enzyme using the Glutathione S-transferase (GST) Gene Fusion System from Pharmacia Biotech. The cDNA was subcloned into the pGEX-4T-1 vector to produce a GST fusion protein. The fusion protein was

directly purified from bacterial lysates using the affinity matrix Glutathione Sepharose 4B. Cleavage of the enzyme from GST was performed using a site-specific thrombin protease whose recognition sequence is located immediately upstream from the multiple cloning site on the pGEX-4T-1 plasmid. However, the attempts to cleave the recombinant enzyme were unsuccessful even at different concentrations of thrombin protease and urea (Chooback et al., 1998). It is possible that the 77 kDa fusion protein is folded in such a way that the thrombin protease site is inaccessible. Interestingly, the fusion enzyme still remains active and gives kinetic parameters that are within error identical to those of the native enzyme. This result suggests that the N-terminus is away from the active site. In fact, this has also been confirmed by the three-dimensional structure of the apoenzyme (Figure 7). Nevertheless, the GST fusion system proved unsuitable for the expression and purification of 6PGDH. Finally, the sheep liver 6PGDH cDNA was cloned into the expression vector pQE30, which adds a 6-histidine tag to the N-terminus of the target protein. The His-tagged recombinant wild type enzyme was expressed, purified, and characterized. As a result, a protein with a subunit molecular weight of approximately 51,000 was obtained as judged by SDS/PAGE. The recombinant enzyme exhibits kinetic parameters within error identical to those measured for the native sheep liver enzyme (Chooback., et al., 1998).

1.3.6 Altered Site II *in vitro* Mutagenesis System.

The Altered site II *in vitro* mutagenesis system from Promega (1995) uses antibiotic selection as a means to obtain a high percentage of mutants. The pALTER-1 vector contains genes for both ampicillin and tetracycline resistance. However, the plasmid is ampicillin sensitive because a frameshift was introduced into this resistance gene by removing the *Pst* I site. During the mutagenesis reaction, an ampicillin repair oligonucleotide is annealed to the single-stranded DNA template at the same time as the mutagenic oligonucleotide. This repair oligonucleotide can restore ampicillin resistance to the mutant strand. The appropriate oligonucleotides can be used simultaneously to inactivate one resistance gene while repairing the other. In this way, multiple rounds of mutagenesis can be carried out on a single construct without subsequent subcloning from the parental mutagenesis vector.

This antibiotic selection method increases the yield of mutants. If no selection method is used, the theoretical yield of mutants is 50% (due to the semi-conservative mode of DNA replication). However, the yield is usually much lower in practice, maybe only a few percent or less. This low yield is caused by several factors such as incomplete *in vitro* polymerization, primer displacement by the DNA polymerase, and *in vivo* host-directed mismatch repair mechanisms which favor repair of the unmethylated newly synthesized DNA strand (Kramer et al., 1984). The use of antibiotic selection for the mutant strand yields a much higher percentage of mutants. The high frequency enables identification of mutants by restriction analysis and direct sequencing of clones, eliminating the need to screen a large number of colonies by hybridization.

The pALTER-1 vector is a phagemid which contains the f1 origin of replication. Under normal circumstances, it replicates as a plasmid. When the host cells are infected with the helper phage R408 or M13KO7, single-stranded DNA will be produced (Dotto et al., 1981; Dotto and Zinder, 1983; Dotto et al., 1984). In this way, a stable single-stranded DNA template is easily obtained.

The stability of the complex between the oligonucleotide and the template is determined by the base composition of the oligonucleotide and the conditions under which it is annealed. In general, for single base mutations, 8-10 perfectly matched nucleotides on either side of the mismatch are required. For mutations involving two or more mismatches, 12-15 perfectly matched nucleotides are needed on either side of the mismatch. For insertions and deletions, longer oligonucleotides are required. The annealing conditions may vary with the base composition of the oligonucleotide. AT-rich complexes may require a lower annealing temperature due to their lower stability compared to GC-rich complexes.

The ES1301 *mutS* strain is a repair minus *E. coli* strain, which suppresses *in vivo* mismatch repair (Zell and Fritz, 1987). It is used for the initial round of transformation to decrease the chance that the antibiotic repair mismatch or the mutagenic mismatch are repaired. A subsequent transformation into a more stable JM109 strain is needed to ensure proper segregation of mutant and wild type plasmids and result in a high proportion of mutants.

1.3.7 QIAexpress Protein Expression and Purification System.

The QIAexpress protein expression and purification system from Qiagen (1996) has been used for the purification of the native and mutant 6PGDH. The system is based on the remarkable selectivity of the Ni-NTA resin for proteins with an affinity tag consisting of six consecutive histidine residues (6xHis tag).

The pQE expression vector adds a 6xHis affinity tag to the target protein and also provides a high-level of expression in *E. coli*. The pQE plasmids contain an optimized, regulatable promoter/operator element, consisting of the *E. coli* phage T5 promoter and two *lac* operator sequences. Expression from this promoter/operator is extremely efficient, and can only be prevented by the presence of high levels of *lac* repressor. M15[pREP4] (Villarejo and Zabin, 1974), the host strain used in this system contains multiple copies of the plasmid pREP4, which carries the *lacI* gene encoding the *lac* repressor (Farabaugh, 1978). The high levels of *lac* repressor present in the cells provide a tight regulation of protein expression. Expression of the recombinant protein from pQE vectors is achieved by addition of IPTG. The combination of the strong promoter and the high levels of *lac* repressor permit control over the level of expression. The tightly regulated expression is critical in cases where the expressed protein is toxic to the cell.

The QIAexpress purification system uses a metal chelate adsorbent Ni-NTA (nitrilo-tri-acetic acid) resin which has an extremely high affinity for proteins and peptides that contain six consecutive histidine residues (Hochuli et al., 1987). The NTA ligand occupies four of the six ligand binding sites of the Ni²⁺ ion, leaving the other two sites open to interact with the 6xHis tag (Figure 11). The affinity between

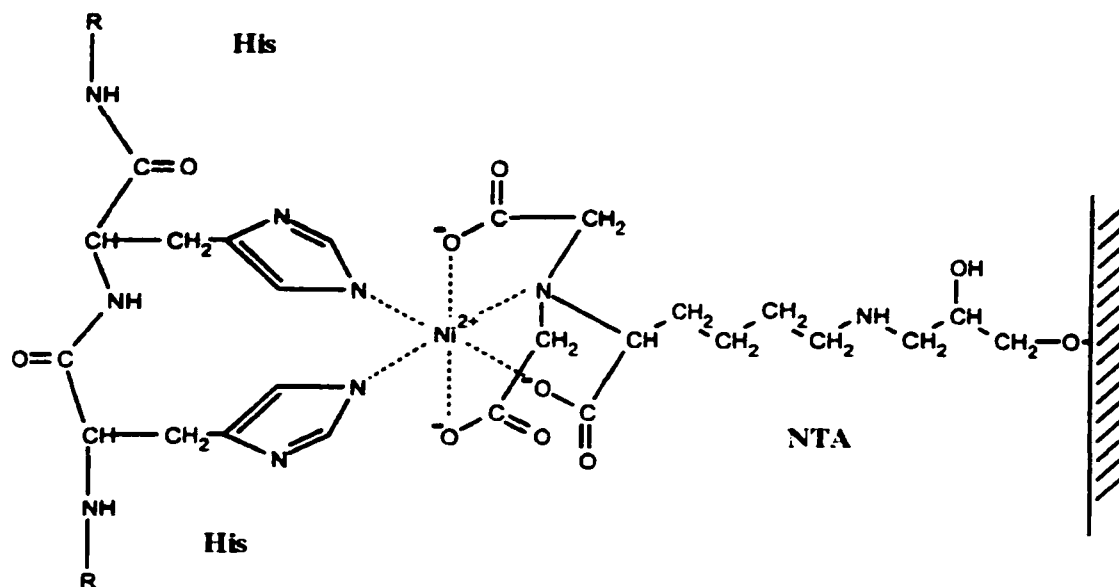


Figure 11. Binding Interaction between 6xHis Tag and Ni-NTA Resin. Nitrilo-tri-acetic acid occupies four ligand binding sites of the Ni^{2+} ion, while 6xHis tag takes the rest two sites.

the 6xHis tag and Ni-NTA resin is far greater than the affinity between most antibodies and antigens, or enzymes and substrates. Unlike other purification systems which rely on antigen/antibody or enzyme/substrate interactions, the Ni-NTA system can be used for almost any protein purification because the binding of the tagged proteins does not require any functional protein structure. The high affinity interaction allows proteins in very dilute solutions to be efficiently bound to the resin. The binding capacity of the Ni-NTA resin is approximately 5-10 mg of 6xHis tagged protein per ml of resin.

The 6xHis affinity tag consists of six consecutive histidine residues which allows the minimal addition of extra amino acids to the recombinant protein. The tag is non-immunogenic and uncharged at physiological pH. Generally, the affinity tag does not affect the secretion, compartmentalization, or folding of the protein to which it is attached. Therefore, the 6xHis tag rarely needs to be removed from the recombinant protein after purification. If the affinity tag must be removed afterwards, a protease cleavage site can be inserted between the 6xHis sequence and the N(C)-terminus of the protein.

The 6xHis affinity tag may be placed at either N- or C-terminus of the recombinant protein. If the protein is to be purified under native conditions, the tag should be placed at the end of the protein that is most likely to be exposed. In the case of 6PGDH, the tag is attached to the N-terminus which is away from the active site.

1.4 Specific Goals of This Study.

Important questions still remain regarding the mechanism of the 6PGDH catalyzed reactions. Site-directed mutagenesis studies have been performed for a few active site amino acids (Glu 190, Arg 446 and Arg 33). However, the functions of most of the important residues still remain unclear. The purpose of the research presented in this dissertation is to identify the functional groups required for catalysis and substrate binding, and to quantitate their contributions.

As discussed above, the best candidate for the general base in the 6PGDH reaction is Lys 183. In the research presented here, Lys 183 was mutated to Glu (could still act as a general base but with a lower pK), Arg (could still act as a general base but with a higher pK), His (still capable of acting as a general base but with a lower pK and a bulky side chain), Gln (loss of general base activity but could still form a hydrogen bond), Met (a side chain about the same size as that of Lys, but no general base or hydrogen-bonding ability), Cys (have a shorter side chain but still capable of forming the hydrogen bond), and Ala (eliminates all functional groups). The mutant proteins were then expressed and purified for further characterization. Kinetic studies of these mutants included initial velocity studies, studies of the pH dependence of the kinetic parameters, and primary deuterium isotope effect studies. Initial velocity studies should provide information on any changes in catalytic and binding abilities upon mutagenesis. Since Lys 183 is expected to serve as a general base, pH studies should give direct indications of the possible role played by this residue. Isotope effects are a very useful method in studying reaction mechanisms, including determination of rate-limiting steps. Finally, circular dichroism spectra

were used to detect any gross conformational changes upon mutagenesis. Although studies of the K183 mutant enzymes are included in this dissertation, they have been published in *Biochemistry* (Zhang et al., 1999).

In addition, three other residues located in the active site were mutated to study their individual contribution to catalysis and substrate binding. Thus, Ser 128, His 186, and Asn 187 were changed to Ala to eliminate all functional groups. The mutant enzymes were prepared and characterized in a manner similar to that discussed above. In all, the above studies should provide identification of the catalytic and binding groups involved in the 6PGDH reaction.

CHAPTER 2

EXPERIMENTAL METHODS

2.1 Materials

2.1.1 Chemicals and Reagents.

Mutagenesis and sequencing primers were either from Biosynthesis or Gibco-BRL. The Altered Sites II *in vitro* Mutagenesis System and the fmol^R DNA Cycle Sequencing System were purchased from Promega. The PERFECTprepTM Plasmid DNA Kit was from 5 prime to 3 prime, Inc. The GeneClean^R II Kit was from Bio 101, Inc. The DNA molecular weight ladder was from New England Biolabs. Restriction endonucleases, Taq DNA polymerase, T₄ DNA ligase and IPTG were purchased from Gibco-BRL. Pfu polymerase was from Stratagene, and deoxynucleoside triphosphates were from Perkin Elmer. T₄ Kinase, protein molecular mass markers, and *Escherichia coli* strain JM 109 were from Promega. The QIAexpress type IV kit was purchased from QIAGEN. The Bio-Rad protein assay kit was used to determine protein concentrations according to Bradford (1976) with bovine serum albumin as a standard. Ampicillin, kanamycin, and 6-phosphogluconic acid trisodium salt were from Sigma. NADPH and NADP was from US Biochemicals. Hepes, Bis-Tris, and Ches buffers were from Research Organics Inc. All other chemicals were the highest quality commercially available.

2.1.2 Bacterial Strains and Plasmids.

The *E. coli* strain JM 109 was used as the host strain for plasmids containing the 6PGDH cDNA with amino acid changes at lysine 183, serine 128, histidine 186, and asparagine 187, while M15[pREP4] was the host strain for expression of the mutant proteins. The plasmid pAlter-1 was used as the mutagenesis vector and plasmid pQE-30 was the expression vector.

2.2 Site-Directed Mutagenesis.

2.2.1 Subcloning of 6-PGDH into the pAlter-1 Vector.

Cloning of the wild type 6PGDH cDNA into the mutagenesis vector pAlter-1 was performed by Karsten et al. (1998). The resulting construct, pPGDH.LC5 (Figure 12), was used as the template for the site-directed mutagenesis.

2.2.2 Preparation of Single-Stranded DNA.

An overnight culture of JM109 cells containing pPGDH.LC5 was prepared by inoculating 1-2 mL of LB broth containing 10 µg/mL tetracycline and shaking at 37 °C. 0.5 mL of the overnight culture was used to inoculate 25 mL of LB broth. After 30 minutes of shaking, the culture was infected with 200 µL of the helper phage R408 and shaken for another 6 hours with vigorous agitation. The culture supernatant was then collected by centrifuging at 12,000 x g for 15 minutes. Another 15 minutes of centrifugation of the supernatant was needed to reduce the level of contaminating

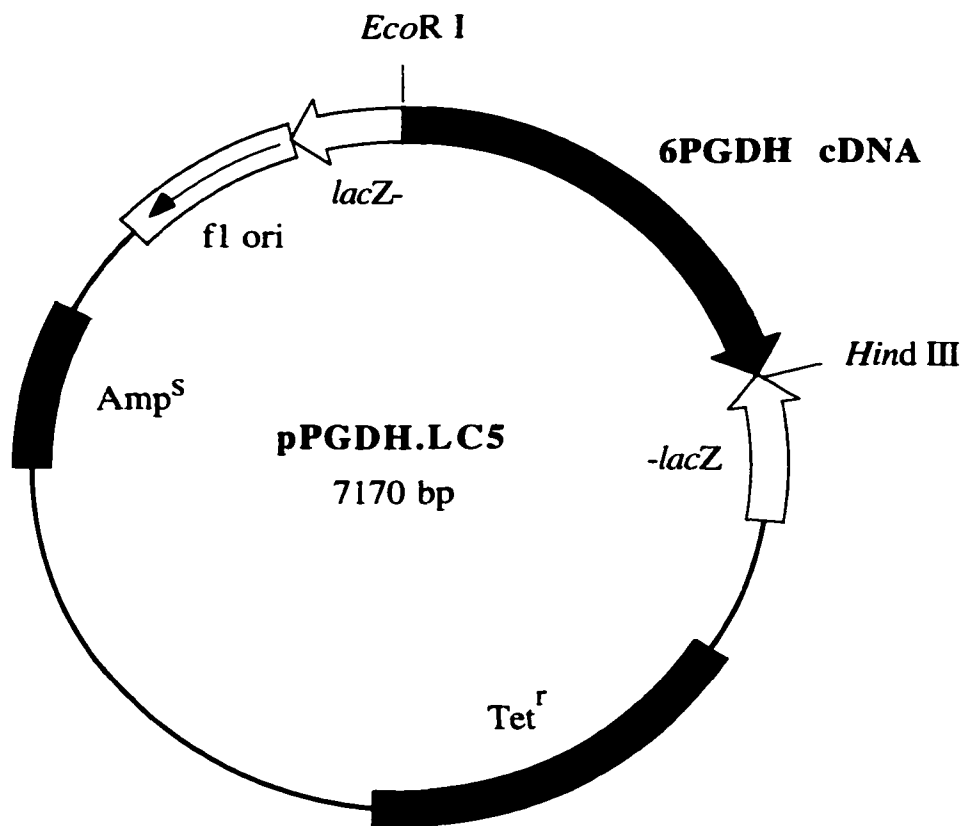


Figure 12. Map of pPGDH.LC5. This plasmid contains a 1.5 kb 6PGDH cDNA insert between the *EcoR* I – *Hind* III sites of pAlter-1 vector.

cellular nucleic acid. Next, the phage was precipitated by adding 0.25 volumes of phage precipitation solution (3.75 M ammonium acetate, pH 7.5 and 20% PEG-8,000) to the supernatant. The overnight precipitation was followed by centrifuging the solution at 12,000 x g for 15 minutes. The pellet was collected and resuspended in TE buffer, followed by several phenol:chloroform extractions. Finally, the ssDNA was purified by ethanol precipitation and resuspension in water. The amount and purity of the final product was estimated by agarose gel electrophoresis.

2.2.3 Site-Directed Mutagenesis.

Site-directed mutagenesis was performed using the Altered Site II *in vitro* mutagenesis system from Promega. The schematic diagram of the mutagenesis procedure was shown in Figure 13 and the synthetic mutagenic oligonucleotides listed in Table 1. Each mutagenesis reaction was prepared by annealing 1.25 pmoles of phosphorylated mutagenic oligonucleotide and 0.25 pmoles of ampicillin repair oligonucleotide to 0.05 pmoles of single-stranded DNA template. The annealing reaction was heated to 75 °C for 5 minutes and cooled slowly to room temperature to minimize nonspecific annealing of the oligonucleotides. The mutant strand was then synthesized by T4 DNA polymerase, with the nick ligated by T4 DNA ligase.

Each mutagenesis reaction was transformed into ES1301 *mutS* electrocompetent cells by using an EC100 electroporator at 1.8 kV. The transformation reaction was added to 4.5 ml LB broth containing 125 µg/mL ampicillin and incubated overnight at 37 °C with shaking. This culture was used for

Figure 13. Schematic Diagram of the Altered Sites II *in vitro* Mutagenesis Procedure from Promega. This system uses antibiotic selection as a means to obtain a high percentage of mutants.

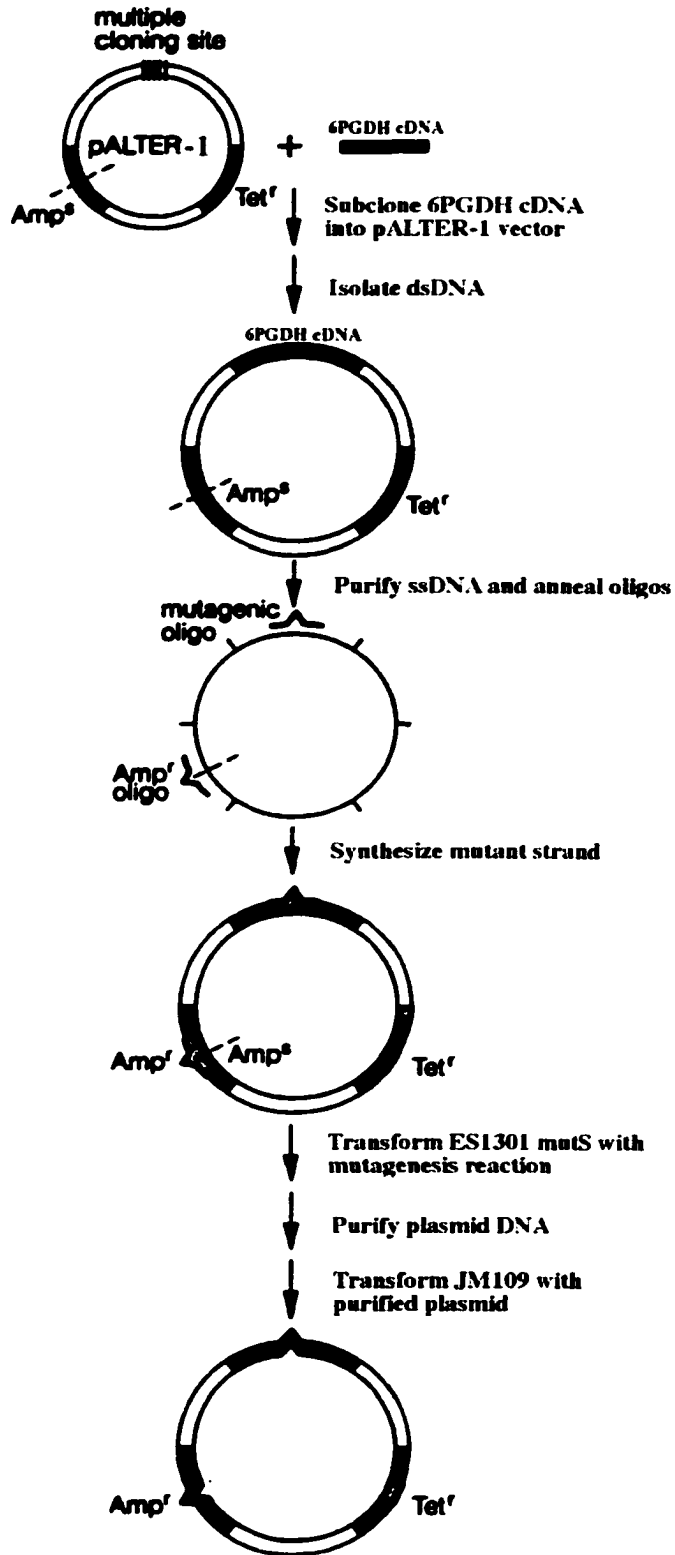


Table.1 Sequence of Mutagenic Oligonucleotides.	
WT	ACACTTTGTGAAGATGGTGCACA
K183A	ACACTTTGTGGCGATGGTGCACA
K183E	ACACTTTGTGGAGATGGTGCACA
K183H	ACACTTTGTGCATATGGTGCACA
K183C	ACACTTTGTGTGTATGGTGCACA
K183R	ACACTTTGTGCCGATGGTGCACA
K183M	ACACTTTGTGATGATGGTGCACA
K183Q	ACACTTTGTGCAGATGGTGCACA
S128A	GGGAGCGGAGTTGCTGGTGGAGAGGA
H186A	GTGAAGATGGTGGCCAACGGCATAGAG
N187A	AAGATGGTGCACGCCGGCATAGAGTAC

The mutation site is underlined.

the plasmid miniprep using PERFECTprep™ Plasmid DNA Kit according to the manufacturer's procedure. The resulting plasmid was further transformed into the host strain JM 109 and plated on LB/Amp plates. Two to four colonies were picked randomly from the plates and their plasmids were purified. The plasmids were digested with restriction endonucleases *EcoR* I and *Hind* III and the mixture checked by agarose gel electrophoresis. Those with the correct insert size were sequenced through the mutation site using the fmol^R DNA Cycle Sequencing System, with sequencing primers located 150-200 base pairs upstream from the mutation sites. Strains containing plasmids with the correct mutations were stored in LB/Amp containing 15% glycerol at -70 °C. The mutated plasmids were designated as K183A.pAlter, K183E.pAlter, K183H.pAlter, K183R.pAlter, K183C.pAlter, K183M.pAlter, K183Q.pAlter, S128A.pAlter, H186A.pAlter, and N187A.pAlter.

2.2.4 Subcloning of the Mutants into the pQE-30 Expression Vector.

Two synthesized oligonucleotides containing the desired restriction sites were constructed. One primer, 5' ACTATAGGGCGCGCATGCATGGCCCAAG 3', creates a *Sph* I restriction site at the start of the gene and the other one 5' TGTAGAGTTGAAAGCTTGGAACAGAAG 3' contains a *Hind* III site at the end of the gene. The two sites were introduced into the gene containing the desired mutation using the polymerase chain reaction. *Taq* DNA polymerase was used in the PCR reactions in the presence of dNTPs. The thermocycling conditions were set to cycle for 30 seconds melting at 95 °C, 30 seconds annealing at 42 °C, and 1 minute

extension at 70 °C, and this was repeated for 38 cycles. The size of the PCR product was confirmed by agarose gel electrophoresis.

The PCR product was purified with the GeneClean^R II Kit according to the manufacturer's procedure, followed by digestion with *Sph* I and *Hind* III. An expression vector, pQE30, was also digested with the same restriction endonucleases. Both digested PCR product and vector were purified using the GeneClean^R II Kit and ligated together by T4 DNA ligase. The ligation reaction was incubated overnight at 15 °C, with the result checked by agarose gel electrophoresis. Next, the ligation mix was added into 125 µl M15[pREP4] competent cells with the mixture incubated on ice for 20 minutes. This was followed by heat-shock at 42 °C for 90 seconds, and the transformation reaction was mixed with 500 µl Psi-broth (LB medium, 4 mM MgSO₄, 10 mM KCl). After being shaken at 37 °C for 90 minutes, the transformation mix was plated on LB-agar plates containing 25 µg/mL kanamycin and 100 µg/mL ampicillin and incubated at 37 °C overnight. Four colonies were picked from the plates with their plasmids purified from the overnight culture. The plasmids were digested with *Hind* III only and checked by agarose gel electrophoresis. The entire gene containing the mutation was sequenced to insure the integrity of the cDNA. The resulting plasmids were designated as K183A.pQE30, K183E.pQE30, K183H.pQE30, K183R.pQE30, K183C.pQE30, K183M.pQE30, K183Q.pQE30, S128A.pQE30, H186A.pQE30, and N187A.pQE30. The schematic representation of the subcloning process is shown in Figure 14, with the resulting pQE30 constructs shown in Figure 15.

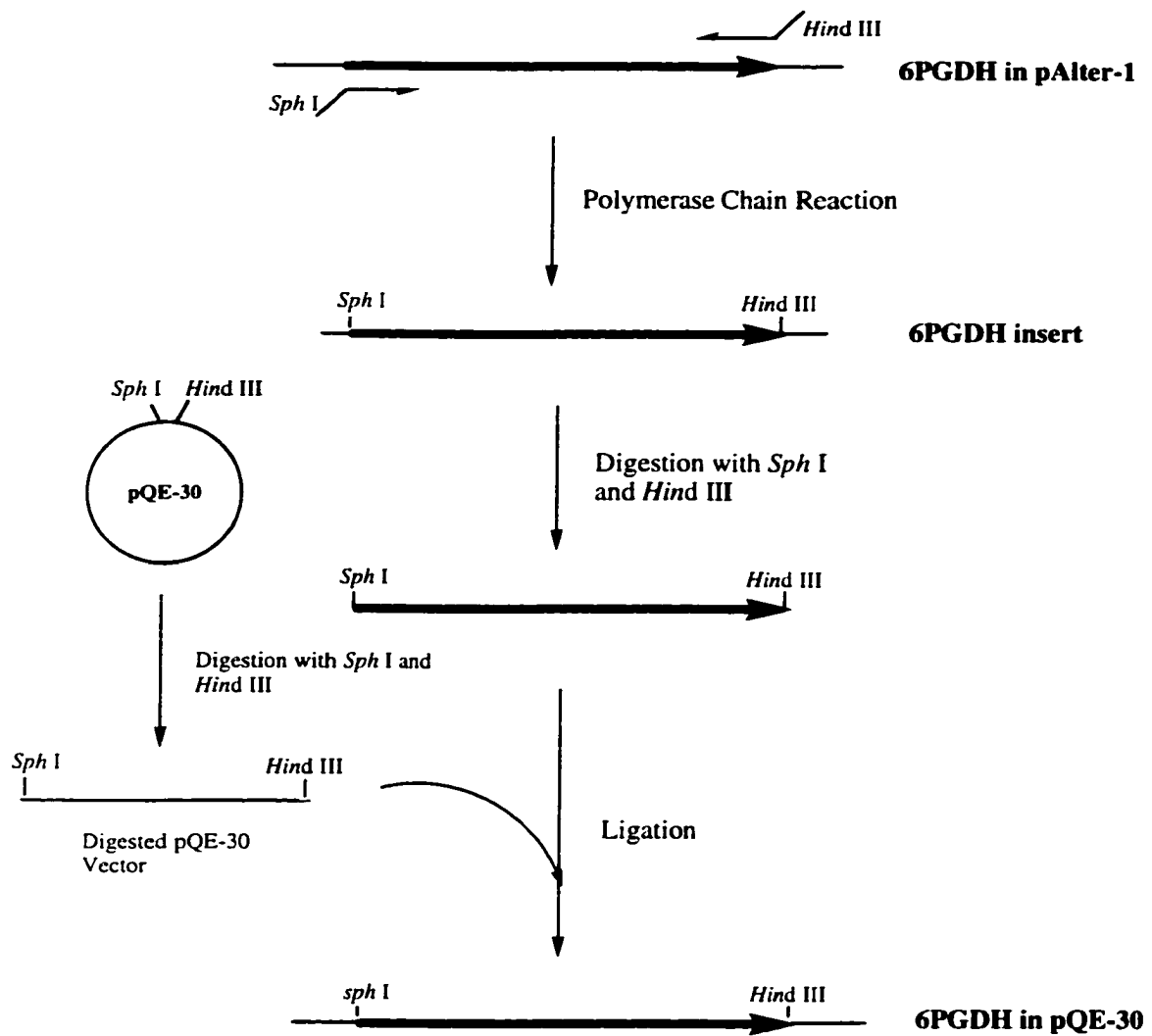
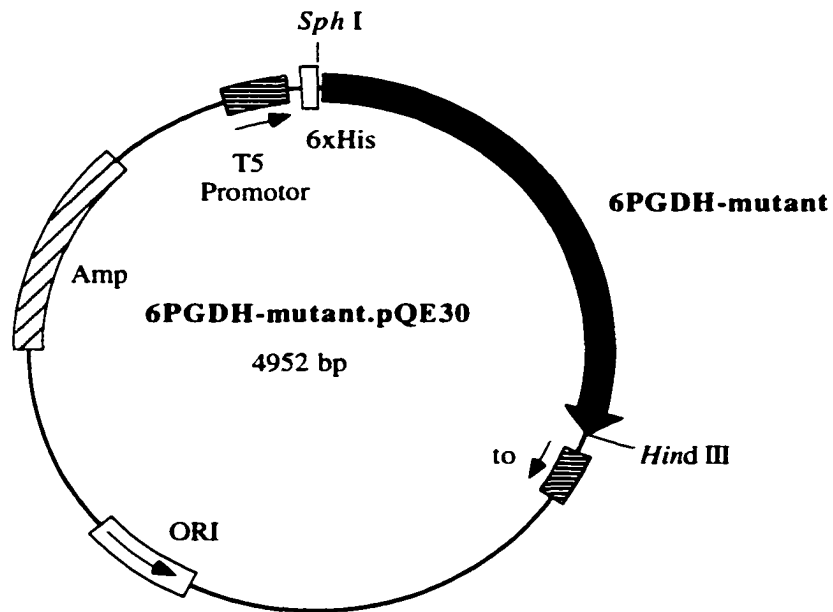


Figure 14. Schematic Representation of Subcloning of Mutated 6PGDH cDNA into pQE-30 Expression Vector.



6PGDH-mutant = K183A, K183E, K183H, K183R, K183C, K183M, K183Q, S128A, H186A, and N187A.

Figure 15. Map of Mutated 6PGDH Gene in pQE-30 Vector. This vector adds a 6xHis tag to the N-terminus of the enzyme.

2.3 Expression and Purification of the Mutant Proteins.

The pQE-30 vector adds a 6xHis tag to the N-terminus of the 6PGDH, which has a specific affinity to the Ni-NTA resin. The expression and purification were performed using the QIAexpress kit. The bacterial strains containing the correct mutated plasmid were grown at 30 °C in 10-20 liters of LB/Amp/Kan medium, and then induced with IPTG to a final concentration of 0.5 mM when the A_{600} reached 0.7-0.9. After another 4.5 hours growth, the cells were harvested by centrifugation at 9,000 x g for 20 minutes. The cell paste was resuspended in 3 x volume sonication buffer (50 mM Na-phosphate, pH 8.0, 300 mM NaCl and 10 mM β -mercaptoethanol), sonicated for 2 minutes on ice, and centrifuged at 22,000 x g for 40 minutes to pellet cell debris. The sonication supernatant was then added to Ni-NTA resin pre-equilibrated with sonication buffer, and stirred on ice for 1-2 hours. The mixture was washed with sonication buffer followed by wash buffer (sonication buffer containing 0.8-40mM imidazole), and finally eluted with an imidazole gradient (0-0.4 M). Protein concentrations were measured for all fractions using the Bradford method with bovine serum albumin as a standard, and fractions corresponding to the peak were collected. The mutant enzymes were then precipitated on ice by 75% ammonium sulfate and stored at 4°C. Before each use, the precipitated enzymes were collected by centrifugation at 18,000 x g for 20 minutes, with the pellets resuspended in protein dilution solution (20 mM Hepes, pH 7.5, 20% glycerol, and 10 mM β -mercaptoethanol). All mutant enzymes were analyzed via SDS-PAGE.

2.4 Characterization of the Mutant Proteins

2.4.1 Circular Dichroism Spectroscopy.

Circular dichroism spectra were recorded on an Aviv 62 DS spectropolarimeter, with the enzymes placed in 0.2-cm quartz cuvettes. Far UV-CD (200-260 nm) spectra at intervals of 1 nm and a dwell time of 3 s were recorded for the wild type 6PGDH and each of the mutants pre-dialyzed in 10 mM K-phosphate buffer, pH 7.0. The same buffer was used as the blank for each spectrum before adding the enzyme, and each spectrum was the average of 3 repeats. Ellipticity values recorded by the instrument in millidegrees (obs) were converted to molar ellipticity values according to the following equation.

$$[\theta] = [\theta]_{\text{obs}}/[10\{\text{MRC}\}l]$$

where $[\theta]$ is molar ellipticity in (degrees)cm²/dmol, $[\theta]_{\text{obs}}$ is ellipticity recorded by the instrument in millidegrees, MRC is the mean residue concentration of the enzyme and is equal to the number of amino acid residues times molar concentration of the protein, and l is the pathlength in centimeters (Rao et al., 1991). The spectra obtained for the mutant proteins were compared to those of the wild type enzyme to detect any gross conformational changes upon mutagenesis.

2.4.2 Initial Velocity Studies.

Initial velocity studies were performed using a HP 8453 diode array spectrophotometer, monitoring the appearance of NADPH ($\epsilon_{340} = 6,220 \text{ M}^{-1} \text{ cm}^{-1}$) at 340 nm. Reactions were carried out in 1 ml volumes using 1 cm pathlength cuvettes. An initial velocity pattern was obtained at 100 mM Hepes, pH 7.3, using variable concentrations of 6PG (50-500 μM) and NADP (25-250 μM).

2.4.3 Product Inhibition Studies.

Product inhibition studies were carried out for mutants S128A, H186A and N187A, using NADPH as a competitive inhibitor. Product inhibition patterns were obtained by varying NADP concentration at a fixed level of 6PG (saturating, or near K_m) and different fixed levels of NADPH. Dixon plots were also obtained by varying NADPH concentration at a fixed level of 6PG and NADP.

2.4.4 pH Studies.

Initial velocity patterns for K183R were measured at pH 5.5 and 10.5 to obtain estimates of the kinetic parameters at the extremes of pH. The pH dependence of V and V/K_{6PG} for the K183R mutant were carried out by measuring the initial velocity at concentrations of 6PG around its K_m and a saturating (1 mM) concentration of NADP⁺, as a function of pH over the range 6 to 9.5. The pH was maintained using the following buffers at 100 mM concentrations: BTP, 5.5-6.5; Hepes, 6.5-8.5; Ches, 8.5-9.5. Sufficient overlap was obtained as buffers were

changed to rule out any nonspecific effects. The pH value was recorded before and after the initial velocity was measured.

2.4.5 Primary Deuterium Isotope Effects.

The *3-deuterio-6-phosphogluconate* was synthesized and purified by Chi-Ching Hwang from the same lab (Hwang et al., 1998). The concentrations of *3-h-6PG* and *3-d-6PG* were determined enzymatically in triplicate by endpoint analysis using 6PGDH. Primary deuterium isotope effects with *3-d-6PG* were obtained for K183R, S128A, H186A, and N187A by direct comparison of initial velocities (Parkin, 1991). V and V/K_{6PG} were measured by varying *3-h-6PG* and *3-d-6PG* at saturating levels of NADP, and $^D V$ and $^D(V/K_{6PG})$ estimated as ratios of intercepts and slopes, respectively.

Isotope effects are defined as the ratio of the rates with light and heavy atom substitutions. For example, deuterium kinetic isotope effects are defined as k_H/k_D , while C-13 isotope effects are k_{C-12}/k_{C-13} . In this study, isotope effects are abbreviated by adding a leading superscript of the heavy atom to the kinetic parameters (Northrop, 1975; Cook and Cleland, 1981). Thus, k_H/k_D , k_{C-12}/k_{C-13} can be given as $^D k$ and ^{13}k , respectively. In enzyme-catalyzed reactions, the isotope effects are often expressed as the limiting macroscopic rate constants, e.g. $^D V$ and $^D(V/K_{6PG})$.

2.4.6 Chemical Rescue

In order to restore the mutant enzyme activity that is lost due to the mutation of the active site lysine residue, several small primary amines were incubated with the mutant enzymes. Amines such as ethylamine, dimethylamine, ethylenediamine, and benzylamine were incubated with the K183A mutant enzyme at amine concentrations from 0 to 1 M, and the incubation time was from 5 to 10 minutes.

In addition, the K183C mutant enzyme was modified chemically by adding 25 mM 2-bromoethylamine to the mutant protein and incubating for 12 hours at room temperature and 4 °C, respectively. The preparation was then used in the enzymatic reactions with both substrates saturating, and the results were compared with that of the K183C mutant enzyme incubated with buffer alone. All enzyme assays were carried out as discussed above.

2.4.7 Data Processing.

Reciprocal initial velocities were plotted against reciprocal substrate concentrations. Data were fitted to the appropriate rate equations (using BASIC versions of the computer programs developed by Cleland (1977)). Initial velocity data were fitted using eq. 1. For pH studies, substrate saturation curves were fitted using eq. 2. Data for pH profiles with one ionization on the acid side were fitted using eq. 3. Data for competitive inhibition were fitted using eq. 4. Data for Dixon plots were fitted using the equation for a straight line. Deuterium kinetic isotope

effect data, obtained by direct comparison of initial velocities, and with independent effects on V and V/K were fitted using eq. 5.

$$v = VAB/(K_{ia}K_b + K_aB + K_bA + AB) \quad (1)$$

$$v = VA/(K_a + A) \quad (2)$$

$$\log y = \log[C/(1+H/K_1)] \quad (3)$$

$$v = VA/(K_a[1+I/K_{is}] + A) \quad (4)$$

$$v = VA/[K_a(1 + F_iE_{v/K}) + A(1 + F_iE_v)] \quad (5)$$

In eqs. 1, 2, 4, and 5, v is the initial velocity, V is the maximum velocity, A and B are reactant concentrations, K_a (K_{NADP}) and K_b (K_{6PG}) are Michaelis constants for NADP and 6PG, K_{ia} is the dissociation constant for NADP, and K_{is} is the inhibition constant for slope. In the case of 6PGDH, K_{6PG} and K_{NADP} are dissociation constants for 6PG and NADP from the E:NADP:6PG complex, respectively. In eq. 5, F_i is the fraction of deuterium label in the substrate and $E_{v/K}$ and E_v are the isotope effects minus 1 for the respective parameters. In eq. 3, y is the value of the parameter of interest, C is the pH independent value of y , H is the hydrogen ion concentration, and K_1 is the acid dissociation constant for an enzyme or substrate functional group important in a given protonation state for optimal binding and/ or catalysis.

CHAPTER 3

RESULTS

3.1 Site-Directed Mutagenesis.

Site-directed mutagenesis was performed using the Altered Site II *in vitro* mutagenesis system from Promega. After the transformation of each mutagenesis reaction into ES 1301 *mutS* electrocompetent cells, the transformation reaction was shaken overnight in LB broth containing ampicillin. The cultures showed good growth the next morning, indicating that the mutant plasmids contained the ampicillin resistance gene. After the second transformation of the mutant plasmids into JM 109 competent cells, about thirty to eighty colonies were obtained on each plate. Two to four colonies were picked and their plasmids were purified. The plasmids were digested with *EcoR* I and *Hind* III and the results were analyzed by agarose gel electrophoresis. All digestion reactions resulted in two bands: a 1.5 kb band representing the insert and a 5.7 kb band representing the vector. Figure 16 shows the digestion results of K183A.pAlter. The sequencing results of these plasmids showed that over 60% of the colonies have the correct mutant gene.

3.2 Subcloning of the Mutants into the pQE-30 Expression Vector.

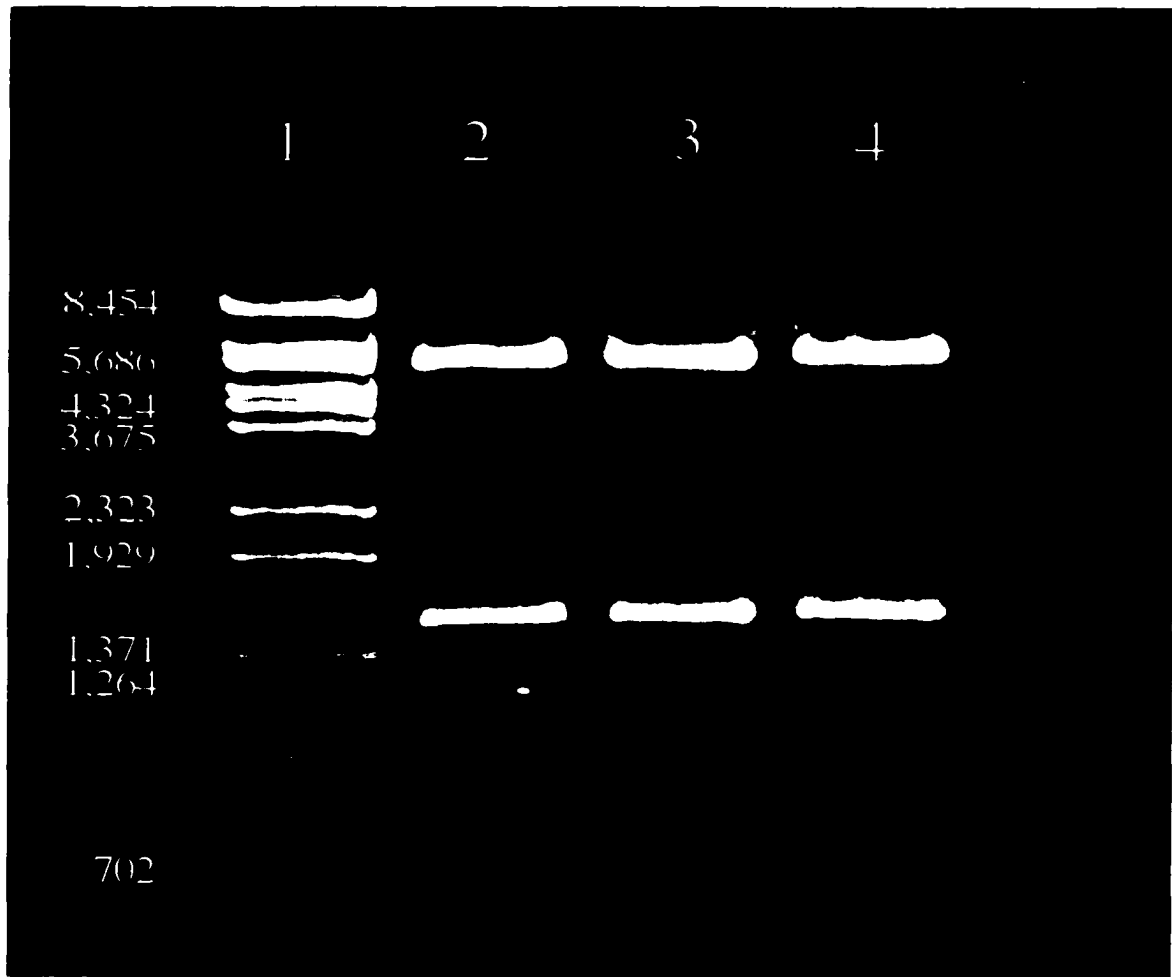


Figure 16. Agarose Gel Electrophoresis of K183A.pAlter Plasmids Digested with *EcoR* I and *Hind* III. Lane 1, molecular weight standards (Lambda DNA-*Bst*E II digest); Lane 2 to Lane 4, K183A.pAlter plasmids from three single colonies, and digested with *EcoR* I and *Hind* III. All three colonies contain a plasmid of the correct insert size.

The PCR product was analyzed by agarose gel electrophoresis, and a 1.5 kb DNA fragment was obtained. The transformation of the ligation reaction into M15 competent cells resulted in thirty to fifty colonies per LB plate, and the *Hind* III digestion showed that 50% of the colonies contained two plasmids: plasmid pREP4 (3.7 kb) from the competent cells and the pQE-30 vector with the mutant insert (4.9 kb). The remaining 50% of the colonies contained the pREP4 plasmid (3.7 kb) and the pQE-30 plasmid without insert (3.4 kb). The digestion results for K183A.pQE30 are shown in Figure 17. The entire gene was then sequenced, and none of the mutants were found to have any non-specific mutations other than the desired one.

3.3 Expression and Purification of the Mutant Proteins.

Expression and purification were performed using the QIAexpress system. In all cases, the mutant proteins were expressed at a level equal to that of the WT enzyme. After the protein was eluted from the column, protein concentrations were measured for all fractions. Figure 18 shows the protein concentration for each fraction of the elution profile using the K183E mutant enzyme as an example. The fractions corresponding to the second peak on the plot were collected as the final mutant enzyme fraction. All the other mutants gave similar results when eluted from the resin. About 1 mg protein is obtained from 1 liter of culture for each mutant. The final enzyme preparation is around 90% pure based on Coomassie blue-stained SDS polyacrylamide gels. The apparent subunit molecular weight of the mutants is

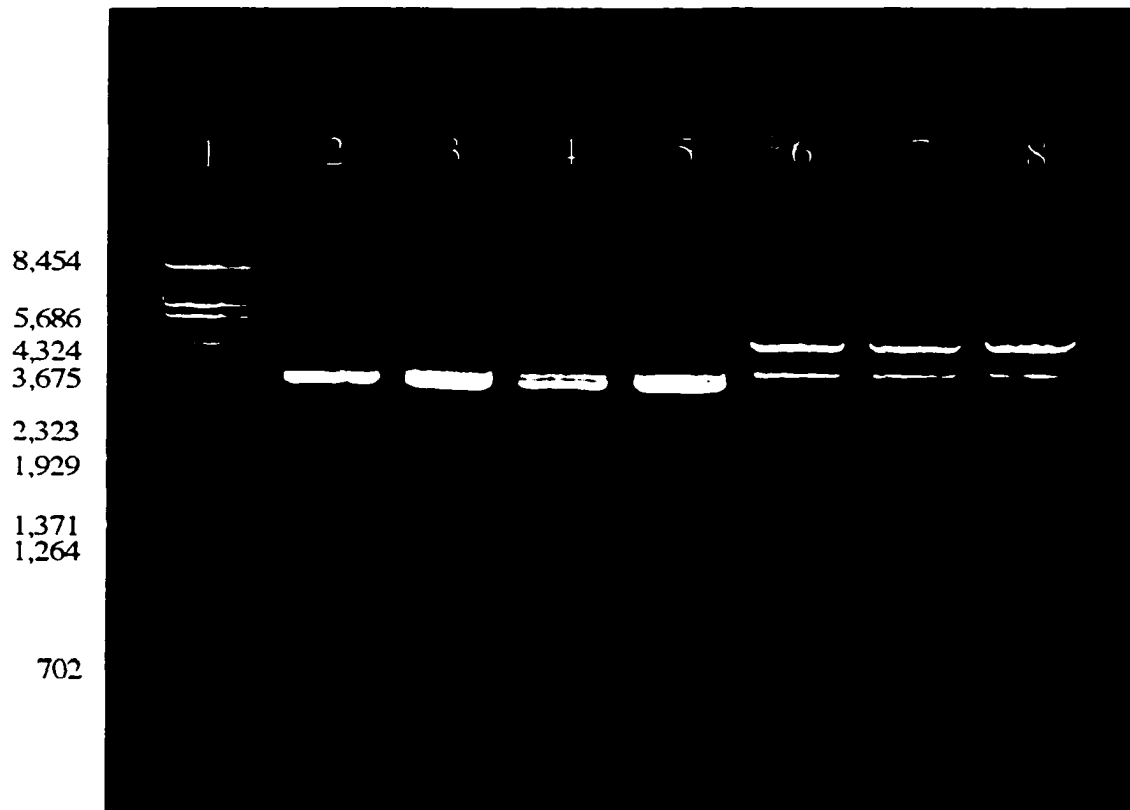


Figure 17. Agarose Gel Electrophoresis of K183A.pQE30 Plasmids Digested with *Hind* III. Lane 1, molecular weight standards (Lambda DNA-*Bst*E II digest); Lane 2 to Lane 8, K183A.pQE30 plasmids from seven single colonies, and digested with *Hind* III. colony 6, 7, and 8 have the plasmids with the correct insert size.

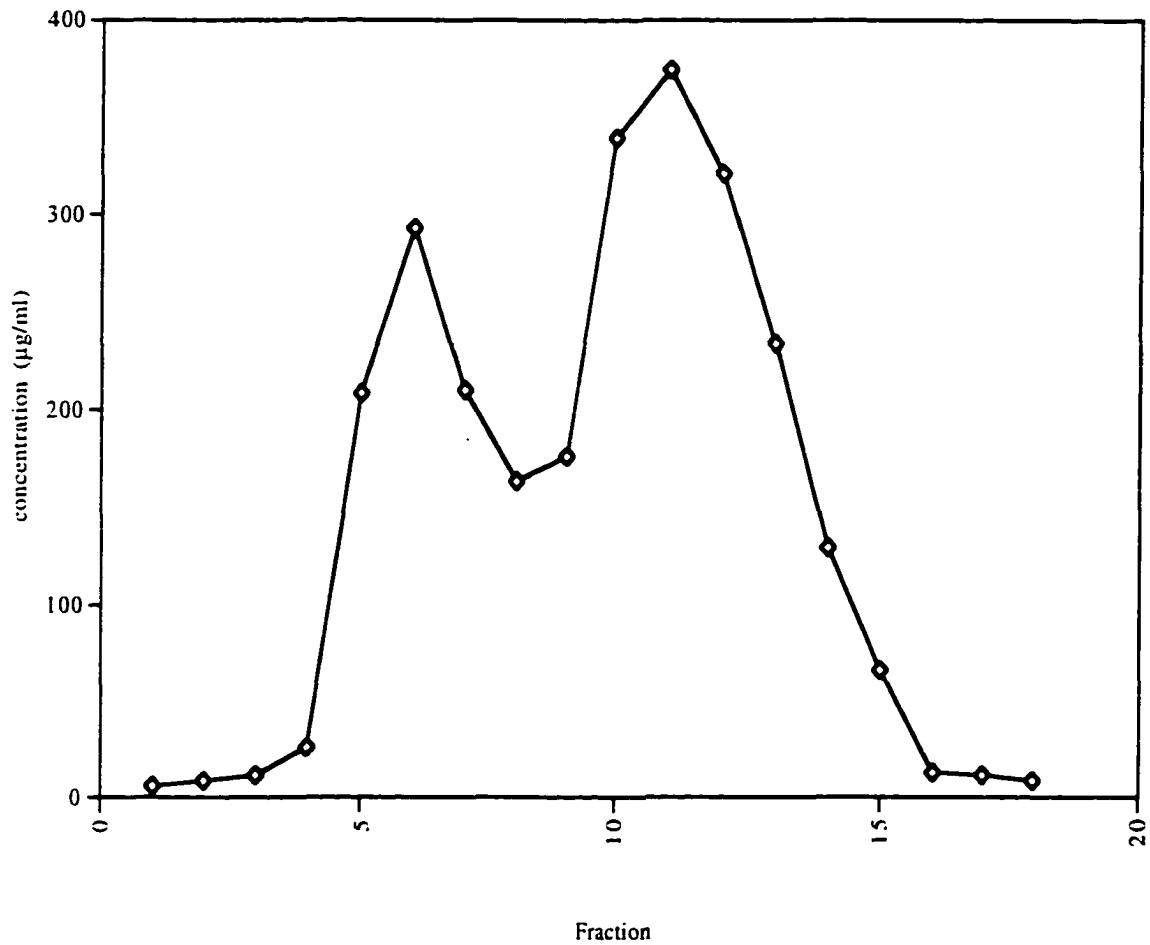


Figure 18. Elution Profile of the K183E Mutant Protein. Elution from the Qiagen Ni-column was affected using an imidazole step gradient. The fractions corresponding to the second peak (0.2 M imidazole) were collected and used for further studies.

51,000. Figure 19 shows an overloaded SDS-PAGE of the K183E mutant protein. All the other mutants gave similar results based on SDS-PAGE.

3.4 Circular Dichroism Spectroscopy.

To determine whether the point mutation in 6PGDH resulted in a loss of overall structural integrity, far-UV CD spectra were measured using an Aviv 62 DS spectropolarimeter. The far-UV spectra were superimposable once corrected to the same protein concentration, with those of the wild type enzyme. Thus, changes in structure, if any, must be localized to the active site. Figure 20 shows the CD spectra of the K183E mutant protein compared with that of the wild type enzyme. All of the other mutant proteins gave qualitatively similar CD spectra.

3.5 Characterization of K183 Mutant Proteins.

3.5.1 Kinetic Parameters.

Initial velocity patterns were obtained at pH 7 by measuring the initial rate as a function of the concentration of NADP at a fixed concentration of 6PG, and then repeating the experiment at several different fixed concentrations of 6PG. The activity was very low for some of the mutant enzymes, and there was not enough enzyme available to determine complete initial velocity patterns; in these cases the 6PG saturation curve was obtained at saturating NADP. The kinetic parameter expected to show the most dramatic effect of the mutation is V/K_{6PG} since K183 is thought to interact with the 3-hydroxyl of 6PG. In order to ensure that NADP was saturating,

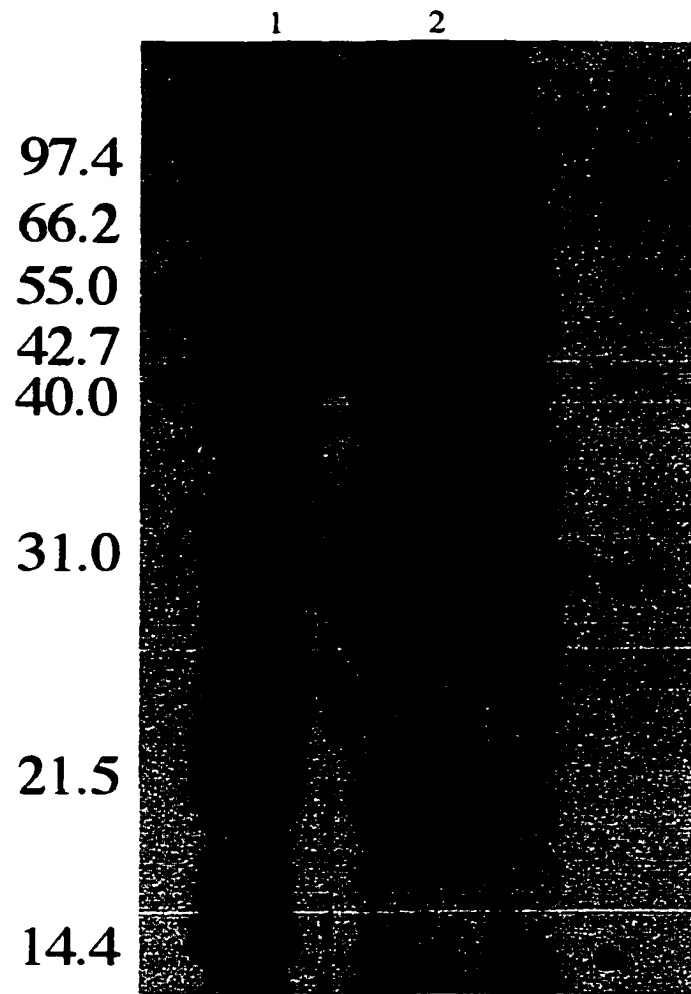


Figure 19. SDS-PAGE of K183E Mutant Protein. Lane 1, molecular mass standards; lane 2, 80 µg K183E mutant protein, final fraction from the Ni-column.

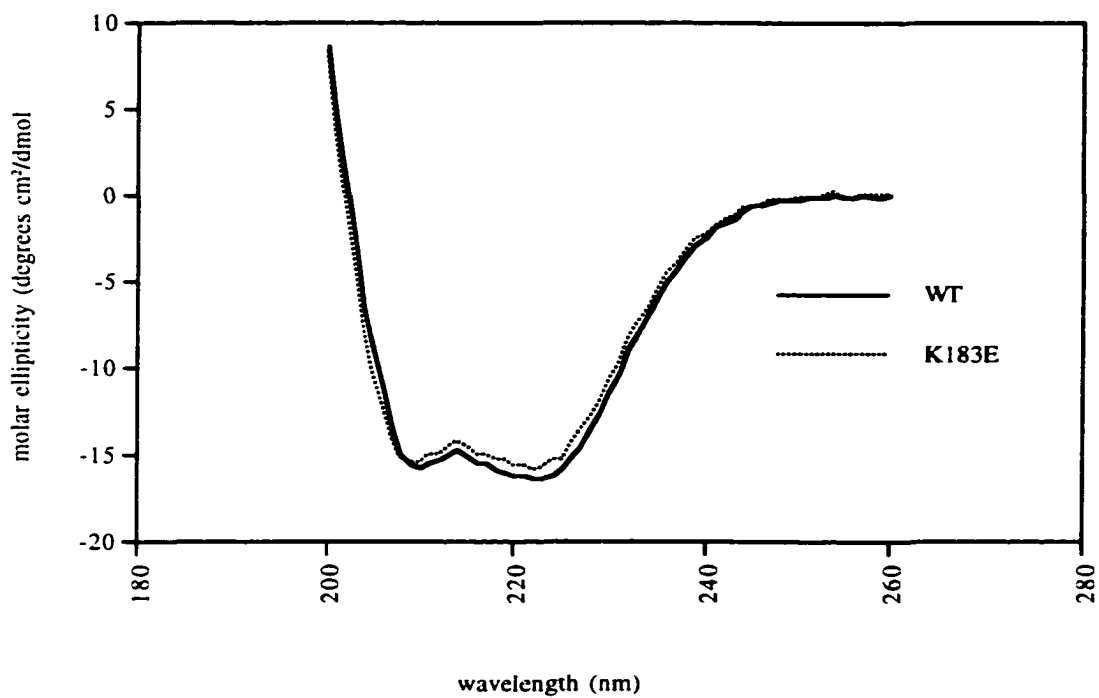


Figure 20. Far-UV CD Spectrum of K183E Mutant Protein Compared with the Wild Type Enzyme. Spectra were recorded with 0.1 mg/mL enzyme in 10 mM KH₂PO₄ buffer, pH 7, at intervals of 1nm and a dwell time of 3 s.

individual rates were repeated at twice the concentration of NADP, with no change observed. A Lineweaver-Burk plot of the initial velocity data for the K183C mutant enzyme is shown in Figure 21 as an example, while an initial velocity pattern obtained for the K183R mutant enzyme is shown in Figure 22. The estimated kinetic parameters for all of K183 mutant enzymes are summarized in Table 2.

The value of V/E_t is decreased by 10^3 - to 10^4 -fold for all of the mutant proteins compared to that of the wild type enzyme. In all cases, with the exception of the K183A, K183R, and K183M mutant enzymes, K_{6PG} is within error identical to the value measured for the wild type enzyme. Of the K_{NADP} values measured, only that for K183R increases significantly compared to that of the wild type. Decreases in V/K_{6PG} and V/K_{NADP} are either similar to or larger than changes in V . In the case of the K183M and K183R mutant proteins, the increase in K_{6PG} likely suggests a decreased affinity for 6PG as a result of steric interference by the bulky guanidinium group of the arginine side chain or the sulfur of the methionine side chain. All of the other changes, with the exception of alanine, will potentially allow a hydrogen bond to the 3-hydroxyl, similar to that observed for the wild type enzyme.

3.5.2 pH Dependence of Kinetic Parameters.

The pH dependence of kinetic parameters should provide the best indicator as to the general base capability of K183, since they give a direct measure of the pK value for the general base functionality of 6PGDH (Berdis and Cook, 1993b, Price and Cook, 1996). Because of the very low activity of most of the mutant proteins, the

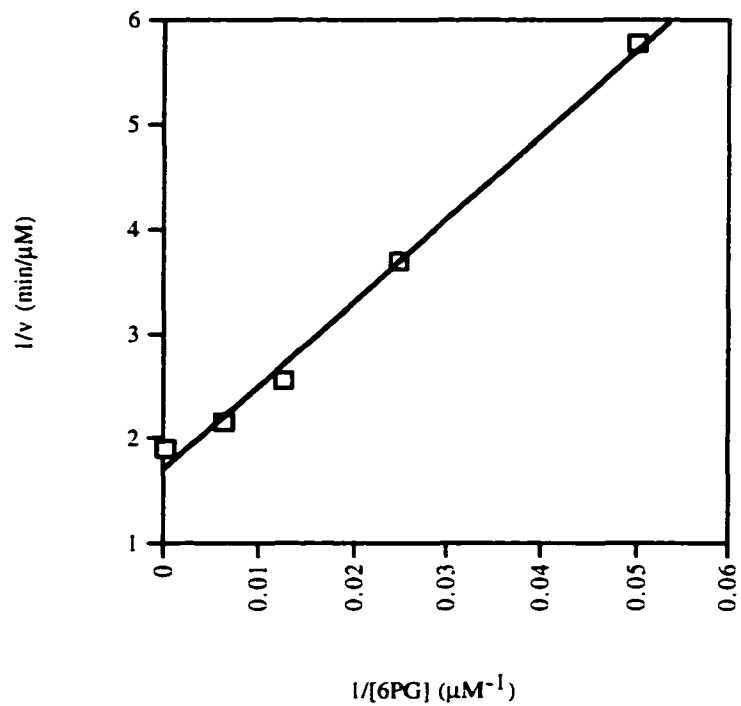


Figure 21. Lineweaver-Burk Plot for the K183C Mutant Protein. Data were obtained at pH 7, 25 °C. The NADP concentration was fixed at 1 mM ($500 K_{NADP}$). The points shown are the experimentally determined values, while the curve is from a fit of the data using eq. 2 shown in chapter 2.

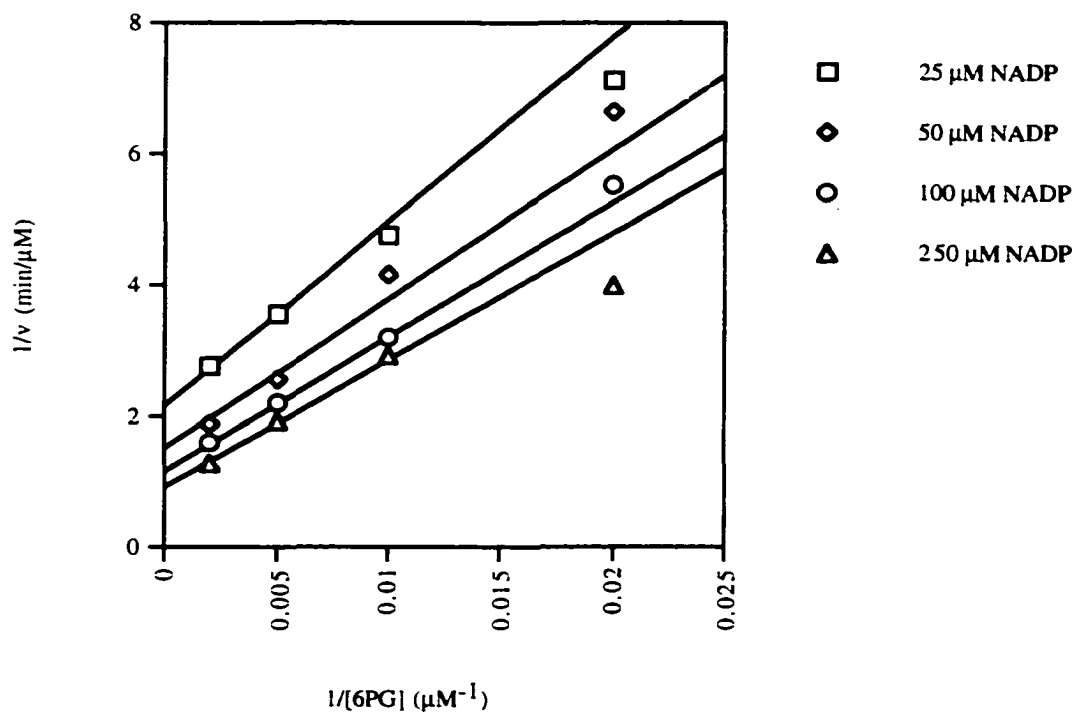


Figure 22. Initial Velocity Pattern for K183R Mutant Protein. Data were obtained at pH 7, 25 °C. The points shown are the experimentally determined values, while the curve is from a fit of the data using eq. 1 shown in chapter 2.

Table 2. Kinetic Parameters for K183 Mutant 6PGDHs^a.

	K_{6PG} (μM)	K_{NADP} (μM)	V/E_t^b (s^{-1})	$V/K_{6PG}/E_t$ ($\text{M}^{-1} \text{s}^{-1}$)	$V/K_{NADP}/E_t$ ($\text{M}^{-1} \text{s}^{-1}$)
WT ^c	36 ± 15	2 ± 1	3.5 ± 0.1	(1 ± 0.4) × 10 ⁵	(1.8 ± 0.6) × 10 ⁶
K183A	150 ± 30 (4 ± 2)	--	(2.5 ± 0.3) × 10 ⁻⁴ (14000 ± 1700)	17 ± 4 (59000 ± 27000)	--
K183E	26 ± 3 --	8 ± 4 (4 ± 3)	(4.7 ± 0.1) × 10 ⁻⁴ (7500 ± 300)	18 ± 2 (5600 ± 2300)	70 ± 40 (25000 ± 17000)
K183H	80 ± 40 (2 ± 1)	9 ± 4 (2 ± 1)	(6.2 ± 0.8) × 10 ⁻⁴ (5600 ± 750)	7 ± 3 (14300 ± 8400)	100 ± 40 (17500 ± 9300)
K183C	45 ± 2 --	-- --	(3.9 ± 0.05) × 10 ⁻⁴ (9000 ± 300)	8.8 ± 0.4 (11400 ± 4600)	-- --
K183Q	27 ± 5 --	-- --	(7.2 ± 0.3) × 10 ⁻⁴ (4900 ± 250)	27 ± 4 (3700 ± 1600)	-- --
K183R	220 ± 30 (6 ± 3)	42 ± 8 (20 ± 11)	(4.4 ± 0.3) × 10 ⁻³ (800 ± 60)	19 ± 1 (5300 ± 2100)	100 ± 10 (17500 ± 6300)
K183M	300 ± 100 (8)	-- --	(4.1 ± 0.6) × 10 ⁻⁴ (8500 ± 1250)	1.4 ± 0.4 (70000 ± 35000)	-- --

^aValues in parentheses indicate the fold increase in K_m or fold decrease in V and V/K compared to those of the wild-type enzyme.

^b E_t is total enzyme concentration.

^cFrom (Chooback et al., 1998).

pH dependence of V and V/K_{6PG} was measured for only the K183R mutant, which has an 800-fold lower V/E_t value. The pH-rate profiles for the wild-type enzyme are shown in Figure 23 (Karsten et al., 1998), and the pH-rate profiles for K183R are shown in Figure 24. The pH-rate profiles for the wild type enzyme are bell-shaped, while the pK on the basic side is missing in both pH-rate profiles for K183R mutant. The pK values calculated for the wild type and K183R are summarized in Table 3. pH independent values of V/E_t and $V/K_{6PG}E_t$ for K183R are $(9 \pm 2) \times 10^{-3} \text{ s}^{-1}$ and $7.4 \pm 0.9 \text{ M}^{-1}\text{s}^{-1}$, respectively.

3.5.3 Kinetic Deuterium Isotope Effect.

To determine which step is impaired in the case of the K183R mutant, the kinetic deuterium isotope effect was assessed using the method of direct comparison of initial velocities, varying the concentration of 6PG-3-(h, d). Data were only obtained for the R mutant because its activity is higher than those of other K183 mutant enzymes. For the wild type enzyme, the deuterium isotope effects are equal on V and V/K_{6PG} with an average value of 2 (Price and Cook, 1996; Hwang et al., 1998). For K183R mutant, the deuterium isotope effect values on V and V/K_{6PG} are within error equal to 1.

3.5.4 Chemical Rescue.

Chemical rescue experiments allow the replacement of a missing enzyme side chain functionality (eliminated by site-directed mutagenesis) with small weak acids or

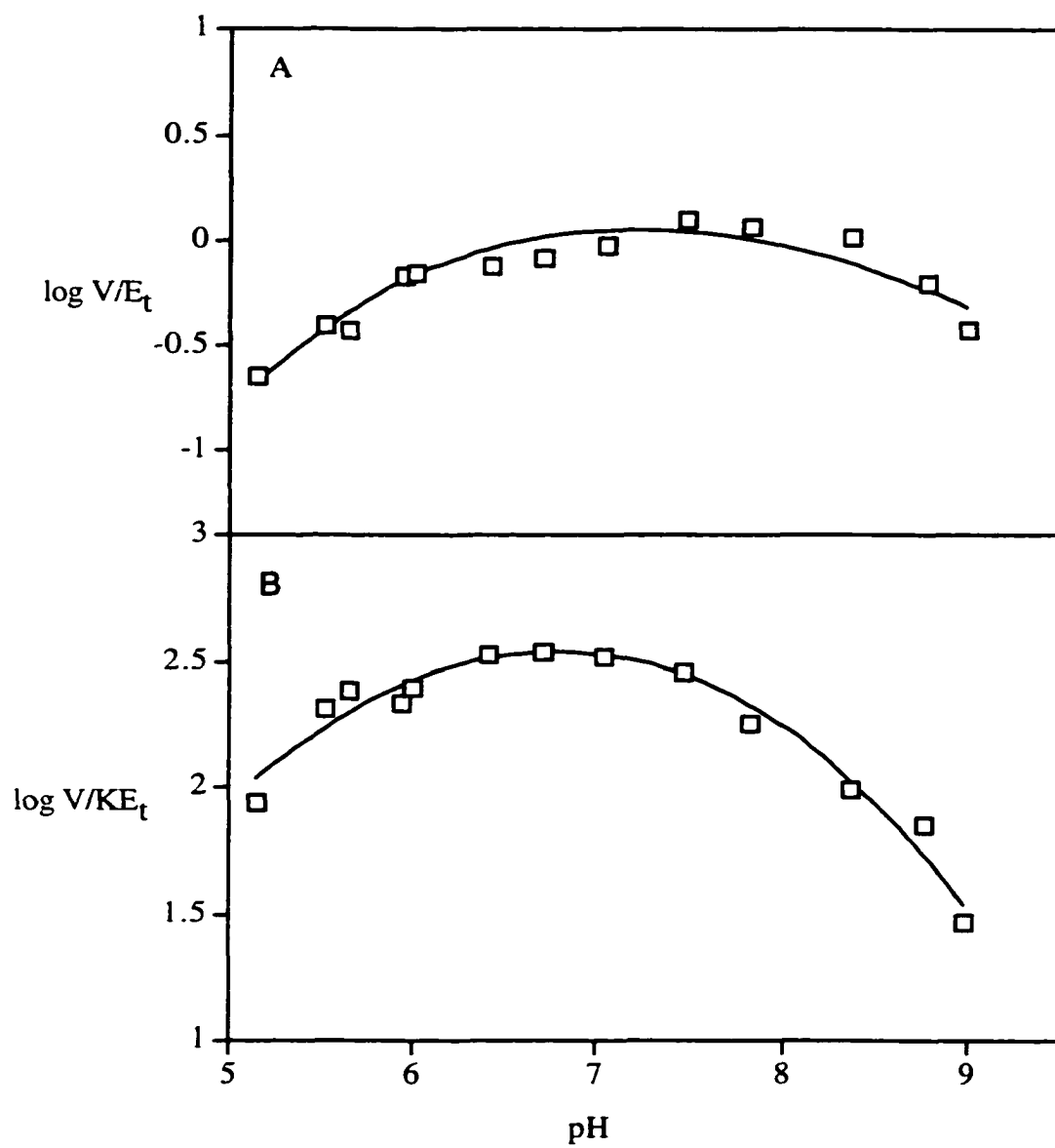


Figure 23. pH Dependence of Kinetic Parameters for Wild Type 6-PGDH. Data were obtained for V (A) and V/K_{6PG} (B) (Karsten et al., 1998)

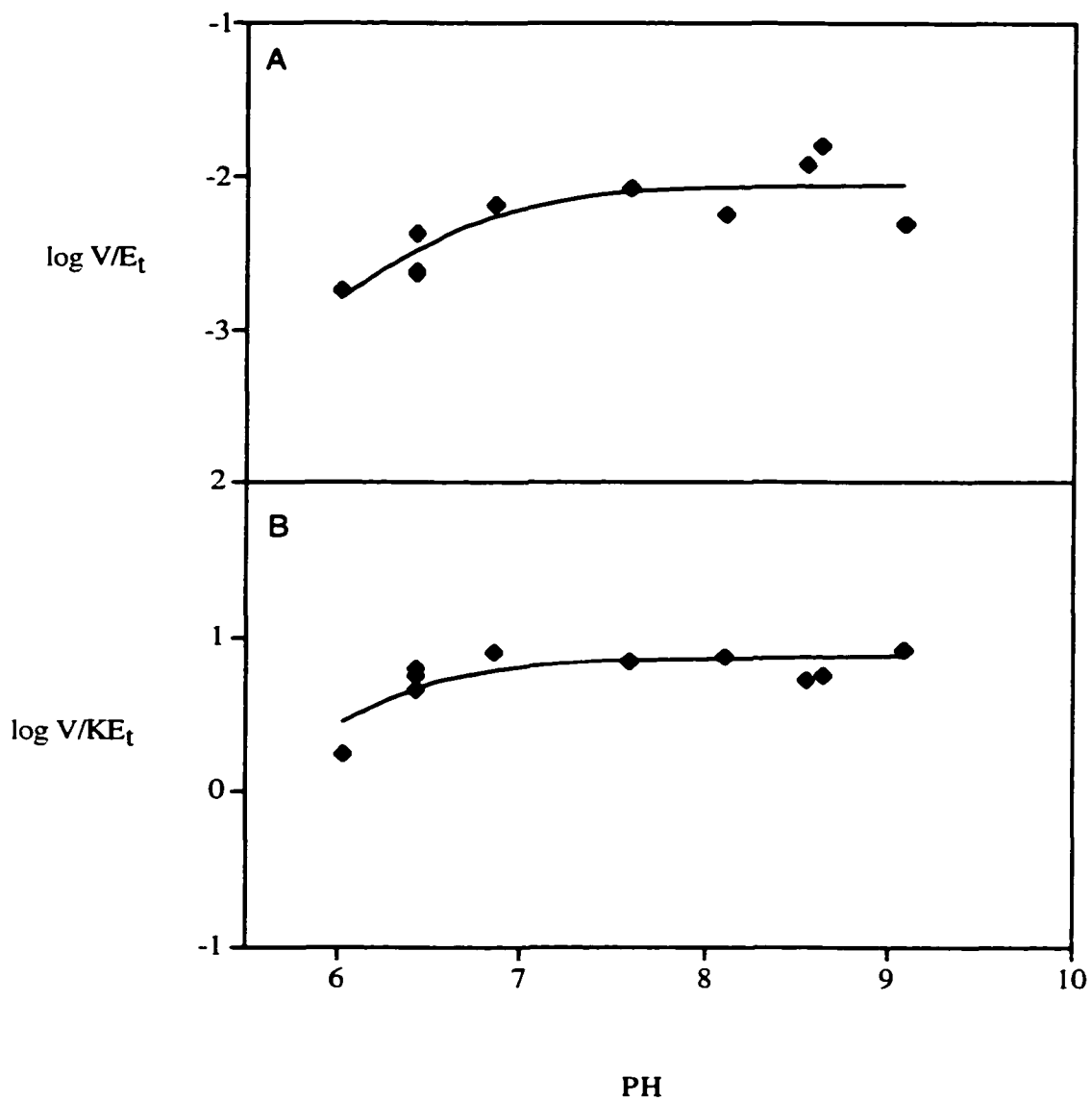


Figure 24. The pH Dependence of Kinetic Parameters for the K183R Mutant of 6-PGDH. Data were obtained at pH 7, 25 °C for V/E_t (A) and $V/K_{6PG}E_t$ (B). The points shown are the experimentally determined values, while the curves are from a fit of the data using eq. 3 shown in chapter 2.

Table 3. pK Values for the Wild Type 6PGDH and K183R Mutant Protein.

		pK _a	pK _b
WT ^a	V/E _t	5.8 ± 0.1	8.8 ± 0.1
	V/K _{6PG} /E _t	5.6 ± 0.1	8.0 ± 0.1
K183R	V/E _t	6.6 ± 0.1	---
	V/K _{6PG} /E _t	6.2 ± 0.1	---

^aFrom (Karsten et al., 1998)

bases (Planas and Kirsch, 1991). Since the ϵ -amino group of lysine is absent in the K183 mutant enzymes, two different methods were attempted to restore activity, i.e., addition of small primary amines to the K183A mutant enzyme and chemical modification of Cys183 of the K183C mutant enzyme with bromoethylamine to form S-aminoethyl-L-cysteine. For the K183A mutant enzyme, primary amines such as ethylamine, dimethylamine, ethylenediamine, and benzylamine were used in an attempt to recover the enzyme activity. None of the above amines has any effect on the activity of the enzyme. The lack of ability of the primary amines to replace lysine may be entropic, since these amines lack the advantage of being locked into place, or may be geometric resulting from the amines being bound at the active site in such a way that they are unable to catalyze the reaction effectively. There is only 2 to 3 fold increase in activity after incubating the K183C mutant enzyme with 2-bromoethylamine for 12 hours. Data suggest either no, or very little conversion of cysteine to S-aminoethyl-L-cysteine.

3.6 Characterization of the Substrate Binding Mutant Proteins.

3.6.1 Kinetic Parameters.

The initial velocity results for S128A, H186A and N187A were obtained in the same manner as those obtained for the K183 mutants. Initial velocity data are shown in Figure 25 using the H186A mutant enzyme as an example, and the estimated kinetic parameters for the mutant enzymes are summarized in Table 4. The value of V/E_0 decreases compared to the wild type enzyme by around 200 fold for

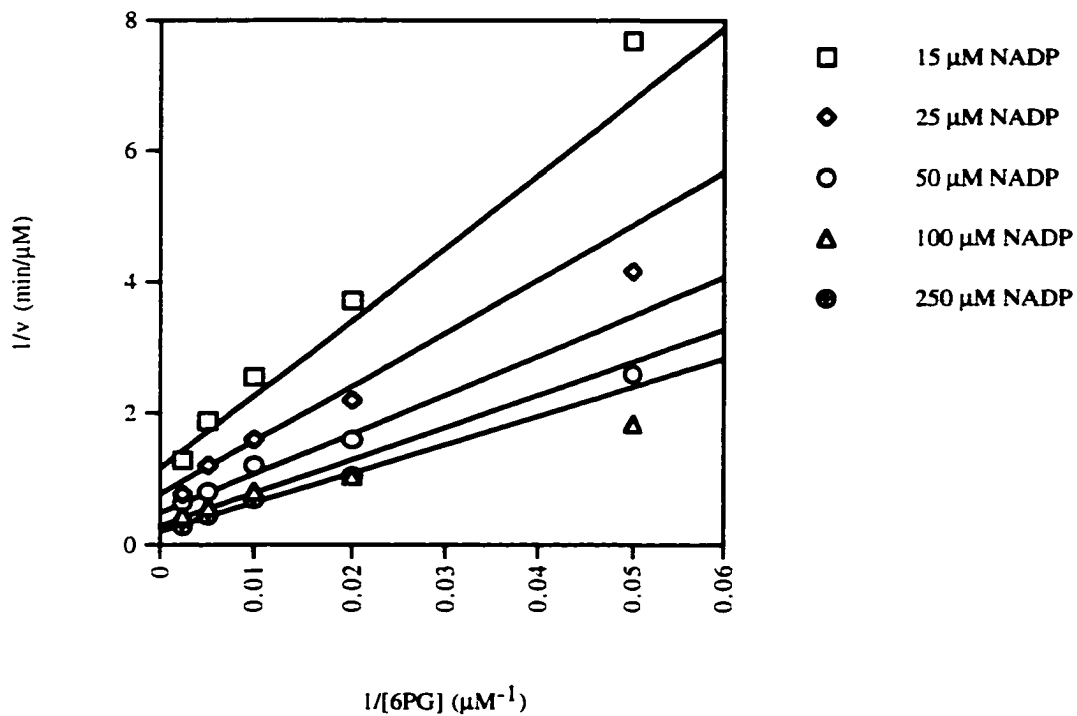


Figure 25. Initial Velocity Pattern for H186A Mutant Protein. Data were obtained at pH 7, 25 °C. The points shown are the experimentally determined values, while the curve is from a fit of the data using eq. 1 shown in chapter 2.

Table 4. Kinetic Parameters for Mutants of Binding Residues in 6PGDH Active Site^a.

	K_{6PG} (μM)	K_{NADP} (μM)	V/E_t (s^{-1})	$V/K_{6PG}/E_t$ ($\text{M}^{-1} \text{s}^{-1}$)	$V/K_{NADP}/E_t$ ($\text{M}^{-1} \text{s}^{-1}$)
WT ^b	36 ± 15	2 ± 1	3.5 ± 0.1	(1 ± 0.4) × 10 ⁵	(1.8 ± 0.6) × 10 ⁶
S128A	232 ± 35 (6 ± 3)	3.7 ± 0.8 (2 ± 1)	0.3 ± 0.03 (12 ± 1)	(1.3 ± 0.07) × 10 ³ (77 ± 31)	(1.1 ± 0.2) × 10 ⁵ (16 ± 6)
H186A	247 ± 61 (7 ± 3)	96 ± 24 (48 ± 27)	(2.2 ± 0.3) × 10 ⁻² (160 ± 22)	92 ± 11 (1100 ± 450)	239 ± 33 (7500 ± 2700)
N187A	560 ± 148 (16 ± 8)	39 ± 10 (20 ± 11)	(1.7 ± 0.1) × 10 ⁻² (200 ± 13)	30 ± 6 (3300 ± 1500)	436 ± 90 (4100 ± 1600)

^aValues in parentheses indicate the fold increase in K_m or fold decrease in V and V/K compared to those of the wild-type enzyme.

^bFrom (Chooback et al., 1998)

the H186A and N187A mutant enzymes, but decreases only 12 fold for the S128A mutant enzyme. K_{6PG} is increased by around 6 fold for both S128A and H186A and 16 fold for N187A. The decreased affinity for 6PG is likely caused by the loss of the hydrogen bond between 6PG and the respective side chain. The value of K_{NADP} is increased by 20 fold for N187A and by 50 fold for H186A, while there is no significant change in the K_{NADP} value for S128A mutant enzyme.

3.6.2 Product Inhibition by NADPH.

Product inhibition studies by NADPH were carried out for S128A, H186A and N187A mutants at both saturating and nonsaturating 6PG concentrations. The K_{is} value obtained in these studies reflects the affinity of enzyme for NADPH. Since all three of the amino acids changed form hydrogen-bonds with the nicotinamide ring of NADPH, it is important to quantitate these interactions (Adams et al., 1994). The inhibition pattern using the H186A mutant enzyme as an example is show in Figure 26, while a Dixon plot is shown in Figure 27 using the N187A mutant enzyme as an example. The calculated K_{is} values for all of the mutant enzymes are summarized in Table 5. For all the mutants, the inhibition remains competitive at both saturating and nonsaturating 6PG. At a saturating concentration of 6PG, the value of K_{is} is increased by 2 to 3 fold for the S128A and H186A mutant enzymes compared to that of the wild type. At nonsaturating 6PG, however, K_{is} is increased by 5 to 6 fold for the S128A and H186A mutant enzymes. No significant change is observed in the K_{is} value for the N187A mutant enzyme at either 6PG concentration.

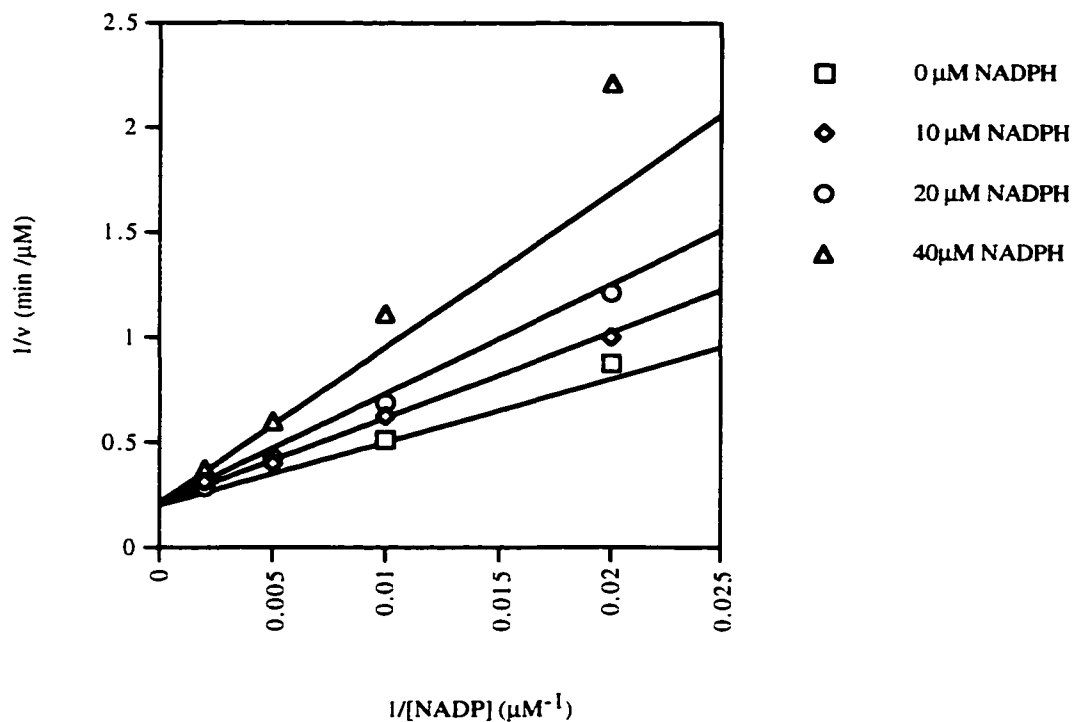


Figure 26. Inhibition Pattern for H186A Mutant Protein at Saturating 6PG Concentration. 6PG concentration was fixed at 5 mM ($20 K_m$). Data were obtained at pH 7, 25 °C. The points shown are the experimentally determined values, while the curve is from a fit of the data using eq. 4 shown in chapter 2.

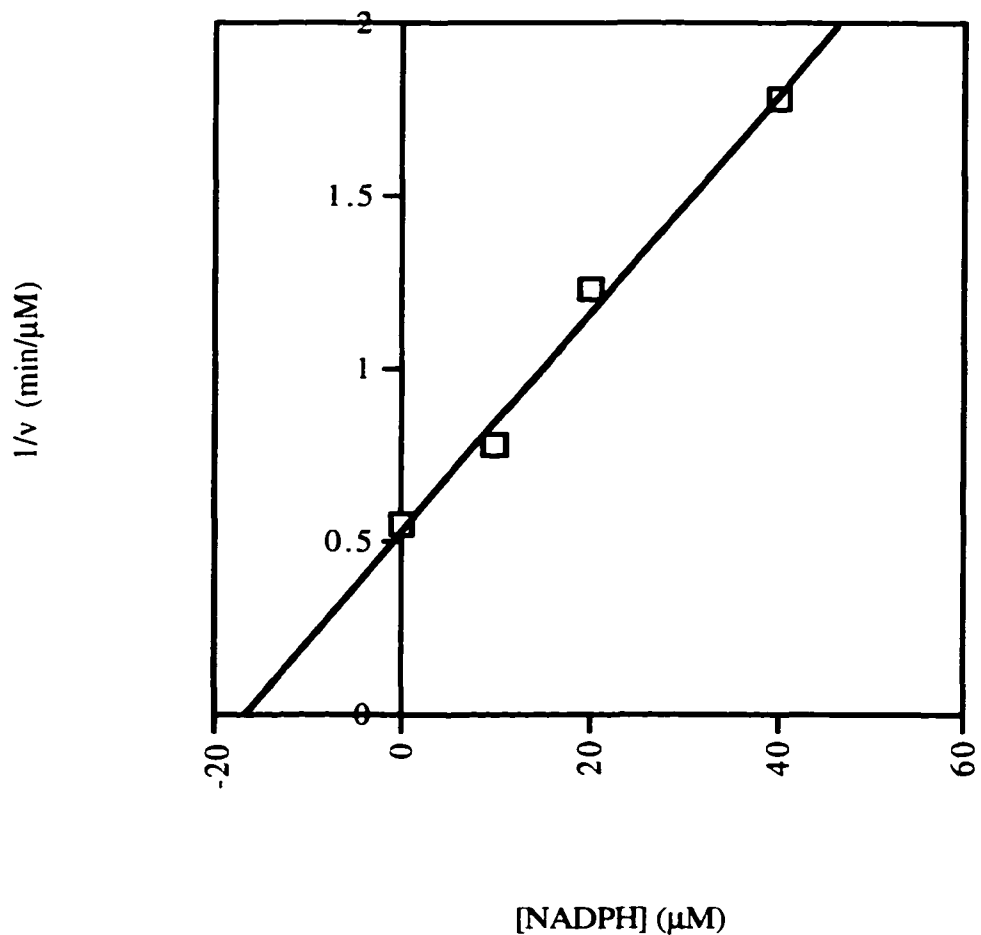


Figure 27. Dixon Plot for N187A Mutant Protein at Saturating 6PG Concentration. 6PG concentration was fixed at 12 mM ($20 K_m$). Data were obtained at pH 7, 25 °C. The points shown are the experimentally determined values, while the curve is from a fit of the data using the equation for a straight line.

Table 5. K_{is} Values (μM) of the Product Inhibition (NADPH vs. NADP) Studies for Mutant 6-Phosphogluconate Dehydrogenases^a.

	6PG (s) ^b	6PG (ns) ^c
WT ^d	8 ± 2	1.8 ± 0.3
S128A	19 ± 7.5 (2 ± 1)	12 ± 0.7 (6 ± 1)
H186A	27 ± 5.7 (3 ± 1)	9.5 ± 1.6 (5 ± 1)
N187A	9.3 ± 1.3	2.8 ± 0.1

^aValues in parentheses represent the fold increase in K_{is} compared to those of the wild-type enzyme.

^bs, saturating (20 K_m).

^cns, nonsaturating (K_m).

^dFrom (Price and Cook, 1996).

3.6.3 Deuterium Isotope Effect.

Primary deuterium isotope effect data have been obtained for S128A, H186A, and N187A in a manner identical to those obtained for K183R, and the initial velocity plot for the H186A mutant enzyme is shown in Figure 28 as an example. The calculated deuterium isotope effects for all three mutant enzymes are summarized in Table 6. For all the mutants, the deuterium isotope effects are within error equal on V and V/K_{6PG} , indicating that the kinetic mechanism of the mutant enzymes remains rapid equilibrium. The isotope effects decrease for S128A and H186A, and increase in the case of N187A compared to those of the wild type enzyme.

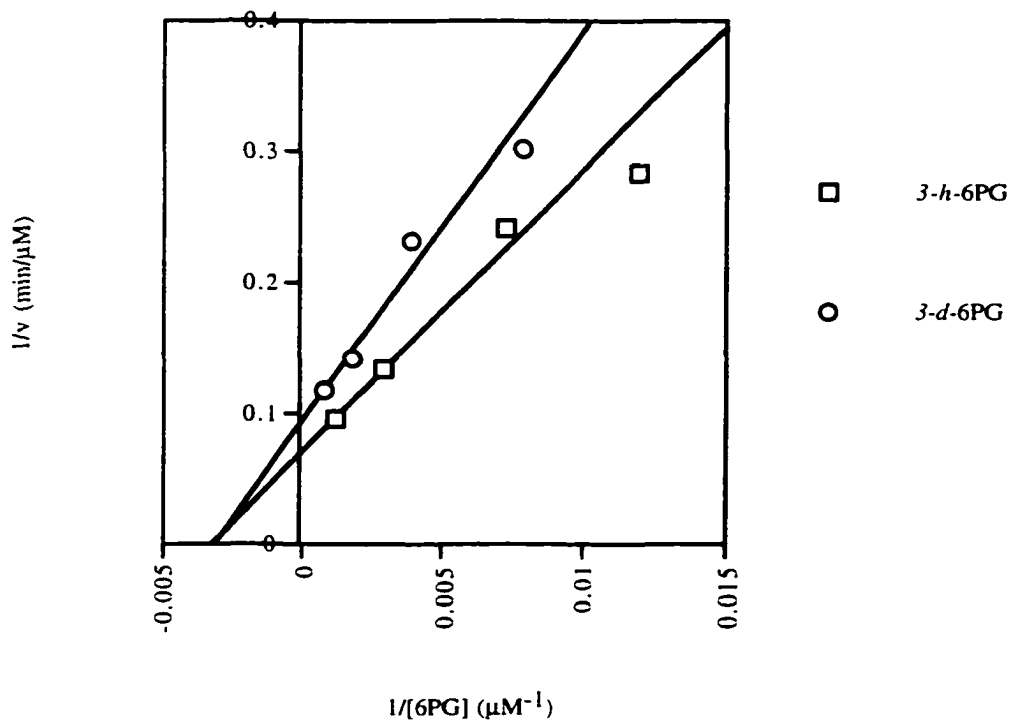


Figure 28. Primary Deuterium Isotope Effects for H186A mutant protein. NADP concentration was fixed at 2 mM (20 K_m). Data were obtained at pH 7, 25 °C. The points shown are the experimentally determined values, while the curve is from a fit of the data using eq. 5 shown in chapter 2.

Table 6. Primary Deuterium Kinetic Isotope Effects for Mutant 6-Phosphogluconate Dehydrogenases^a.

	^D V	^D (V/K _{6PG})
WT ^b	2.1 ± 0.1	2.1 ± 0.1
S128A	1.5 ± 0.1	1.2 ± 0.1
H186A	1.4 ± 0.1	1.4 ± 0.2
N187A	3.0 ± 0.4	2.7 ± 0.7

^aAssays were carried at 25 °C and saturating concentrations (20K_m) of NADP.

^bFrom (Hwang et al., 1998).

CHAPTER 4

DISCUSSION

4.1 Circular Dichroism spectroscopy.

The CD spectra of the mutant enzymes are identical to that of the wild type 6PGDH, indicating that there are no gross conformational changes upon mutagenesis. This result is not unexpected, since the mutation sites are all located in the active site of the enzyme. The side chains of the active site amino acid residues are usually more flexible due to their substrate binding function. The result of the CD spectroscopy suggests that any changes of the mutant enzyme activities are not due to the loss of structural integrity, rather to the alteration of an important amino acid residue.

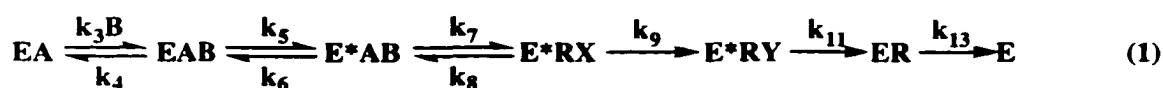
4.2 K183 mutant proteins.

As shown in Figure 10, K183 is completely conserved in 6PGDH from all species for which a primary sequence has been determined. It is likely then that the lysine side chain is important to the mechanism of 6PGDH. In agreement with this hypothesis, K183 is found in the active site within hydrogen-bonding distance to the 3-hydroxyl of 6PG, Fig. 9 (Adams et al., 1994). An overlay of the three dimensional structures of the E, E:NADP, E:NADPH, and E:6PG complexes (Adams et al., 1991;

Adams et al., 1994), indicates no gross conformational changes throughout the structure, and only very slight changes in side chain positions within the active site (data not shown). Thus, the stereo representation shown in Fig. 9 is a reasonable view of the interactions of K183 with the 3-hydroxyl of 6PG at the active site. Finally, since there is also no change in the position of K183 with NADPH bound, it is likely that the position of the side chain is fixed (with the possible exception of small changes in the K183-NE to 6PG-O β hydrogen-bonding distance) in all intermediates formed along the reaction pathway.

4.2.1 Interpretation of Kinetic Data.

A minimal kinetic mechanism for 6PGDH (Berdis and Cook, 1993a; Price and Cook, 1996; Hwang and Cook, 1998), including 6PG binding, and all three of the catalytic steps is given in eq. 1



where the A, B, R, X, and Y represent NADP, 6PG, NADPH, 3-keto-6PG, and the 1,2-enediol of ribulose 5-phosphate, the E to E* interconversion represents a conformational change prior to catalysis, k_3 and k_4 are binding and dissociation constants for 6PG, k_5 and k_6 are rate constants for the enzyme isomerization, k_7 and k_8 represent forward and reverse hydride transfer, k_9 represents decarboxylation and release of CO₂, k_{11} represents either tautomerization and release of ribulose 5-

phosphate or release of the enediol intermediate, and k_{13} represents release of NADPH. Based on the assigned rapid equilibrium random kinetic mechanism (Price and Cook, 1996), and the proposed rapid release of CO_2 , eqs. 2-4 are obtained.

$$V = [k_7/(1 + k_6/k_5)]/[1 + \{k_7(1/k_5 + 1/k_{11})\}/(1 + k_6/k_5)] \quad (2)$$

$$V/K_{6\text{PG}} = [k_3k_5k_7/k_4k_6]/[1 + (k_7/k_6)] \quad (3)$$

$$K_{6\text{PG}} = K_d(1 + (k_7/k_6))/[1 + k_5/k_6 + k_7(1/k_5 + 1/k_{11})] \quad (4)$$

The effect of changing K183 is easily understood via eqs. 2-4. Two classes of mutant enzymes are obtained (Table 2). The first group is composed of the E, H, C, and Q mutants, which show little significant change in the $K_{6\text{PG}}$, and thus equal decreases in V/E_t and $V/K_{6\text{PG}}E_t$. None of the mutant side chains likely function in a general base capacity at pH 7, given pK values of the side chains as compared to the pK of the 3-hydroxyl of 6PG. Hwang et al. (1998) have measured deuterium and ^{13}C kinetic isotope effects for the sheep liver enzyme, and on the basis of the value of observed and intrinsic deuterium isotope effects, one can estimate that the hydride transfer step is 20-30% limiting overall, while decarboxylation limits the overall rate by about 15-20%. Since the general base is required to accept a proton from the 3-hydroxyl in the oxidation step, and is also utilized to polarize the carbonyl and as a general acid in the decarboxylation step, it is of interest to determine whether hydride transfer or decarboxylation is impaired. The lack of a significant deuterium isotope effect on V and $V/K_{6\text{PG}}$ suggests that it is a decrease in the rate of the decarboxylation

step, k_9 , that is reflected by the several-fold decreases in V and V/K shown in parentheses in Table 2; that is, both kinetic parameters (V and V/K) are dominated by k_9 in the mutant enzymes. The several-fold decrease in V/E_i for the E, H, C, and Q mutants is about the same for all, with a weighted average value of 6800 ± 800 estimated from the V/E_i values with the lowest standard error. As suggested above, correcting for percent rate-limitation, this value is likely closer to 35,000–45,000. The decrease thus represents an estimate of the catalytic advantage realized from the general acid-electrostatic properties of K183, a $\Delta\Delta G^\ddagger$ of about 6 kcal/mol. However, it should be realized that the rate enhancement is a weighted average that largely reflects the rate of the decarboxylation step (see above).

On the basis of the identity within error of K_{6PG} for the E, H, C, and Q mutant enzymes, it is likely that the hydrogen-bonding interaction between the 3-hydroxyl and the mutant side chains is allowed in all four of the above mutant enzymes. This conclusion is not unexpected, despite the apparent differences in the length of the mutant side chains, especially for cysteine and glutamate, compared to a fully extended lysine side chain. A glance at Fig. 9 shows the side chain of K183 is not fully extended, but folded such that a fully extended cysteine or glutamate side chain could easily be within hydrogen-bonding distance to the 3-hydroxyl of 6PG. Thus, the carbonyl oxygen of glutamine, an unprotonated imidazole, ionized thiol and glutamate side chains may be able to accept a hydrogen bond from the 3-hydroxyl of 6PG.

A second class of K183 changes includes the A, M, and R mutants. This class exhibits an increase in K_{6PG} and a decrease in V/E_t , yielding a greater decrease on $V/K_{6PG}E_t$ than that observed in V/E_t . For these mutant enzymes, a decrease in the affinity for 6PG (an increase in the K_d term in eq. 4 shown above, reflecting the dissociation constant for 6PG from the E:NADP:6PG ternary complex) is observed in addition to a decrease in k_p . Each of the three mutations, however, derives its effect differently. In the case of the M mutant, the bulky sulfur likely causes a local disruption in the 6PG binding pocket in the vicinity of the 3-hydroxyl, and this along with the hydrophobicity of the thiomethyl group give the observed approximately 8-fold decrease in 6PG affinity. The R mutant also presents a bulky side chain that likely interferes slightly with 6PG binding, but the guanidinium functional group can still function, albeit weakly, as a general base as discussed further below. Finally, the A mutation eliminates the side chain for K183, and any real possibility of acid-base catalysis. A possible exception could be a bound water molecule occupying the site of the missing side chain, but the water would have a very weak basicity. In addition, the decrease in V/E_t is larger, not smaller, than the average value of 6800-fold estimated above. (This would include the glutamine side chain, which presumably occupies a space similar to that of lysine.)

The A mutant provides an opportunity to estimate the contribution of the ϵ -amine of K183 to 6PG binding affinity. The overall ΔG° for the binding energy of 6PG in the combined E:NADP:6PG and E*:NADP:6PG complexes, based on the measured dissociation constant of 36 μM is -6.1 kcal/mol. The decrease in binding

affinity of 2- to 6-fold, based on the data in Table 2, and assuming no effect of the mutation on the isomerization equilibrium represented by k_5 and k_6 , gives a $\Delta\Delta G^\circ$ of 0.4 to 1.1 kcal/mol, with an average value of 0.8 kcal/mol for the contribution of K183 to 6PG binding. Thus, although the amine contributes to 6PG binding, the contribution is relatively modest.

Prior to a discussion of the pH-rate data, it is worth noting that substantial changes are also observed in $V/K_{\text{NADP}}E_t$ (for all those measured) as expected in a rapid equilibrium random kinetic mechanism. However, one would expect changes in k_7 to be identically expressed in both V/K values, and they are not as shown in Table 2. Differences in the decrease in the $V/K_{\text{6PG}}E_t$ and $V/K_{\text{NADP}}E_t$ values compared to those of the WT enzyme must reflect differences in affinity for NADP and 6PG for mutant vs. WT enzymes. Although the errors are substantial, there is evidence that significant changes in the K_{NADP} occur that are larger, at least in the case of the R mutant, than the change in K_{6PG} . This result is not surprising given the close juxtaposition of the 6PG and NADP binding sites. Indeed, changes in the nicotinamide position are thought to occur as reduction of the ring takes place, resulting in a displacement of the 1-carboxyl of 6PG (Adams et al., 1994).

4.2.2 Interpretation of the pH-Rate Profiles for the K183 Mutant Enzymes.

On the basis of the likely identity of the general base (K183) and the general acid (E190) from structural studies (Adams et al., 1994), previously determined pH-rate profiles have been interpreted in terms of reverse protonation states between the

two groups. That is, although K183 is the general base, its pK is observed on the basic side of the pH profiles, while that of E190, although it is the general acid, is observed on the acidic side of the pH profile (Price and Cook, 1996). The two groups exist in protonation states in the E:6PG and E:6PG:NADP complexes that are opposite that expected based on the pKs of Lys and Glu in solution (Cleland, 1977). Thus, in the WT enzyme, the pK of 5.6 in the V/K_{6PG} profile is thought to be that of E190, while the pK of 8 is thought to reflect K183. The lysine and glutamate pKs must then be perturbed to lower and higher pH values as a result of the hydrophobic nature of the active site.

As stated above, only the R mutant was active enough to obtain pH-rate profiles. The V and V/K_{6PG} pH profiles are similar for the R mutant, with a pK of 6.2-6.8 observed on the acid side, and no decrease on the basic side up to pH 9. Thus, although the pK for E190 is increased slightly, it is the pK for R183 that is not observed, likely because it is above pH 9. The latter is not unexpected since the pK of the arginine guanidinium is about 12.5 in solution (Dawson et al., 1986), and would, by analogy to K183 be expected to be decreased by 2.5 pH units to a pK around 10 (the solution pK of a lysine side chain is 10.5 and the observed pK is 8). Data are thus fully consistent with the predicted general base nature of K183.

4.3 Substrate Binding Mutants.

As stated above, in order to facilitate the decarboxylation process after the hydride transfer step has occurred, hydrogen bonds between the 1-carboxyl group of

6PG and the side chains of Ser 128 and Glu 190 must be broken. Structural evidence of such changes has been obtained by comparing the E:NADP and E:NADPH complexes, Figure 29 and Figure 30, (Adams et al., 1994). The conformations of the adenine, adenine ribose and 2'-phosphate are very similar in both structures, while the nicotinamide ribose and nicotinamide of the oxidized and reduced dinucleotides have different conformations. In the oxidized coenzyme complex, the dinucleotide is less extended, i.e. the nicotinamide ring is positioned near the pyrophosphate backbone of the dinucleotide with the *si* face of the cofactor directed toward C-3 of 6PG. The distance between the N1 of the pyridine ring of NADP and the O2'' of the pyrophosphate is 5.2 Å (Figure 29). In the reduced coenzyme complex, the nicotinamide ring rotates by almost 180°. This conformational change results in a more extended structure of NADPH, and the distance between the N1 of the nicotinamide ring and O2'' increases to 7.6 Å (Figure 30). It is suggested that this structural difference is a consequence of the charge difference at N1 of the nicotinamide ring (Adams et al., 1994). Indeed, there is likely an electrostatic interaction between the positively charged pyridinium ring of NADP and the pyrophosphate backbone in the E:NADP complex. The different conformations of the oxidized and reduced dinucleotide results in a difference in interactions between enzyme side chains and the carboxamide side chain of NADP(H). The oxidized coenzyme makes contacts only with residues in the coenzyme domain, with the carboxamide of NADP within hydrogen-bonding distance of the main chain NH of Met 13 and the carboxylate of Glu 131 (Table 7). Both hydrogen bonds are relatively

Figure 29. Stereopair of the Active Site Region of the 6PGDH:Nbr⁸ADP Binary Complex. The atoms are labeled as, N, blue, O, red, P, orange, and S, cyan. The carbon backbones of enzyme side chains are labeled in yellow, and the carbon backbone of coenzyme is in green. The nicotinamide moiety of Nbr⁸ADP binds to residues from only dinucleotide binding domain (Adams et al., 1994). Note the interaction between the pyridine nitrogen and the pyrophosphate backbone.

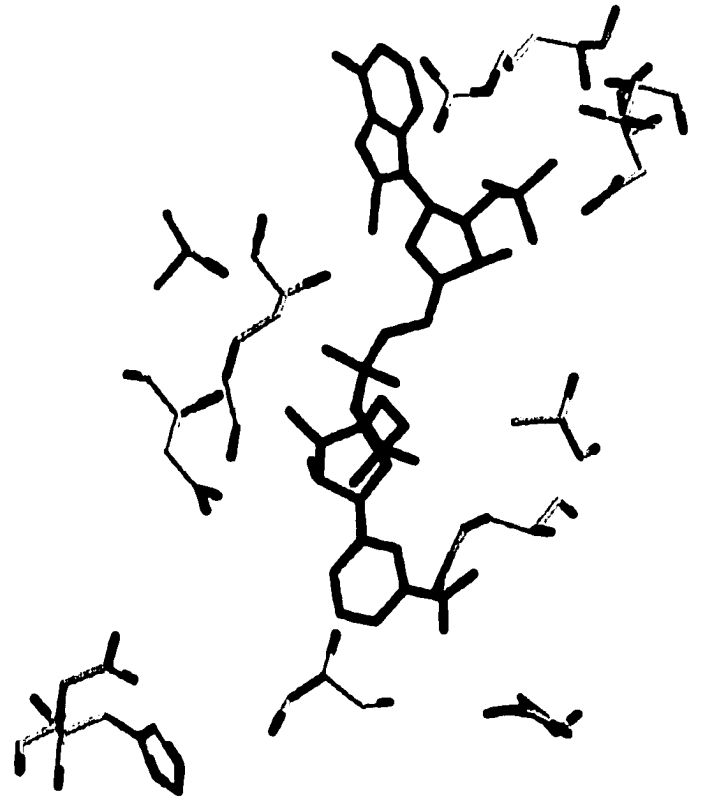
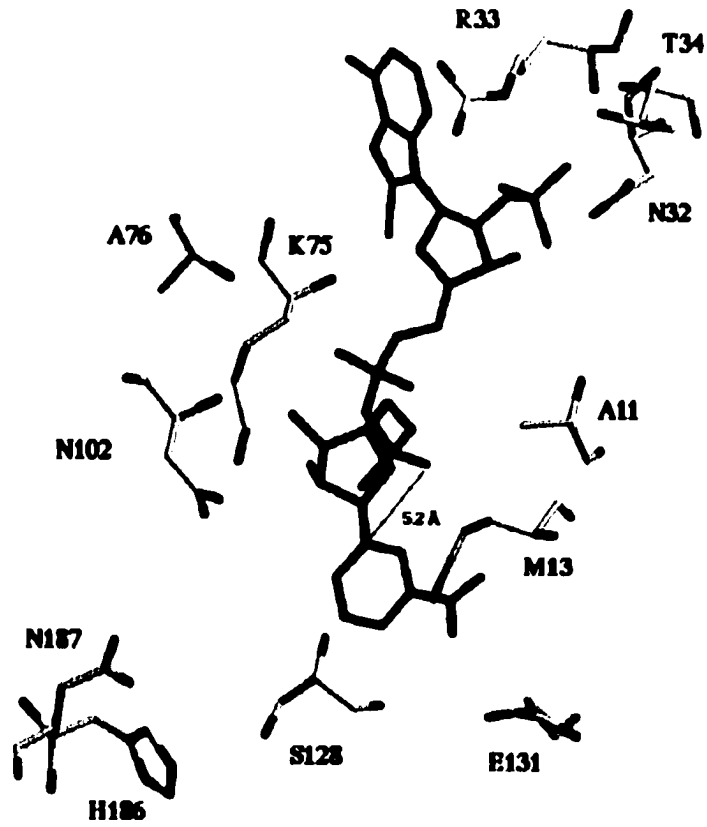


Figure 30. Stereopair of the Active Site Region of the 6PGDH:NADPH Binary Complex. The atoms are labeled as, N, blue, O, red, P, orange, and S, cyan. The carbon backbones of enzyme side chains are labeled in yellow, and the carbon backbone of coenzyme is in green. The nicotinamide moiety of NADPH binds to residues from both the dinucleotide binding and helical domains (Adams et al., 1994). Note the long distance between the pyridine nitrogen and the pyrophosphate backbone.

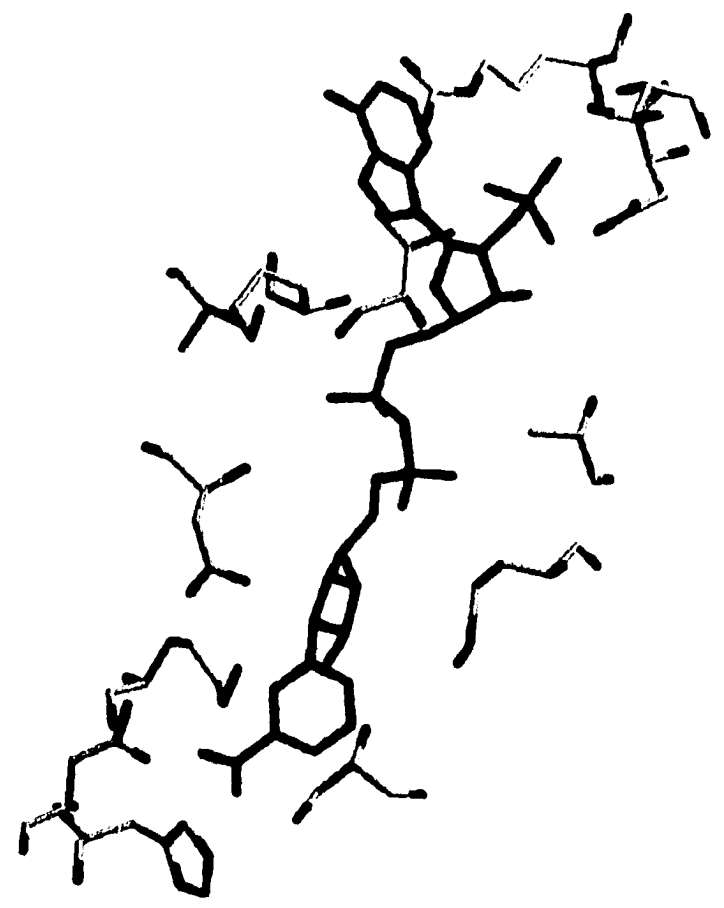
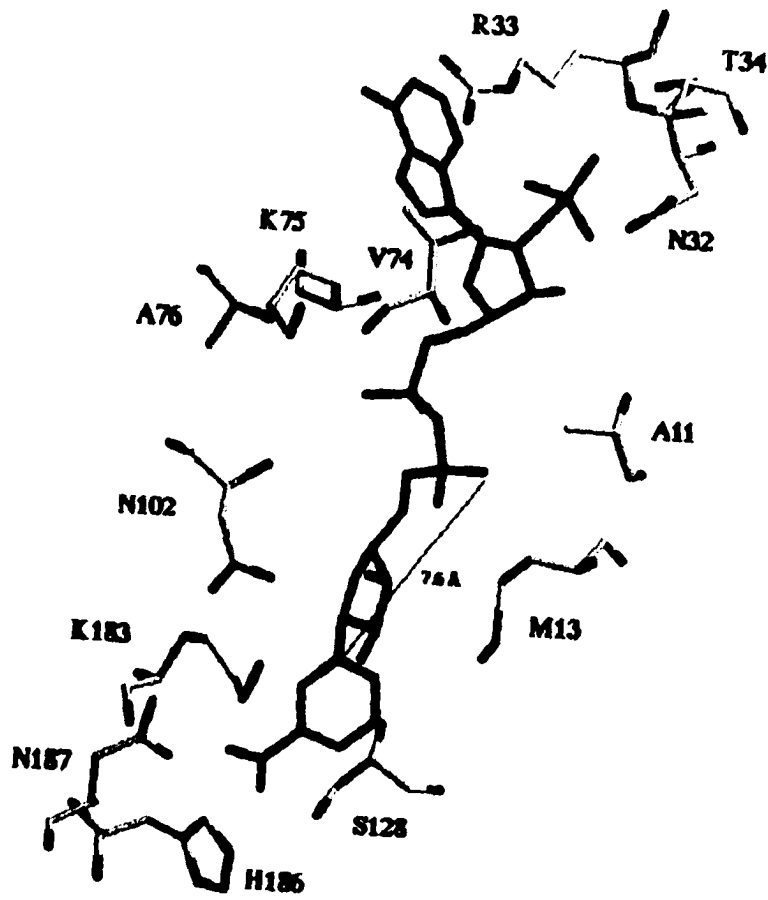


Table 7. Interactions between Enzyme and Coenzymes. ^a		
Coenzyme moiety	Nbr ^a ADP	NADPH
Adenine ribose	O3-NH Leu10 O3-Nδ2 Asn32 O4-NH Lys75	O3-NH Leu10 O3-Oδ1 Asn32 O4-NH Lys75
2'-phosphate	O1(P)-Nη2 Arg33 O2(P)-Oδ1 Asn32 O2(P)-Nε Arg33 O2(P)-Oγ1 Thr34 O3(P)-Oδ1 Asn32 O3(P)-Nδ2 Asn32	O2(R)-Nδ2 Asn32 O1(P)-Nε Arg33 O1(P)-Nη2 Arg33 O2(P)-Nδ2 Asn32 O2(P)-NH Thr34 O2(P)-Oγ1 Thr34 O3(P)-Oδ1 Asn32
Pyrophosphate		O1''-O Wat692 O2''-O Wat589 O5(R)-O Wat516
Nicotinamide ribose		O4-Nδ2 Asn102
Nicotinamide	O7-NH Met13 N7-Oε2 Glu131	O7-Oγ Ser128 O7-Nε2 His186 N7-Oδ1 Asn187
Waters	O614-Oγ Ser128 O614-Oε1 Glu190 O886-Nε2 His452 O886-O4 SO ₄ 505	O516-NH Asn102 O589-NH Ala11 O589-NH Gly14 O589-O Leu73 O589-O Gly9 O692-NH Met13

^aFrom Adams et al., 1994.

weak or modest, at least based on the distances shown in Table 8. The reduced coenzyme, on the other hand, interacts with residues in both the coenzyme and helical domains. The nicotinamide carboxamide of NADPH is within hydrogen-bonding distance to O γ of Ser 128, N ϵ 2 of His 186, and O δ 1 of Asn 187 (Table 7). Thus, the structural rearrangement of the dinucleotide that accompanies reduction of NADP to NADPH likely eliminates the hydrogen bonds between the 1-carboxyl group of 6PG, Ser 128 and Glu 190 (Table 9). Consistent with this suggestion, it has been reported that decarboxylation of 3-keto-2-deoxy-6PG is enhanced upon binding of the reduced (but not oxidized) coenzyme (Hanau et al., 1992). From the sequence alignment of 6PGDHs from different sources (Figure 10), Ser 128, His 186, and Asn 187 are absolutely conserved among all the known sequences, indicating the important roles they may play in the binding and catalytic processes. Therefore, studies of the S128A, H186A, and N187A mutant proteins should provide a further understanding of the catalytic mechanism of 6PGDH.

4.3.1 Interpretation of Kinetic Data.

The value of V/E_0 for the three mutant enzymes is decreased by 10 to 200 fold compared to that of the wild type enzyme. The decrease is much less, however, than those observed for the K183 mutant enzymes, eliminating the possibility that these three residues participate directly in the acid-base chemistry of the reaction. K_{6PG} is increased by 6 to 7-fold for both S128A and H186A mutant enzymes, respectively, and by 16-fold for the N187A mutant enzyme. The decrease in affinity for 6PG is

Table 8. Distances from Specific Enzyme Side Chains to Substrate and Coenzymes.			
Binary complex		Hydrogen bond	Distance (Å)
E:Nbr ^δ ADP	Nicotinamide	O7-NH Met13	3.1
		N7-Oε2 Glu131	3.4
E:NADPH	Nicotinamide	O7-Oγ Ser128	3.0
		O7-Nε2 His186	3.1
		N7-Oδ1 Asn187	3.1
E:6PG	1-carboxy (O9, O10)	O10-Oγ Ser128	2.8
		O9-Oε1 Glu190	3.0
	C2-C6	O7-Nζ Lys183	3.2
		O7-Nδ2 Asn187	2.8
	6-phosphate	O3-Oη Tyr191	2.7
		O3-NH Lys260	2.9
		O3-Oγ1 Thr262	3.5
		O2-Nη1 Arg287	2.9
		O2-O Wat528	2.6

6PG region	6PG complex	Inorganic ion	Apo-enzyme
1-carboxy (O9, O10)	O10-O γ Ser128 O9-O ϵ 1 Glu190	SO ₄ 507	O1-N ζ Lys183 O1-O Wat613 O1-O Wat614 O2-N δ 2 Asn102 O2-N δ 2 Asn187 O3-O Wat886 O4-O Wat699
C2-C6	O8-O Wat1109 O8-O Wat1232 O7-N ζ Lys183 O7-N δ 2 Asn187 O5-N ϵ 2 His452# ^b		
6-phosphate	O3-O η Tyr191 O3-NH Lys260 O3-O γ 1 Thr262 O2-N η 1 Arg287 O2-N η 1 Arg446# O2-O Wat528 O1-N η 1 Arg446#	SO ₄ 505	O1-O Wat886 O2-O η Tyr191 O2-NH Lys260 O2-O Wat953 O3-N η 1 Arg287 O3-N η 1 Arg446# O3-O Wat528 O4-N η 1 Arg446#
Water neighbors Wat528 Wat1109 Wat1232	O-O ϵ 2 Glu190 O-N η 3 Arg287 (O-O2 6PG) (O-O8 6PG) O-NH Gly130 (O-O8 6PG)	Water neighbors Wat528 Wat613 Wat614 Wat699	O-O ϵ 2 Glu190 O-N η 2 Arg287 (O-O3 SO ₄ 505) O-NH Gly129 O-NH Gly130 (O-O1 SO ₄ 507) O-O Wat614 (O-O4 SO ₄ 507) O-O γ Ser128 O-O Wat613 O-N ϵ 2 His186 (O-O1 SO ₄ 507) O-O Val127 (O-O4 SO ₄ 507)

^aFrom Adams et al., 1994.

^btwo-fold related subunit by (#).

likely caused by a loss of the hydrogen-bonding interaction between 6PG and the mutated residues. In the case of H186A mutant enzyme, although there is no direct interaction between 6PG and H186, the increase in K_{6PG} is not surprising since Nε2 of the histidine is only 3.6 Å from one of the 1-carboxyl oxygens of 6PG (Adams et al., 1994). H186 interacts with S128 and could provide a positive charge to aid in neutralizing the 1-carboxylate of 6PG, although the imidazole pK is expected to be quite low based on the observed pK of 8 for K183. If there is an electrostatic interaction between the positively charged side chain of H186 and 1-carboxylate, the dielectric constant calculated based on the change in binding energy is 93, larger than the dielectric constant for water, which is 78.6. This result is highly unlikely given the hydrophobic environment of the enzyme's active site. Therefore, the side chain of H186 is probably neutral. Another possibility is that there is a secondary effect caused by the loss of the bulky imidazolium of H186, since it is in close proximity to S128, N187 and E190, all of which interact with 6PG.

As discussed before, the overall ΔG° for the binding energy of 6PG based on a K_d of 36 μM is -6.1 kcal/mole. The estimated decrease in the binding affinity of 6PG for the S128A and H186A mutant enzymes gives an average $\Delta\Delta G^\circ$ value of 1 kcal/mol, while a value of 1.6 kcal/mol is calculated for the N187A mutant enzyme. Therefore, the contribution of N187 to 6PG binding, via a hydrogen bond to the 3-hydroxyl, is the largest among all of the mutant enzymes studied. It is not surprising that the binding energy contributed by N187 is larger than that of K183 despite the fact that both residues make hydrogen bond to the same hydroxyl group of 6PG. The

distance between N δ 2 of N187 and O7 of 6PG is 2.8 Å, while N ζ of K183 is 3.2 Å away from the same oxygen of 6PG (Table 8). Thus, N187 makes a stronger hydrogen bond to the substrate. It is worth noting that the values of the binding energies estimated above are much lower than the average value of 5 kcal/mol estimated for a normal hydrogen bond (Fersht, 1977). This is not unexpected since the hydrogen-bonding energy estimated for the substrate binding is not an absolute binding energy. Indeed, the value reflects the increase in energy of the enzyme-substrate interactions compared to substrate-solvent interactions.

On the basis of each of the calculated binding energies estimated by comparing WT and mutant enzymes, the contribution of different enzyme side chains to the total substrate binding energy can be estimated. The 1-carboxylate of 6PG makes hydrogen bonds with S128 and E190, with a total $\Delta\Delta G^\circ$ value of -1.0 kcal/mole. The 3-hydroxyl group interacts with both N187 and K183, and these contribute about -2.4 kcal/mole to the overall ΔG° for the binding energy of 6PG, -6.1 kcal/mol. Thus, the combination of the binding energy contributed by the 1-carboxylate and the 3-hydroxyl groups of 6PG is -3.4 kcal/mol, leaving -2.7 kcal/mol undetermined. Based on the potential hydrogen bonds suggested in Table 8, the remainder is likely to be obtained through the interactions made by 6-phosphate group of 6PG.

None of the residues mutated have a direct interaction with NADP (Table 7), but a decrease in the V/K_{NADP} value has been observed for the H186A and N187A mutant enzymes. This is not unexpected since the 6PG and NADP binding sites are

juxtaposed, and a steric effect in one site may cause a local disruption in the other site. In the case of the H186A mutant enzyme, the bulky imidazole group has been replaced by a proton, which may result in a local conformational change. A similar situation also exists in the case of N187A mutant enzyme, but to a lesser extent, likely because a smaller carboxamide side chain is replaced by a proton. Thus, the increase in the K_{NADP} value for N187A is smaller than that for H186A. By extrapolation, the small to no change in the NADP binding affinity for the S128A mutant enzyme is also explained.

4.3.2 Interpretation of Product Inhibition Data.

S128, H186, and N187 are all located within hydrogen-bonding distance of the amide of the nicotinamide ring in E:NADPH complex (Table 7). The affinity of these enzyme side chains and NADPH can be estimated using the K_{is} values obtained from product inhibition studies (Table 5). In the case of the N187A mutant enzyme, the K_{is} value is within error identical to that of the wild type at both saturating and nonsaturating 6PG concentrations, indicating either a very weak or no interaction between N187 and NADPH. As to S128A and H186A, K_{is} values are increased by 2 to 3-fold at saturating 6PG, and by 5-6 fold at nonsaturating 6PG. The change in affinity in the absence and presence of 6PG is expected since the 1-carboxylate of 6PG and the carboxamide of NADPH compete with each other for hydrogen-bonding to S128 and H186. The affinity for NADPH in the E:6PG:NADPH complex is not important to the overall mechanism since this is a dead-end complex. The estimated

$\Delta\Delta G^\circ$ value for the S128A and H186A mutant enzymes is 0.9-1.1 kcal/mol at low concentration of 6PG. In all, the binding between the amide and these three residues is not very tight given the overall ΔG° value of -7.8 kcal/mol estimated for the binding energy of NADPH. Thus, the major contribution to NADPH binding must come from the residues that bind the remainder of the NADPH. This result is consistent with the fact that the nicotinamide ring of the coenzyme is rather flexible, as it must be, in order to change its position upon oxidation. As discussed above, this conformational change of the dinucleotide likely plays an important role in the decarboxylation reaction.

4.3.3 Interpretation of Deuterium Isotope Effects

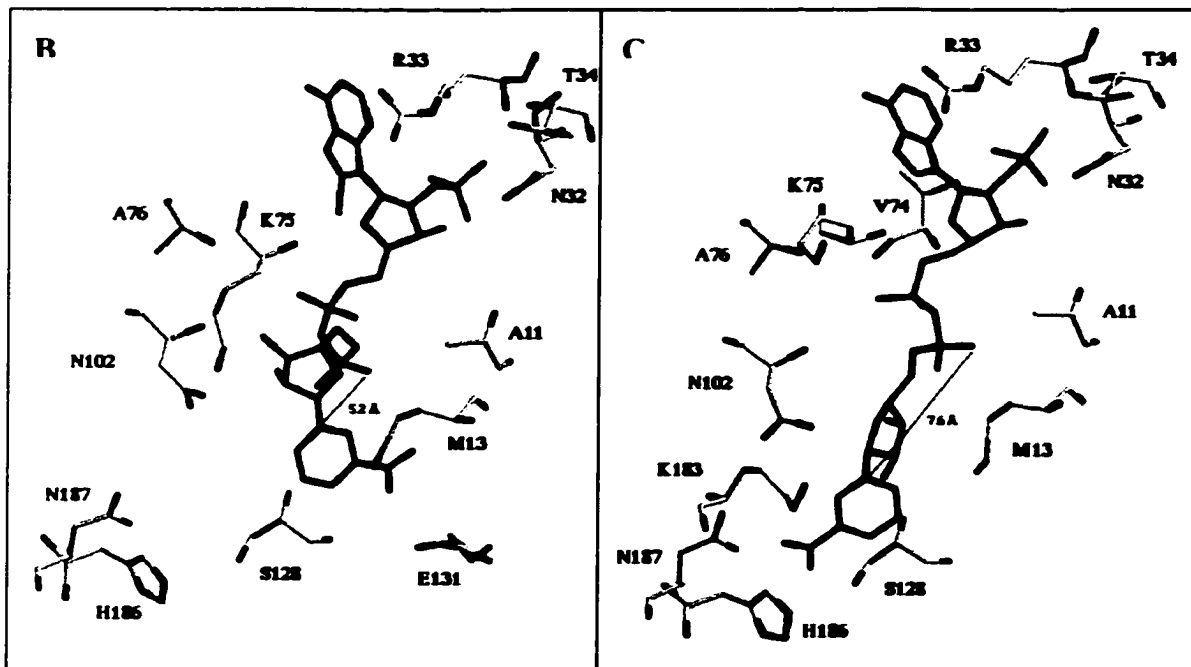
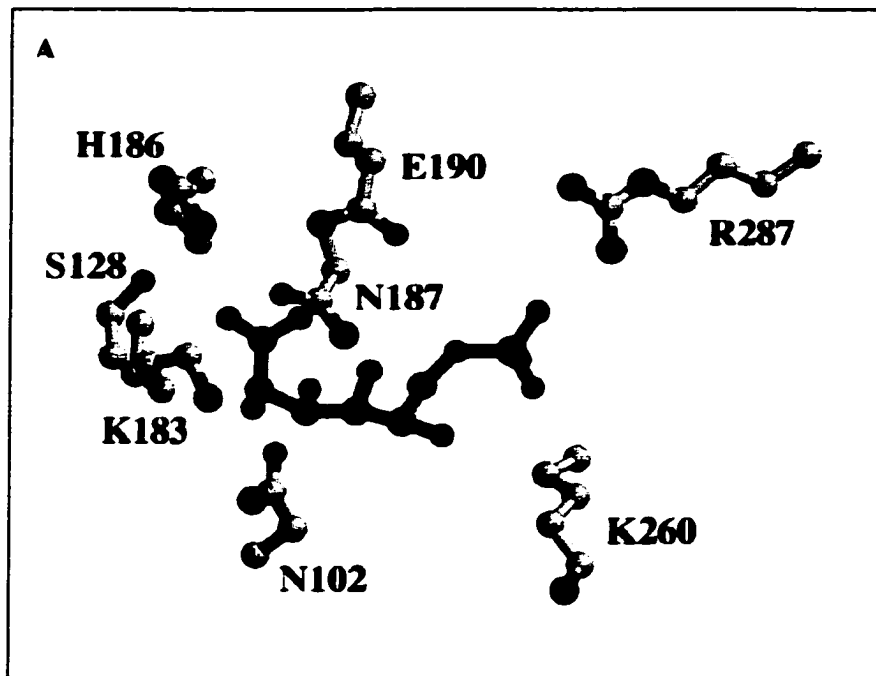
Isotope effects are a useful tool for studying enzyme mechanisms, especially in determination of the identity and amount of rate-limitation of rate-limiting steps, and in the elucidation of transition state structure. The values of $^D V$ and $^D(V/K)$ are equal for the wild type enzyme, indicating a rapid equilibrium random kinetic mechanism, that is a mechanism in which interconversion of E:NADP:6PG and E:NADPH:Ru5P:CO₂ is rate-limiting overall (Price and Cook, 1996). Further, the multiple isotope effect studies of Hwang et al (1998) suggest that the overall reaction is stepwise with oxidation preceding decarboxylation and that the hydride transfer step is partially rate-limiting. For the S128A, H186A, and N187A mutant enzymes, the $^D V$ values are all within error identical to the $^D(V/K)$ values (Table 6), indicating no change in kinetic mechanism. Primary deuterium isotope effects decrease for the

S128A and H186A mutant enzymes compared to those of the wild type enzyme, suggesting a decrease in the rate of the decarboxylation step, or k_9 in eq. 1, as observed for the K183 mutant enzymes. That is, both S128 and H186 must play an important role in the decarboxylation process. This suggestion is consistent with the initial velocity and product inhibition results that suggest the two residues are responsible for stabilizing the nicotinamide ring of NADPH, therefore facilitating the displacement of the 1-carboxylate of 6PG (see above). In the case of the N187A mutant enzyme, the deuterium isotope effects increase compared to those of the wild type enzyme, indicating a decrease in the rate of the hydride transfer step, or k_7 . It is worth noting that the average isotope effect for N187A is 2.85, which is very close to the estimated intrinsic deuterium isotope effect of 3.1 (Hwang et al., 1998). Thus, it appears that it is the oxidation step that has been affected as a result of the mutation. The role for N187 based on the isotope effect data is also consistent with the initial velocity data. As indicated above, N187 binds the 3-hydroxyl group of 6PG, and thus likely helps to maintain the 3-hydroxyl group in the right position, and facilitates proton transfer from the 3-hydroxyl of 6PG to the ϵ -amine of K183.

4.4 Mechanism.

From the above mutagenesis studies, the following mechanism is proposed. The binding of 6PG is such that the 1-carboxyl is hydrogen-bonded to S128 and E190, and the 3-hydroxyl is hydrogen-bonded to K183 and N187 (Figure 31A). Thus, in Figure 6, the oxidation of the 3-hydroxyl of 6PG is facilitated by K183,

Figure 31. Active Site Regions of the Enzyme-Substrate and Enzyme-Coenzyme Binary Complexes. A. E:6PG complex; B. E:Nbr⁸ADP complex; C. E:NADPH complex.



which accepts a proton from the 3-hydroxyl as the hydride is transferred to the *si* face of the nicotinamide ring. The nicotinamide ring is thought to be held in position by an electrostatic interaction between the positively charged N1 of the nicotinamide and the negatively charged pyrophosphate moiety of NADP (Figure 31B, Adams et al., 1994). Once the hydride has been transferred, the nicotinamide ring rotates by about 180° and presumably displaces the 1-carboxyl from its hydrogen-bonded position in preparation for decarboxylation (Figure 31C). The hydrogen bonds between the 1-carboxyl and E190 and S128 are broken, and new hydrogen bonds form between the carboxamide of the nicotinamide ring and S128 and H186. The positively-charged K183 is now set to polarize the carbonyl of 3-keto-6PG in the decarboxylation step. Therefore it is reasonable to conclude that the 6PGDH has evolved to have reverse protonation states between E190 and K183, the amino acid residues serving as the general acid and general base. There is no divalent metal ion required for the 6PGDH reaction, unlike other β -hydroxyacid oxidative decarboxylases, e.g. malic enzyme. Thus, an enzyme residue must be present to polarize the carbonyl in the decarboxylation step, and protonated K183 fills this role. In the decarboxylation step, K183 donates a proton to give the 1,2-enediol of ribulose 5-phosphate. CO₂ is then released, and tautomerization of the enediol occurs with acid-base catalysis by E190 and K183.

4.5 Summary

Based on the kinetic studies of all of the K183 mutant 6PGDHs, and especially the pH studies of the K183R mutant enzyme, the effect of changing K183 is significant. Thus, all data are consistent with the general base function of K183. From the kinetic data of the S128A, H186A and N187A mutant enzymes, it is reasonable to conclude that S128, H186 and N187 are all responsible for binding the substrate, and both S128 and H186 play an important role in the decarboxylation process, while N187 facilitates the hydride transfer step.

4.6 Future Studies

Additional research must still be carried out to obtain a further understanding of the mechanism of the 6PGDH catalyzed reaction. First, pH profiles will be obtained for the S128A, H186A and N187A mutant enzymes to study possible effects on the pK values of the enzyme catalytic groups by the above mutations. In order to probe the function of each amino acid residue mutated in the decarboxylation step, ¹³C isotope effects will also be performed for all of the above mutant proteins and the K183R mutant enzyme. Next, due to the very high activity of the wild type 6PGDH, it is impossible to obtain the structure of E:NADP:6PG ternary complex. However, with the low turnover number of some of the mutant enzyme, e.g. K183A, crystallization can be performed to solve the ternary complex structure of the mutant enzyme. This structure will provide valuable information concerning the reaction mechanism. Finally, additional site-directed mutagenesis studies will be carried out for several other residues to study their potential substrate binding and catalytic

functions. Residues include Tyr 191, Arg 287 and Arg 447, all of which make hydrogen bonds to the 6-phosphate group of 6PG, and Asn 32, Arg 33 and Thr 34, which bind the 2'-phosphate of NADP. Mutagenesis studies of the above amino acid residues will allow an estimation of the contribution of enzyme side chains to substrate and coenzyme binding.

LITERATURE CITED

Adams, M. J., Gover, S., Leaback, R., Phillips, C., and Somers, D. O. (1991) The structure of 6-Phosphogluconate Dehydrogenase refined at 2.5 Å Resolution. *Acta Cryst. B47*, 817-820.

Adams, M. J., Ellis, G. H., Cover, S., Naylor, C. E., and Phillips, C. (1994) Crystallographic Study of Coenzyme, Coenzyme Analogue and Substrate Binding in 6-Phosphogluconate Dehydrogenase: Implications for NADP Specificity and the Enzyme Mechanism. *Structure* 2, 651-668.

Berdis, A. J., and Cook, P. F. (1993a) Overall Kinetic Mechanism of 6-Phosphogluconate Dehydrogenase from *Candida utilis* . *Biochemistry* 32, 2036-2040.

Berdis, A. J., and Cook, P. F. (1993b) Chemical Mechanism of 6-Phosphogluconate Dehydrogenase from *Candida utilis* from pH Studies. *Biochemistry* 32, 2041-2046.

Berdis, A. J., and Cook, P. F. (1993c) The 2'-Phosphate of NADP is Critical for Optimum Productive Binding to the 6-Phosphogluconate Dehydrogenase from *Candida utilis*. *Arch. Biochem. Biophys.* 305, 551-558.

Boros, L. G., Puigjaner, J., Cascante, M., Lee, W. N., Brandes, J. L., Bassilian, S., Yusuf, F. I., Williams, R. D., Muscarella, P., Melvin, W. S., and Schirmer, W. J. (1997) Oxythiamine and Dehydroepiandrosterone Inhibit the Nonoxidative Synthesis of Ribose and Tumor Cell Proliferation. *Cancer Res.* 57, 4242-4248.

Bradford, M. M. (1976) A Rapid and Sensitive Method for the Quantitation of Microgram Quantities of Protein Utilizing the Principle of Protein-Dye Binding. *Anal. Biochem.* 72, 248-254

Chooback, L., Price, N. E., Karsten, W. E., Nelson, J., Sundstrom, P. R., and Cook, P. F. (1998) Cloning, Expression, Purification, and Characterization of the 6-Phosphogluconate Dehydrogenase from Sheep Liver. *Protein Expression and Purification* 13, 251-258.

Cleland, W. W. (1977) Determining the Chemical Mechanisms of Enzyme-Catalyzed Reactions by Kinetic Studies. *Adv. Enzymol. Relat. Areas Mol. Biol.* 45, 273-387.

Cook, P. F., and Cleland, W. W. (1981) Mechanistic Deduction from Isotope Effects for Bi-reactant Enzyme Reactions. *Biochemistry* 20, 1790-1796.

Dalocchio, F., Matteuzzi, M., and Bellini, T. (1985) Half-Site Reactivity in 6-Phosphogluconate Dehydrogenase from Human Erythrocytes. *Biochem. J.* 227, 305-310.

Dawson, T. M. C., Elliott, D. C., Elliott, W. H., and Jones, K. M. (1986) Amino Acids, Amines, Amides, Peptides, and Their Derivatives. in *Data for Biochemical Research* (3rd ed.), pp. 6-7, Clarendon Press, Oxford, U.K.

Dotto, G. P., Enea, V., and Zinder, N. D. (1981) Functional Analysis of Bacteriophage f1 Intergenic Region. *Virology* 114, 463-473.

Dotto, G. P., and Zinder, N. D. (1983) The Morphogenetic Signal of Bacteriophage f1. *Virology* 130, 252-256.

Dotto, G. P., Horiuchi, K., and Zinder, N. D. (1984) The Functional Origin of Bacteriophage f1 DNA Replication. Its Signals and Domains. *J. Mol. Biol.* 172, 507-521.

Farabaugh, P. J. (1978) Sequence of the *lacI* Gene. *Nature* 274, 765-769.

Fersht, A. (1977) Forces between Molecules, and Enzyme-Substrate Binding Energies. in *Enzyme Structure and Mechanism* , pp.230-231, W. H. Freeman and Company, New York.

Ganea, E., and Harding, J. J. (1996) Inhibition of 6-Phosphogluconate Dehydrogenase by Carbamylation and Protection by Alpha-Crystallin, a Chaperone-Like Protein. *Biochem. Biophys. Res. Commun.* 222, 626-631.

Grissom, C. B., and Cleland, W. W. (1988) Isotope Effect Studies of Chicken Liver NADP Malic Enzyme: Role of the Metal Ion and Viscosity Dependence. *Biochemistry* 27, 2927-2934.

Hanau, S., Dallochio, F., and Rippa, M. (1992) NADPH Activates a Decarboxylation Reaction Catalysed by Lamb Liver 6-Phosphogluconate Dehydrogenase. *Biochemica et. Biophysica Acta.* 1122, 273-277.

Hanau, S., Rippa, M., Bertelli, M., Dallochio, F., and Barrett, M. P. (1996) 6-Phosphogluconate Dehydrogenase from *Trypanosoma brucei*. Kinetic Analysis and Inhibition by Trypanocidal Drugs. *Eur. J. Biochem.* 240, 592-599.

Hermes, J. D., Roeske, C. A., O'Leary, M. H., and Cleland, W. W. (1982) Use of Multiple Isotope Effects to Determine Enzyme Mechanisms and Intrinsic Isotope

Effects, Malic Enzyme and Glucose-6-Phosphate Dehydrogenase. *Biochemistry* 21, 5106-5114.

Hochuli, E., Döbeli, H., and Schacher, A. (1987) New Metal Chelate Adsorbents Selective for Proteins and Peptide Containing Neighboring Histidine Residues. *J. Chromatography* 411, 177-184.

Hsu, R. Y., and Lardy, H. A. (1967) Pigeon Liver Malic Enzyme. II. Isolation, Crystallization, and Some Properties. *J. Biol. Chem.* 242, 520-526.

Hwang, C-C., Berdis, A. J., Karsten, W. E., Cleland, W. W., and Cook, P. F. (1998) Oxidative Decarboxylation of 6-Phosphogluconate by 6-Phosphogluconate Dehydrogenase Proceeds by a Stepwise Mechanism with NADP and APADP as Oxidants. *Biochemistry* 37, 12596-12602.

Hwang, C-C., and Cook, P. F. (1998) Multiple Isotope Effects as a Probe of Proton and Hydride Transfer in the 6-Phosphogluconate Dehydrogenase Reaction. *Biochemistry* 37, 15698-15702.

Karsten, W. E., and Cook, P. F. (1994) Stepwise versus Concerted Oxidative Decarboxylation Catalyzed by Malic Enzyme: a Reinvestigation. *Biochemistry* 33, 2096-2103.

Karsten, W. E., Chooback, L., and Cook, P. F. (1998) Glutamate 190 is a General Acid Catalyst in the 6-Phosphogluconate Dehydrogenase-Catalyzed Reaction. *Biochemistry* 37, 15691-15697.

Kiick, D. M., Harris, B. G., and Cook, P. F. (1986) Protonation Mechanism and Location of Rate-Determining Steps for the *Ascaris suum* Nicotinamide Adenine Dinucleotide-Malic Enzyme Reaction from Isotope Effects and pH Studies. *Biochemistry* 25, 227-235.

Kramer, B., Kramer, W., and Fritz, H. J. (1984) Different Base/Base Mismatches Are Corrected with Different Efficiencies by the Methyl-Directed DNA Mismatch-Repair System of *E. coli*. *Cell* 38, 879-887.

Luzzato, L., and Mehta, A. (1989) Glucose-6-Phosphate Dehydrogenase Deficiency. in *The Metabolic Basis of Inherited Disease*, 6th ed., (Scriver, C. R., Beudet, A., Sly, W. S., and Valle, D., Eds.), pp. 2237-2265, McGraw-Hill, Inc., USA.

Niehuas, W. G., Richardson, S. B., and Wolz, R. L. (1996) Slow-Binding Inhibition of 6-Phosphogluconate Dehydrogenase by Zinc Ion. *Arch. Biochem. Biophys.* 333, 333-337.

Northrop, D. B. (1975) Steady-State Analysis of Kinetic Isotope Effects in Enzymic Reactions. *Biochemistry* 14, 2644-2651.

Parkin, D. W. (1991) Methods for the Determination of Competitive and Noncompetitive Kinetic Isotope Effects. in *Enzyme Mechanism from Isotope Effects* (Cook, P. F., Ed.), pp. 284-285, CRC Press, Inc., Boca Raton.

Phillips, C., Dohnalek, J., Gover, S., Barrett, M. P., Adams, M. J. (1998) A 2.8 Å Resolution Structure of 6-Phosphogluconate Dehydrogenase from the Protozoan Parasite *Trypanosoma brucei*: Comparison with the Sheep Enzyme Accounts for Difference in Activity with Coenzyme and Substrate Analogues. *J. Mol. Biol.* 282, 667-681.

Planas, A., and Kirsch, J. F. (1991) Reengineering the Catalytic Lysine of Aspartate Aminotransferase by Chemical Elaboration of A Genetically Introduced Cysteine. *Biochemistry* 30, 8268-8276.

Pontremoli, S., de Flora, A., Grazi, E., Mangiarotti, G., Bonsignore, A., and Horecker, B. L. (1961) Crystalline D-Gluconate 6-Phosphate Dehydrogenase. *J. Biol. Chem.* 236, 2975-2980.

Price, N. E., and Cook, P. F. (1996) Kinetic and Chemical Mechanisms of the Sheep Liver 6-Phosphogluconate Dehydrogenase. *Arch. Biochem. Biophys.* 336, 215-223.

Promega Corp. (1995) Altered Sites II *in vitro* Mutagenesis Systems Technical Manual. TM001.

QIAGEN Inc. (1996) The QIAexpressionist: The High Level Expression and Protein Purification System. 1.000735

Quinn, D. M., and Sutton, L. D. (1991) Theoretical Basis and Mechanistic Utility of Solvent Isotope Effects. in *Enzyme Mechanism from Isotope Effects* (Cook, P. F., Ed.), pp. 88-92, CRC Press, Inc., Boca Raton.

Rao, G. S. J., Cook, P. F., and Harris, B. G. (1991) Effector-Induced Conformational Transitions in *Ascaris suum* Phosphofructokinase. *J. Biol. Chem.* 266, 8884-8890.

Rendina, A. R., Hermes, J. D., and Cleland, W. W. (1984) Use of Multiple Isotope Effects to Study the Mechanism of 6-Phosphogluconate Dehydrogenase. *Biochemistry* 23, 6257-6762.

Rippa, M., Signorini, M., and Dallochio, F. (1973) A Multiple Role for the Coenzyme in the Mechanism of Action of 6-Phosphogluconate Dehydrogenase. *J. Biol. Chem.* 248, 4920-4925.

Rippa, M., Giovannini, P. P., Barrett, M. P., Dallochio, F., and Hanau, S. (1998) 6-Phosphogluconate Dehydrogenase: the Mechanism of Action Investigated by a Comparison of the Enzyme from Different Species. *Biochim. Biophys. Acta.* 1429, 83-92.

Siebert, G., Carsiotis, M., and Plaut, G. W. E. (1957) The Enzymatic Properties of Isocitric Dehydrogenase. *J. Biol. Chem.* 226, 977-991.

Somers, D., Medd, S. M., Walker, J. E., and Adams, M. J. (1992) Sheep 6-Phosphogluconate Dehydrogenase: Revised Protein Sequence Based upon the Sequences of cDNA Clones Obtained with the Polymerase Chain Reaction. *Biochem. J.* 288, 1061-1067.

Tetaud, E., Hanau, S., Wells, J. M., Le Page, R. W., Adams, M. J., Arkison, S., and Barrett, M. P. (1999) 6-Phosphogluconate Dehydrogenase from *Lactococcus lactis*: A Role for Arginine Residues in Binding Substrate and Coenzyme. *Biochem. J.* 338, 55-60.

Topham, C. M., Matthews, B., and Dalziel, K. (1986) Kinetic Studies of 6-Phosphogluconate Dehydrogenase from Sheep Liver. *Eur. J. Biochem.* 156, 555-567.

Topham, C. M., and Dalziel, K. (1986) The Chemical Mechanism of Sheep Liver 6-Phosphogluconate Dehydrogenase. A Schiff-base Intermediate Is Not Involved. *Biochem. J.* 234, 671-677.

Tsai, C. S., and Chen, Q. (1998) Purification and Kinetic Characterization of 6-Phosphogluconate Dehydrogenase from *Schizosaccharomyces pombe*. *Biochem. Cell. Biol.* 76, 637-644.

Villafranca, J. J., and Colman, R. F. (1974) Frequency and Temperature Dependence of the Proton Relaxation Rates of Solvent and Substrate Interaction with Isocitrate Dehydrogenase Bound Mn(II). *Biochemistry* 13, 1152-1160.

Villarejo, M. R., and Zabin, I. (1974) Beta-Galactosidase from Termination and Deletion Mutant Strains. *J. Bacteriol.* 120, 466-474.

Voet D., and Voet J. G. (1995) The Pentose Phosphate Pathway. in *Biochemistry* (2nd ed.), pp. 617-625, John Wiley and Sons, Inc, USA.

Weiss, P. M., Gavva, S. R., Harris, B. G., Urbauer, J. L., Cleland, W. W., and Cook, P. F. (1991) Multiple Isotope Effects with Alternative Dinucleotide Substrates as a Probe of the Malic Enzyme Reaction. *Biochemistry* 30, 5755-5762.

Yoon, H., Anderson, C. D., and Anderson, B. M. (1989) Kinetic Studies of *Haemophilus influenzae* 6-Phosphogluconate Dehydrogenase. *Biochim. Biophys. Acta.* 994, 75-80.

Zell, R., and Fritz, H. J. (1987) DNA Mismatch-Repair in *Escherichia coli* Counteracting the Hydrolytic Deamination of 5-Methyl-Cytosine Residues. *EMBO J.* 6, 1809-1815.

Zhang, L., Chooback, L., and Cook, P. F. (1999) Lysine 183 Is the General Base in the 6-Phosphogluconate Dehydrogenase-Catalyzed Reaction. *Biochemistry* 38, 11231-11238.

APPENDIX

SEQUENCE ALIGNMENT OF 6-PHOSPHOGLUCONATE DEHYDROGENASES

	70	80	90	100	110	120
Bakers yeast	QSKVDHFLANE---	AKGKSIIGATSIEDFTIS	SKLKRPRKVMMLVKA	GAPVDALINQIVPLL		
Candida albicans	TAKVDREFLANE---	AKGKSIIGAHSIKELVD	QLRPRRIMMLVKA	GAPVDFINQLLPLL		
Fission yeast	TSRVDEFLANE---	AKGKSIIVGAHSLLEEF	VSKLKRPRVCIILV	KAGKPVVDYLIEGLAPLL		
Drosophila melanogaster	VAKVKEFLANE---	AKDTKVIIGADSLKDM	VSKLKSFRKVMMLV	KAGSAVDDFTIQQLVPLL		
Drosophila simulans	VAKVKEFLANE---	AKGTNVIIGADSLKDM	VSKLKSFRKVMMLV	KGSSAVDDFTIQQLVPLL		
Ceratitidis capitata	VEKVNQFLKNE---	AKGTNVIIGATSIQDM	VNKLKLRKIMMLV	KAGSAVDDFTIQQLVPLL		
Human	VSKVDDFLANE---	AKGTKVVGQAQSLKEM	VSKLKRPRRIILV	KAGQAVDDFTIEKLVPLL		
Sheep	VSKVDDFLANE---	AKGTKVVGQAQSLKEM	VSKLKRPRRIILV	KAGQAVDDFTIEKLVPLL		
Actinobacillus	TSKVDEFLEGA---	AKGTNVIIGAYSLEDL	ANKLEKPRKVMMLV	RAGEVVDHFDALLPHL		
Haemophilus influenzae	TSKVDEFLEGA---	AKGTNVIIGAYSLEDL	AAKLEKPRKVMMLV	RAGDVVDQFTEALLPHL		
Treponema pallidum	TTVVDRFLAGR---	AHGKRITGAHSIAELV	SLLARPRKIMMLV	KAGSAVDAVICQLLPLL		
Shigella boydii	REKTEEVIAE----	NPGKKLVPIYYTVKEF	VESLETPRRIILM	VKAGAGTDA/AIDS/LKPYL		
Shigella dysenteriae	REKTEEVIAE----	NPGKKLVPIYYTVKEF	VESLETPRRIILM	VKAGAGTDA/AIDS/LKPYL		
Shigella flexneri	REKTEEVIAE----	NPGKKLVPIYYTVKEF	VESLETPRRIILM	VKAGAGTDA/AIDS/LKPYL		
Shigella sonnei	REKTEEVIAE----	NPGKKLVPIYYTVKEF	VESLETPRRIILM	VKAGAGTDA/AIDS/LKPYL		
Salmonella typhimurium	REKTEEVIAE----	NPGKKLVPIYYTVKEF	VESLETPRRIILM	VKAGAGTDA/AIDS/LKPYL		
Citrobacter diversus	REKTEEVIAE----	NPGKKLVPIYYTVKEF	VESLETPRRIILM	VKAGAGTDA/AIDS/LKPYL		
Citrobacter freundii	REKTEEVIAE----	NPGKKLVPIYYTVKEF	VESLETPRRIILM	VKAGAGTDA/AIDS/LKPYL		
Escherichia vulneris	REKTEEVIAE----	NPGKKLVPIYYTVQEF	VESLETPRRIILM	VKAGAGTDA/AIDS/LKPYL		
Escherichia coli	REKTEEVIAE----	NPGKKLVPIYYTVQEF	VESLETPRRIILM	VKAGAGTDA/AIDS/LKPYL		
Klebsiella pneumoniae	REKTEEVIAE----	NTGKKLVPIYYTVQEF	VESLETPRRIILM	VKAGAGTDA/AIDS/LKPYL		
Klebsiella planticola	REKTEEVIAE----	NPGKKLVPHYTVKEF	VESLETPRRIILM	VKAGAGTDA/AIDS/LKPYL		
Klebsiella terrigena	REKTEEVIAE----	NPGKKLVPHYTVKEF	VESLETPRRIILM	VKAGAGTDA/AIDS/LKPYL		
Citrobacter amalonaticus	REKTEEVIAE----	NPGKKLVPIYYTVQEF	VESLETPRRIILM	VKAGAGTDA/AIDS/LKPYL		
Bacillus subtilis	SSKTEEFLOE----	AKGKNVVGTYSLIEEF	VESLETPRRIILM	VKAGATDATIQSLLPHL		
Synechococcus sp	AEKTEAFADR---	AQGKNIVPAYSLDFV	ASLERPRRIILM	VKAGGPVDAVVEQLKPLL		
Synechocystis sp	PNKTEKFAER---	AVGKDIKAAAYTVVEE	FVQLLERPRRIILM	VKAGGPVDAVINE/LKPLL		
Bacillus licheniformis	RDLTDQLVQK---	TGGQTVKPYELEDV	VQSLEKPRKIFL	MVTAGKPVLSVIDSLVPLL		
Trypanosoma brucei	YSKSEEFKANASAP	FAGNLKAFETMEAFAS	LKKPRKALILVQ	AGAAATDSTTEQLKKVF		
Primary consensus	REKTEEFLAEEASA	APGKKLVPIYYTVKEF	VESLETPRRIILM	VKAGAGTDA/AIDS/LKPYL		

	130	140	150	160	170	180
Bakers yeast	EKGDII	IDGGNSHFPDSNRRYEELK	KKKGI	LFVSGSVSGGEEGARYG	PSL	MPGGSEEAWPH
Candida albicans	EEGDII	IDGGNSHFPDSNRRYEELAK	KKGI	LFVSGSVSGGEEGARTG	PSL	MPGGNEKAWPH
Fission yeast	EKGDII	VDGGNSHYPDTRPCCEELAK	KKGI	LFVSGSVSGGEEGARYG	PSL	MPGGNPAAWPR
Drosophila melanogaster	SAGDVI	IDGGNSEYQDTSRRCDELAK	LGLL	LVFVSGSVSGGEEGARHG	PSL	MPGGHEAAWPL
Drosophila simulans	SAGDVI	IDGGNSEYQDTSRRCDELAK	LGLLYV	SGSVSGGEEGARHG	PSL	MPGGHEAAWPL
Ceratitidis capitata	SPGDVI	IDGGNSEYQDTSRRCDELRA	KKIL	LVFVSGSVSGGEEGARHG	PSL	MPGGHPEAWPL
Human	DTGDI	IDGGNSEYRDTTRPCRD	LKKG	ILFVSGSVSGGEEGPRYG	PSL	MPGGNKEAWPH
Sheep	DIGDII	IDGGNSEYRDTTRPCRD	LKKG	ILFVSGSVSGGEEGARYG	PSL	MPGGNKEAWPH
Actinobacillus	EAGDII	IDGGNSNYPTNRRVAALRE	KGIR	IFVSGSVSGGEEGARHG	PSL	MPGGNEEAWQF
Haemophilus influenzae	EEGDII	IDGGNSNYPTNRRVKA	LAEK	GIRFVSGSVSGGEEGARHG	PSL	MPGGNQEAWQY
Treponema pallidum	EKGDIV	ICGGNSHYQDTSRRCDEL	AKL	GLLVFVSGSVSGGEEGAL	RGPS	MPGGSAQAWPL
Shigella boydii	DKGDI	IDGGNTFFQDTIRRNRELS	AE	GFNFVSGSVSGGEEGAL	KGPS	MPGGQKEAYEL
Shigella dysenteriae	DKGDI	IDGGNTFFQDTIRRNRELS	AE	GFNFVSGSVSGGEEGAL	KGPS	MPGGQKEAYEL
Shigella flexneri	DKGDI	IDGGNTFFQDTIRRNRELS	AE	GFNFVSGSVSGGEEGAL	KGPS	MPGGQKEAYEL
Shigella sonnei	DKGDI	IDGGNTFFQDTIRRNRELS	AE	GFNFVSGSVSGGEEGAL	KGPS	MPGGQKEAYEL
Salmonella typhimurium	EKGDII	IDGGNTFFQDTIRRNRELS	AE	GFNFVSGSVSGGEEGAL	KGPS	MPGGQKDAYEL
Citrobacter diversus	DKGDI	IDGGNTFFQDTIRRNRELS	AE	GFNFVSGSVSGGEEGAL	KGPS	MPGGQKEAYEL
Citrobacter freundii	DKGDI	IDGGNTFFQDTIRRNRELS	AE	GFNFVSGSVSGGEEGAL	KGPS	MPGGQKEAYEL
Escherichia vulneris	DKGDI	IDGGNTFFHDTIRRNRELS	AE	GFNFVSGSVSGGEEGAL	KGPS	MPGGQKEAYEL
Escherichia coli	DKGDI	IDGGNTFFQDTIRRNRELS	AE	GFNFVSGSVSGGEEGAL	KGPS	MPGGQKEAYEL
Klebsiella pneumoniae	DKGDI	IDGGNTFFQDTIRRNRELS	AE	GFNFVSGSVSGGEEGAL	KGPS	MPGGQKEAYEL
Klebsiella planticola	NKGDII	IDGGNTFFQDTIRRNRELS	AE	GFNFVSGSVSGGEEGAL	KGPS	MPGGQKEAYEL
Klebsiella terrigena	DKGDI	IDGGNTFFQDTIRRNRELS	AE	GFNFVSGSVSGGEEGAL	KGPS	MPGGQKEAYEL
Citrobacter amalonaticus	DKGDI	IDGGNTFFQDTIRRNRELS	EE	GFNFVSGSVSGGEEGAL	KGPS	MPGGQKEAYEL
Bacillus subtilis	EKDDIL	IDGGNTYYKDTQRRNKEL	AE	SGIHVSGSVSGGEEGAL	KGPS	MPGGQKEAHEL
Synechococcus sp	DPGELI	IDGGNSLFTDTERBVKDL	EAL	GLGFMGMVSGGEEGAL	NGPS	MPGGTQAAYEA
Synechocystis sp	EEGDMI	IDGGNSLYEDTERBTKDL	EAT	GLGFMGMVSGGEEGAL	LGPS	MPGGTQAAYKE
Bacillus licheniformis	EEGDVI	MDGGNSHYEDTERBYDSL	KAKG	IGYLGISGSEV	GALKGPS	MPGGDRDVYEK
Trypanosoma brucei	EKGDIL	VDTGNNAHFQDQGFPAQ	QLEA	AGLRFLMGI	SGGEEGARKG	PAFFPGTSLVWEE
Primary consensus	DKGDI	IDGGN2FFQDTIRRNRELS	AE	GFNFVSGSVSGGEEGAL	KGPS	MPGGQKEAYEL

	190	200	210	220	230	240								
Bakers yeast	IKNI	FQSI	SAKS	-DGE--	PCCEWV	GPA	GAGHYV	KQV	VHNGIEY	GDMQ	LICEAY	DI	MR	LG
Candida albicans	IKEI	FQD	VAAKS	-DGE--	PCCDWV	GD	GAGHYV	KQV	VHNGIEY	GDMQ	LICEAY	DL	MR	VGK
Fission yeast	IKPI	FQTL	AAKAGN	NE--	PCCDWV	GE	QAGHYV	KQV	VHNGIEY	GDMQ	LICEAY	DI	MR	GLG
Drosophila melanogaster	IQPI	FQA	ICAKAD	-GE--	PCCEWV	GD	GAGHYV	KQV	VHNGIEY	GDMQ	LICEAY	HI	MI	SLG
Drosophila simulans	IQPI	FQA	ICAKAD	-GE--	PCCEWV	GD	GAGHYV	KQV	VHNGIEY	GDMQ	LICEAY	HI	MI	SLG
Ceratitidis capitata	IQPI	FQSI	CAKAD	-KE--	PCCEWV	GE	GAGHYV	KQV	VHNGIEY	GDMQ	LICEAY	QI	MI	ALG
Human	IKTI	FQGI	AAKAV	GTGE--	PCCDWV	GD	GAGHYV	KQV	VHNGIEY	GDMQ	LICEAY	HL	MD	VLG
Sheep	IKAI	FQGI	AAKAV	GTGE--	PCCDWV	GD	GAGHYV	KQV	VHNGIEY	GDMQ	LICEAY	HL	MD	VLG
Actinobacillus	VKPI	LQAI	SAKTE	QGE--	PCCDWV	GK	DGAGHYV	KQV	VHNGIEY	GDMQ	LICEAY	QF	LE	GVG
Haemophilus influenzae	VKPI	LQAI	SAKTE	QGE--	PCCDWV	GE	GAGHYV	KQV	VHNGIEY	GDMQ	LICEAY	QF	LE	GLG
Treponema pallidum	VSPI	FCAI	AAKAD	DGT--	PCCDWV	GS	DGAGHYV	KMI	VHNGIEY	GDMQ	LIAEAY	SW	FM	HALG
Shigella boydii	VAPI	ILTK	IAA	VAEDGE--	PCVTYI	IG	DGAGHYV	KQV	VHNGIEY	GDMQ	LIAEAY	SL	LL	GGGLN
Shigella dysenteriae	VAPI	ILTK	IAA	VAEDGE--	PCVTYI	IG	DGAGHYV	KQV	VHNGIEY	GDMQ	LIAEAY	SL	LL	GGGLN
Shigella flexneri	VAPI	ILTK	IAA	VAEDGE--	PCVTYI	IG	DGAGHYV	KQV	VHNGIEY	GDMQ	LIAEAY	SL	LL	GGGLN
Shigella sonnei	VAPI	ILTK	IAA	VAEDGE--	PCVTYI	IG	DGAGHYV	KQV	VHNGIEY	GDMQ	LIAEAY	SL	LL	GGGLN
Salmonella typhimurium	VAPI	ILTK	IAA	VAEDGE--	PCVTYI	IG	DGAGHYV	KQV	VHNGIEY	GDMQ	LIAEAY	SL	LL	GGGLN
Citrobacter diversus	VAPI	ILTK	IAA	VAEDGE--	PCVTYI	IG	DGAGHYV	KQV	VHNGIEY	GDMQ	LIAEAY	SL	LL	GGGLN
Citrobacter freundii	VAPI	ILTK	IAA	VAEDGE--	PCVTYI	IG	DGAGHYV	KQV	VHNGIEY	GDMQ	LIAEAY	SL	LL	GGGLN
Escherichia vulneris	VAPI	ILTK	IAA	VAEDGE--	PCVTYI	IG	DGAGHYV	KQV	VHNGIEY	GDMQ	LIAEAY	SL	LL	GGGLN
Escherichia coli	VAPI	ILKQ	IAA	VAEDGE--	PCVTYI	IG	DGAGHYV	KQV	VHNGIEY	GDMQ	LIAEAY	AL	LL	GGGLT
Klebsiella pneumoniae	VAPI	ILKQ	IAA	VAEDGE--	PCVTYI	IG	DGAGHYV	KQV	VHNGIEY	GDMQ	LIAEAY	AL	LL	GGGLA
Klebsiella planticola	VAPI	ILEQ	IAA	RAEDGE--	PCVAYI	IG	DGAGHYV	KQV	VHNGIEY	GDMQ	LIAEAY	AL	LL	GGGLA
Klebsiella terrigena	VAPI	ILEQ	IAA	RAEDGE--	PCVAYI	IG	DGAGHYV	KQV	VHNGIEY	GDMQ	LIAEAY	AL	LL	GGGLA
Citrobacter amalonaticus	VAPI	ILKQ	IAA	VAEDGE--	PCVTYI	IG	DGAGHYV	KQV	VHNGIEY	GDMQ	LIAEAY	SL	LL	GGGLN
Bacillus subtilis	VKPI	LEAI	SAK	VD-GE--	PCVTYI	IG	PDGAGHYV	KQV	VHNGIEY	GDMQ	LISESY	FI	LS	QVLG
Synechococcus sp	VEPI	VRTI	AAQ	VDDG---	PCVTYI	IG	PGSSG	HYV	KQV	VHNGIEY	GDMQ	LIAEAY	DL	LSVAG
Synechocystis sp	LEPI	ILTK	IAA	QVED	PDNPA	CVTFI	PGGAGHYV	KQV	VHNGIEY	GDMQ	LIAEAY	DI	LN	GLG
Bacillus licheniformis	AAP	ILTK	IAA	QVE	-GD--	PCCVYI	IG	PKGAGHYV	KQV	VHNGIEY	AD	MQ	LIAEAY	TFL
Trypanosoma brucei	IRPI	VEA	AAA	KADDGR--	PCVTM	NSG	SAGS	CVF	YHNS	GEYAI	LQ	EW	GEV	FDILR-AMG
	*	*	..	*	..	*	..	*	..
Primary consensus	VAPI	IL2K	IAA	KAED	GENP	PCVTYI	IG	DGAGHYV	KQV	VHNGIEY	GDMQ	LIAEAY	SL	LL

	310	320	330	340	350	360
Bakers yeast	AINALDLGMPVTLIGEAVFARCLSA	LKNERIRASKVLP	GPPEVP----	KDAVKDREQFVDD		
Candida albicans	AVNALDLGIPVTLIGEAVFSRCLSA	MFAERVEASKALKGPQVTG---	ESPIITDKKQFIDD			
Fission yeast	AQNALDMGTPVSLITEAVFAPCLSS	LKSERVRASKKLTGPNTK-----	FTGDKKQLIDD			
Drosophila melanogaster	AIAALQYGVVPTLIGEAVFSRCLSA	LKDERVQASSVVLKGPSTK-----	AQVANLTKFLDD			
Drosophila simulans	AIAALQYGVVPTLIGEAVFSPCLSA	LKDERVQASSVVLKGPSTK-----	AEVANLTKFLDD			
Ceratitis capitata	AISALQYGVVPTLIGEAVFSRCLSA	LKDERVAASKQLKGPVNV-----	AKVEDLPKFLNH			
Human	AISALEYGVVPTLIGEAVFARCLSS	LKDERIQASKKLGPKKF-----	QFDGDKKSFLED			
Sheep	AISALEYGVVPTLIGEAVFARCLSS	LKDERIQASKKLGPKQNI-----	PFEGDKKSFLED			
Actinobacillus	GINALDFGIPPLTLITESVFAFCVSA	FFDQ RVAASKLFFHKTIGK-----	VEGDKKVWIEA			
Haemophilus influenzae	GINALDFGIPPLTLITESVFAFCVSS	FKDQ RVAANQLFGKTIITP-----	VEGDKKVWIEA			
Treponema pallidum	CVAALEEGSPPLTLITESVMARSLSA	QFQARCKAHRVFGSPVKVSKAETLSA	QQREELVSA			
Shigella boydii	SQSALDLGEPPLSLITESVFAFYISS	LKQ RVAASKVLSGPPAQAPAG-----	NKAEFIEK			
Shigella dysenteriae	SQSALDLGEPPLSLITESVFAFYISS	LKQ RVAASKVLSGPPAQAPAG-----	DKAEFIEK			
Shigella flexneri	SQSALDLGEPPLSLITESVFAFYISS	LKQ RVAASKVLSGPPAQASAG-----	DKAEFIEK			
Shigella sonnei	SQSALDLGEPPLSLITESVFAFYISS	LKQ RVAASKVLSGPPAQASAG-----	DKAEFIEK			
Salmonella typhimurium	SQSALDLGEPPLSLITESVFAFYISS	LKQ RVAASKVLSGPKAQAPAG-----	DKAEFIEK			
Citrobacter diversus	SQSSLDLGEPLSLITESVFAFYISS	LKEQ RVAASKVLSGPKAQLAG-----	DKAEFIEK			
Citrobacter freundii	SQSSLDLGEPLSLITESVFAFYISS	LKQ RVAASKVLSGPPAQAKLAG-----	DKAEFVEK			
Escherichia vulneris	SQSSLDLGEPLSLITESVFAFYISS	LKEQ RVAASKVLSGPPQSQPAG-----	DKAEFIEK			
Escherichia coli	SQSSLDLGEPLSLITESVFPFYISS	LKQ RVAASKVLSGPPAQAPAG-----	DKAEFIEK			
Klebsiella pneumoniae	SQSSLDLGEPLSLITESVFAFYISS	LKQ RVAASKVLSGPPAQAPVAG-----	DKAGFIEK			
Klebsiella planticola	SQSSLDLGEPLSLITESVFAFYISS	LKQ RVAASKVLTGPKAQAPAG-----	DKAEFVEK			
Klebsiella terrigena	SQSSLDLGEPLSLITESVFAFYISS	LKQ RVAASKVLTGPKAQAPAS-----	DKAEFIEK			
Citrobacter amalonaticus	SQSSLDLGEPLSLITESVFAFYISS	LKTQ RVAASKVLTGPPAQAPAG-----	DKAEFIEK			
Bacillus subtilis	SQSALDLGVPLPIITESVFAFFISAM	EERVKASGLLSGPEVKPVTE-----	NKEELIEA			
Synechococcus sp	VETALEIGVAIPTIIAAVNARILSS	IKAEQAASEILSGPITEPFSG-----	DRQAFIDS			
Synechocystis sp	VMSGLELGVPIPTIYAAVNAPVMS	SLKEERVAASGQLSGP-SKTFSG-----	DVEAWIPK			
Bacillus licheniformis	SLQAIDNGIPSSIIITESLFAFYLS	SLKDERTAENVLGAPETEERPL-----	DQNVWIDR			
Trypanosoma brucei	AQEALEIGVPAPSLNMAVVSROFT	MYKTERQANASNAPGITQSPGYTL	KNKSPSGPEIKQ			
	::: * . . . : :: * . . . : * * . . . :					
Primary consensus	SQSALDLGEPPLSLITESVFAFYISS	LKQ RVAASKVLSGPPAQAPAG24AFVGD	KAEFIEK			

	370	380	390	400	410	420
Bakers yeast	LEQALYASKI	IISYAQGFML	IREAAATY	GWKLN	NPALMWR	GGCIIRSVFLGQITKAYRE
<i>Candida albicans</i>	LEQALYASKI	IISYDQGFML	MNQAAKDY	GWKLN	NAGIALMWR	GGCIIRSVFLAEITAAAYRK
Fission yeast	LEDALYASKI	IISYAQGFML	MREAKEY	GWKLN	NAGIALMWR	GGCIIRSVFLKDI TEAFRE
<i>Drosophila melanogaster</i>	IKHALYCAKIV	SYAQGFML	MREAARENK	WRLNY	GGIALMWR	GGCIIRSVFLGNIKDAYTS
<i>Drosophila simulans</i>	IKHALYCAKIV	SYAQGFML	MREAARENK	WRLNY	GGIALMWR	GGCIIRSVFLGNIKDAYTS
<i>Ceratitidis capitata</i>	IKHALYCSKIV	SYAQGFML	MREAAKENN	WNLNY	GGIALMWR	GGCIIRSVFLGNIKDAYTR
Human	IRKALYASKI	IISYAQGFML	LRQAATE	FGWTL	NYGGIALMWR	GGCIIRSVFLGKIKDAFDR
Sheep	IRKALYASKI	IISYAQGFML	LRQAATE	FGWTL	NYGGIALMWR	GGCIIRSVFLGKIKDAFDR
<i>Actinobacillus</i>	VRKALLASKI	IISYAQGFML	IREASEHFN	WNI	NYGNTALLWR	EGCIIRSRFLGNIRDAYEA
<i>Haemophilus influenzae</i>	VRKALLASKI	IISYAQGFML	IREASEQFG	WD	INYGATALLWR	EGCIIRSRFLGNIRDAYEA
<i>Treponema pallidum</i>	LEDALYCAKIV	SYAQGFEL	LSHTAKR	RGWTL	DFSRIASLWR	GGCIIRSGFLSKISAFAQ
<i>Shigella boydii</i>	VRRALYLGKIV	SYAQGFSQL	RAASEEY	NWDL	NYGEIAKI	FRAGCIIRAQFLQKITDAYAE
<i>Shigella dysenteriae</i>	VRRALYLGKIV	SYAQGFSQL	RAASEEY	NWDL	NYGEIAKI	FRAGCIIRAQFLQKITDAYAE
<i>Shigella flexneri</i>	VRSALYLGKIV	SYAQGFSQL	RAASEEY	NWDL	NYGEIAKI	FRAGCIIRAQFLQKITDAYAE
<i>Shigella sonnei</i>	VRRALYLGKIV	SYAQGFSQL	RAASEEY	NWDL	NYGEIAKI	FRAGCIIRAQFLQKITDAYAE
<i>Salmonella typhimurium</i>	VRRALYLGKIV	SYAQGFSQL	RAASDEY	NWDL	NYGEIAKI	FRAGCIIRAQFLQKITDAYAE
<i>Citrobacter diversus</i>	VRRALYLGKIV	SYAQGFSQL	RAASDEY	NWDL	NYGEIAKI	FRAGCIIRAQFLQKITDAYAE
<i>Citrobacter freundii</i>	VRRALYLGKIV	SYAQGFSQL	RAASDEY	NWDL	NYGEIAKI	FRAGCIIRAQFLQKITDAYAE
<i>Escherichia vulneris</i>	VRRALYLGKIV	SYAQGFSQL	RAASEEY	NWDL	NYGEIAKI	FRAGCIIRAQFLQKITDAYAE
<i>Escherichia coli</i>	VRRALYLGKIV	SYAQGFSQL	RAASDEY	NWEL	NYAEIAKI	FRAGCIIRAQFLQKITDAYAQ
<i>Klebsiella pneumoniae</i>	VRRALYLGKIV	SYAQGFSQL	RAASDEY	NWDL	NYGEIAKI	FRAGCIIRAQFLQKITDAYAQ
<i>Klebsiella planticola</i>	VRRALYLGKIV	SYAQGFSQL	RAASNEY	NWDL	NYGEIAKI	FRAGCIIRAQFLQKITDAYEQ
<i>Klebsiella terrigena</i>	VRRALYLGKIV	SYAQGFSQL	RAASNEY	SWDL	NYGEIAKI	FRAGCIIRAQFLQKITDAYEE
<i>Citrobacter amalonaticus</i>	VRRALYLGKIV	SYAQGFSQL	RAASDEY	NWDL	NYGEIAKI	FRAGCIIRAQFLQKITDAYAE
<i>Bacillus subtilis</i>	VRKALFMSKI	CSYAQGF	FAQMKAA	SEY	NWDLKY	GEIAMI FRGGCIIRAAF
<i>Synechococcus</i> sp	VRDALYCSKI	CSYAQGM	ALLAKAS	QVY	NYG	INLGEIARIWGGCIIRAGFLN
<i>Synechocystis</i> sp	VRDALYCSK	MCSYAQGM	ALLAKAS	QVY	NYG	INLGEIARIWGGCIIRAGFLD
<i>Bacillus licheniformis</i>	VRQALYMGKV	CAYAQGF	FAQYKMT	SDLN	GWHLPLK	DIALI FRGGCIIRAQFLN
<i>Trypanosoma brucei</i>	LYDSVCIAI	IISYAQMF	QCLREMD	KVHN	FGLNLP	AT IAT FRAGCIIRAGFLD
Primary consensus	: :: . : .*	* : :	: :	:: **	:: .*	: :

	430	440	450	460	470	480
Bakers yeast	EPDLENLLFNKFFADAVTKAQS	GWRKSLALAT-TYGIPTPAFSTALS	IFYDGYRS-ERLPA			
<i>Candida albicans</i>	KPDLENLLLYPFFNDAITKAQSGWRAS	WGKAI-QYGIPTFAFSTALAFYDGLRS-ERLPA				
Fission yeast	DPNLESILFHPPFTNGVEKAQAGWR	RVVAQAA-MLGIPVATSTGLSFYDGYRS-AVLPA				
<i>Drosophila melanogaster</i>	QPELSNLLLDFFFKKAIERGQDSWRE	VANAF-RWGI PVFALSTALSIFYDGYRT-AKLPA				
<i>Drosophila simulans</i>	QPQLSNLLLDFFFKKAIERGQDSWRE	VANAF-RWGI PVFALSTALSIFYDGYRT-AKLPA				
<i>Ceratitis capitata</i>	NPQLSNLLLDFFFKKAIIEVQNSWR	QVAVANAF-LWGI PVFALSTALSIFYDGYRT-EKLPA				
Human	NPELQNLNLLDFFFKSAVENCQDSWR	RAVSTGV-QAGI PMFCFTTALSIFYDGYRH-EMLPA				
Sheep	NPGLQNLNLLDFFFKSAVENCQDSWR	RAVSTGV-QAGI PMFCFTTALSIFYDGYRH-AMLPA				
<i>Actinobacillus</i>	NPDLIFLGSDSYFKGILENAMSDWR	KVVAKSI-EVGI PMFCMASAITFLDGYTS-ARLPA				
<i>Haemophilus influenzae</i>	NPNLVFLGSDSYFKGILENALS	SDWRKVVAKSI-EVGI PMFCMASAITFLDGYTS-ARLPA				
<i>Treponema pallidum</i>	QHDLENLVLAPFFAEELKRACPGWRTI	VAESV-RQALPVPALSAALAWFDGFTG-AALPA				
<i>Shigella boydii</i>	NPQIANLLLLAPYFKQIADDYQQAL	RDVVAYAV-QNGI PVVTFAAAVAYYDSYRA-AVLPA				
<i>Shigella dysenteriae</i>	NPQIANLLLLAPYFKQIADDYQQAL	RDVVAYAV-QNGI PVVTFAAAVAYYDSYRA-AFLPA				
<i>Shigella flexneri</i>	NPQIANLLLLAPYFKQIADDYQQAL	RDVVAYAV-QNGI PVVTFAAAVAYYDSYRA-AVLPA				
<i>Shigella sonnei</i>	NPQIANLLLLAPYFKQIADDYQQAL	RDVVAYAV-QNGI PVVTFAAAVAYYDSYRA-AVLPA				
<i>Salmonella typhimurium</i>	NADIANLLLLAPYFKKIADDEYQQAL	RDVVAYAV-QNGI PVVTFSAAVAYYDSYRA-AVLPA				
<i>Citrobacter diversus</i>	NAGIANLLLLAPYFKKIADDEYQQAL	RDVVAYAV-QNGI PVVTFSAAVAYYDSYRA-AVLPA				
<i>Citrobacter freundii</i>	NKGIANLLLLAPYFKNIADDEYQQAL	RDVVAYAV-QNGI PVVTFSAAVAYYDSYRS-AVLPA				
<i>Escherichia vulneris</i>	TPAIANLLLLAPYFKQIADDYQQAL	RDVVAYAV-QNGI PVVTFGAAVAYYDSYRA-AVLPA				
<i>Escherichia coli</i>	NAGIANLLLLAPYFKQIADDYQQAL	RDVVAYAV-QNGI PVVTFSAAIAYYDSYRS-AVLPA				
<i>Klebsiella pneumoniae</i>	NAGIANLLLLAPYFKQIADDYQQAL	RDVVAYAV-QNGI PVVTFVSAAIAYYDSYRS-AVLPA				
<i>Klebsiella planticola</i>	NAGIANLLLLAPYFKQIADDEYQQAL	RDVVAYAV-QNGI PVVTFSAAIAYYDSYRS-AVLPA				
<i>Klebsiella terrigena</i>	NAGIANLLLLAPYFKQIADDEYQQAL	RDVVAYAV-QNGI PVVTFSAAIAYYDSYRS-AVLPA				
<i>Citrobacter amalonaticus</i>	NPAIANLLLLAPYFKQIADDYQQAL	RDVVSAYAV-QNGI PVVTFSAAVAYYDSYRA-AVLPA				
<i>Bacillus subtilis</i>	EPELDNLLLDYSYFKNIVESYQGAL	RQVIVSLAV-AQGVVPSFSSALAYYDSYRT-AVLPA				
<i>Synechococcus</i> sp	DPTLANLLLLAPEFRQITLDRQLR	WRVVAIAAA-ERGI PVFAFSASLDYFDSYR--ASPAQ				
<i>Synechocystis</i> sp	NPQLPNLLLLAPEFKQSILDRQGP	WRVVMMLAN-EMGI AVPAFSSSLDYFDSYRR-AVLPAQ				
<i>Bacillus licheniformis</i>	QPDLNLLLVAPDFAEKLKEYQSG	LRKVVCEGI-SSGI SFFCLSTALSIFYDGYRT-GRSNA				
<i>Trypanosoma brucei</i>	NPNI SNLMCA--FQTEIRAGLQNY	RDVVALITSKLEVSI PVLSASLNVTAMFTPTLKYG				
	:	:	*	:	:	*
	:	:	:	:	:	:
Primary consensus	NP2LANLLLLAPYFKQIADDYQQAL	RDVVAYAVSQNGI PVVTFSAALAYYDSYRSPAVLPA				

	490	500	510	520	530
Bakers yeast	NLLQAQRDYFGAHTFRVLPECASDNL	FPVDKDIHINWTGHGGNVSSSTYQA			
<i>Candida albicans</i>	NLLQAQRDYFGAHTFKVLPQENELLK	KDEWIHINWTGRGGDVSSTTYDA			
Fission yeast	NLLQAQRDYFGAHTFRVLPEAADKSL	PADKDIHINWTGHGGNISATTYDA			
<i>Drosophila melanogaster</i>	NLLQAQRDYFGAHTYELLG-----	QEQFHHTNWTGTGGNVSASTYQA			
<i>Drosophila simulans</i>	NLLQAQRDYFGAHTYELLG-----	QEQFHHTNWTGTGGNVSASTYQA			
<i>Ceratitidis capitata</i>	NLLQAQRDYFGAHTYELLG-----	AEGKFVHTNWTGTGGNVSASTYQA			
Human	SLIQAQRDYFGAHTYELLA-----	KPGQFIHTNWTGHGGTVSSSSYNA			
Sheep	NLIQAQRDYFGAHTYELLA-----	KPGQFIHTNWTGHGGSVSSSSYNA			
<i>Actinobacillus</i>	NLLQAQRDYFGAHTYERTDK-----	PRGEFFHTNWTGRGGNTASTTYDV			
<i>Haemophilus influenzae</i>	NLLQAQRDYFGAHTYERTDK-----	PRGEFFHTNWTGRGGNTASTTYDV			
<i>Treponema pallidum</i>	NLLQAQRDYFGAHTYERTD-----	APRGEFFHTNWTGTGGDTIAGTYSI			
<i>Shigella boydii</i>	NLIQAQRDYFGAHTYKRI-----	-----			
<i>Shigella dysenteriae</i>	NLIQAQRDYFGAHTYKRI-----	-----			
<i>Shigella flexneri</i>	NLIQAQRDYFGAHTYKRIDKEGV-----	FHTEWLD-----			
<i>Shigella sonnei</i>	NLIQAQRDYFGAHTYKRI-----	-----			
<i>Salmonella typhimurium</i>	NLIQAQRDYFGAHTYKRTDKEGI-----	FHTEWLE-----			
<i>Citrobacter diversus</i>	NLIQAQRDYFGAHTYKRT-----	-----			
<i>Citrobacter freundii</i>	NLIQAQRDYFGAHTYKRT-----	-----			
<i>Escherichia vulneris</i>	NLIQAQRDYFGAHTYKRT-----	-----			
<i>Escherichia coli</i>	NLIQAQRDYFGAHTYKRTDKEGV-----	FHTEWLE-----			
<i>Klebsiella pneumoniae</i>	NLIQAQRDYFGAHTYKRTDKEGV-----	FHTEWLE-----			
<i>Klebsiella planticola</i>	NLIQAQRDYFGAHTYKRT-----	-----			
<i>Klebsiella terrigena</i>	NLIQAQRDYFGAHTYKRT-----	-----			
<i>Citrobacter amalonaticus</i>	NLIQAQRDYFGAHTYKRT-----	-----			
<i>Bacillus subtilis</i>	NLIQAQRDYFGAHTYERTDKEGI-----	FHTEWMK-----			
<i>Synechococcus</i> sp	NLTQAQRDYFGAHTYERTDRSGS-----	FHAQWF-----			
<i>Synechocystis</i> sp	NLTQAQRDYFGAHTYERTDKPRGE-----	FFHTEWLD-----			
<i>Bacillus licheniformis</i>	NLLQAQRDYFGAHTYERTDMEGV-----	FHTDWY-----			
<i>Trypanosoma brucei</i>	QLVSLQRDVFGRHGYSRVDKDKGR-----	ESFQWPELQ-----			
	. * . * . : * * * . :				
Primary consensus	NLIQAQRDYFGAHTYKRTDKEGVE3LP2G2	FFHTNWTG2GGNVSSSTY2A			

Alignment length : 530
 Identity (*) : 27 is 5.09 %
 Strongly similar (:): 34 is 6.42 %
 Weakly similar (.) : 16 is 3.02 %
 Different : 453 is 85.47 %